INFORMATION TO USERS

This manuscript has been reproduced from the microfilm master. UMI films the text directly from the original or copy submitted. Thus, some thesis and dissertation copies are in typewriter face, while others may be from any type of computer printer.

The quality of this reproduction is dependent upon the quality of the copy submitted. Broken or indistinct print, colored or poor quality illustrations and photographs, print bleedthrough, substandard margins, and improper alignment can adversely affect reproduction.

In the unlikely event that the author did not send UMI a complete manuscript and there are missing pages, these will be noted. Also, if unauthorized copyright material had to be removed, a note will indicate the deletion.

Oversize materials (e.g., maps, drawings, charts) are reproduced by sectioning the original, beginning at the upper left-hand corner and continuing from left to right in equal sections with small overlaps.

ProQuest Information and Learning
300 North Zeeb Road, Ann Arbor, MI 48106-1346 USA
800-521-0600

DETERMINING THE FUNCTIONAL NEUROANATOMY OF SPEECH PERCEPTION AND READING

by

Ryan C.N. D'Arcy

Submitted in partial fulfillment of the requirements
for the degree of Doctor of Philosophy

at

Dalhousie University
Halifax, Nova Scotia
February 15, 2002

DALHOUSIE UNIVERSITY

FACULTY OF GRADUATE STUDIES

The undersigned hereby certify that they have read and recommend to the Faculty of Graduate Studies for acceptance a thesis entitled "Determining the Functional Neuroanatomy of Speech Perception and Reading", in partial fulfillment of the requirements for the degree of Doctor of Philosophy.

Dated: February 15, 2002

External Examiner:

Research Supervisor:

Examining Committee:

DALHOUSIE UNIVERSITY

DATE: February 15, 2002

AUTHOR: RYAN C.N. D'ARCY

TITLE: DETERMING THE FUNCTIONAL NEUROANATOMY OF SPEECH PERCEPTION AND READING

DEPARTMENT OR SCHOOL: DEPARTMENT OF PSYCHOLOGY

DEGREE: Ph.D. **CONVOCATION:** MAY **YEAR:** 2002

Permission is herewith granted to Dalhousie University to circulate and to have copied for non-commercial purposes, at its discretion, the above title upon the request of individuals or institutions.

Signature of Author

Dedications

To my wife, Wendy K. Smith-D'Arcy, and to my father, Michael G.N. D'Arcy:

Thank-you both for teaching me to enjoy the journey, while always daring greatly...

Table of Contents

List of Figures

List of Tables

Abstract

Brain imaging studies are advancing our knowledge of the anatomy of language. In this investigation, the spatiotemporal nature of phonological and semantic processing was explored along with the influence of working memory (WM) on these functions. Semantic comprehension was the common theme across three experiments, each of which involved either speech perception or reading. Neural activity was imaged using event-related brain potentials (ERPs) and functional magnetic resonance imaging (fMRI). The first experiment examined ERP correlates of phonology and semantics in a visual to auditory semantic priming task. The results supported the role of phonological processing in the formulation of lexical candidates; a process that likely utilized WM to provide 'bottom-up' input for semantic analysis. Spatial analyses confirmed that the phonological mismatch negativity (PMN) and semantic N400 response had specific activation patterns, with intracranial generators localized to different regions of the left perisylvian cortex. The second experiment examined WM influences on the N400 in a visual semantic priming task in which WM load was also varied. Increased WM load delayed the response latency (and reduced the relative amplitude). Intracranial generators were localized to left perisylvian language areas as well as memory regions in the bilateral anterior temporal lobes and left inferior parietal lobe. The effects of increased WM load were observed within these memory regions (particularly the latter). The third experiment explored fMRI correlates of the N400 in a reading task that used contextually constrained sentences. While a number of foci corresponded with left perisylvian N400 generators, the activation patterns varied across individuals. The findings demonstrated that hemodynamic correlates of the N400 were detectable in fMRI, but are likely at or near

threshold levels. Overall, the investigation provided convergent evidence across stimulus and imaging modalities for a distributed neural architecture; one that supports cognitive processes essential to semantic comprehension.

Abbreviations and Symbols Used

AMLT	anterior medial temporal lobe
ANOVA	analysis of variance
BA	brodmann's area
BESA	brain electromagnetic source analysis
BOLD	blood-oxygen level-dependent contrast
cm	centimeters
CSD	current sources density
dB	decibels
DLPFC	dorsolateral prefrontal cortex
EEG	electroencephalogram
EOG	electro-oculogram
EP	evoked potential
ERP	event-related brain potential
fMRI	functional magnetic resonance imaging
Hz	hertz
KΩ	kilo-ohms
LTM	long-term memory
$\underline{M}$	mean
MEG	magnetoencephalography
MIP	maximum intensity projection
MRI	magnetic resonance imaging
MRS	magnetic resonance spectroscopy

ms	milliseconds
μV	micro-volts
nAm	nano-ampere
PET	positron emission tomography
SD	standard deviation
SE	standard error
SPM	statistical parametric mapping
STG	superior temporal gyrus
STP	superior temporal plane
TE	echo time
TR	repetition time
WM	working memory

Acknowledgments

In a prior attempt at acknowledgments (my M.Sc. thesis), I received feedback from a number of people, all of whom told me the same thing: "two sentences might be too brief." At the time, I promised that there was more to come.

I am extremely grateful for all of the guidance and support provided by my supervisor, Dr. John F. Connolly. Amongst all that I have learned, the pleasures of conducting vertical, creative research that influences basic and applied realms alike, has featured prominently. This thesis is a direct reflection of such a philosophy. Also, many of the core ideas that formed the basis of this work were generated from discussions with Dr. Elisabet Service, and I extend my sincere gratitude. I must thank my thesis committee for their enthusiasm and assistance in this project. Dr. Kazue Semba (my neuroscience supervisor) has continually provided me with valuable guidance and has always made time for impromptu visits. Dr. Peter Gregson and Dr. Kenneth Campbell have dedicated their time and effort to this thesis and provided valuable input.

My family has been vital in helping me along the way. I am particularly indebted to my wife, Wendy K. Smith-D'Arcy, who provides unfaltering love and support along with the ability to refresh and motivate. For this, I am forever grateful. I extend my sincere thanks to my father, Michael G.N. D'Arcy, my sister, Megan P. D'Arcy, and my brother, Trevor J.P. D'Arcy for all of their love and encouragement over the years. I have also always appreciated the keen interest and support from Gina D'Arcy, Len Smith, and Dolores Goodwin.

I must thank my friends for keeping me grounded solidly in insanity. My sincere gratitude is extended to Ian M. Guise, Dr. (to be) Scott Fairless, Dr. Michael A. Kuzyk,

and Dr. Yannick Marchand. I have always benefited from their joie de vive and endeavored to match their wit. I am very grateful to Alma and John Major, ambassadors to Newfoundland, without them our experiences in the east would not have been nearly as rewarding. I have appreciated my many discussions with Dr. (to be) Randy-Lynn Newman, who has always provided much needed, and timely, motivation. Many former, present, or affiliate colleagues have helped me in countless ways. Along with Alma ('lab mom'), I want to extend my thanks to Drs. (some now, others soon enough) Bruce Dick, Christopher A. Dywan, Jason G. Emsley, Kelly A.K. Forbes, Colin S. Hawco, Carl A. Helmick, Celeste LeFebvre, Frank P. MacMaster, and Jingtian Wang. I believe that it is a rare circumstance to find so many bright and talented people working together with the same research setting.

I also want to thank a number of other professors for their guidance throughout graduate school, including Drs. Sultan Darvesh, Gail A. Eskes, Tracy Taylor-Helmick, Michael E. Houlihan, Ray Klein, Catherine A. Mateer, Patrick McGrath, Myong Yoon, Matthias Schmidt, and Sherry Stewart. You have all taught me a great deal about science and research.

Before starting this, I wanted to prove that I could meet the challenges. In the process, I have learned that any true accomplishment can only be realized in the presence of others.

Thank-you, Ryan. (Winter, 2001)

Chapter One

General Introduction - Neuroanatomy and Language

Chapter One - Summary

Our understanding of the complex relationship between the brain and language in humans has become increasingly more advanced. Early neurological and subsequent neuropsychological investigations have led to the development of valuable aphasiological models of language, with many of the fundamental discoveries still exerting their influence on contemporary research (e.g., brain areas named after early aphasiologists such as Broca's and Wernicke's areas: verbal expression and reception, respectively). In addition to lesion work, behavioural studies on the processes that support language function in healthy individuals have enhanced the theoretical constructs that form the framework needed for integrating anatomical and physiological evidence (e.g., mental lexicon: "a dictionary or memory store in the brain of words and their meanings"; Kolb and Whishaw, 1996, pp. 647). Advances in neuroimaging have provided complementary evidence for many of the neurological and behavioural studies, and have a considerable potential for enhancing our understanding of the brain/language relationship. While a number of different neuroimaging techniques exist, event-related brain potentials (ERPs) and functional magnetic resonance imaging (fMRI) are commonly used to elucidate the neural basis of language (as well as other sensory, perceptual, and cognitive processes). The objective of this thesis was to investigate the spatiotemporal nature of language systems in the brain. In particular, the investigation focused on phonology (the sounds of words), semantics (the knowledge of words), and working memory (WM) during speech perception and reading. While these cognitive processes do not represent all that is fundamental to language, comprehension cannot exist without them.

Chapter One – Neuroanatomy and Language

One of the implicit universals of language is its definition, which has been succinctly summarized as: "Language is a code that relates form to meaning." (Caplan, Carr, Gould, and Martin, 1999, pp. 1493). It is the mental faculty that gives rise to the dominant forms of communication in humans, and is reliant on the ability to associate sounds and symbols with meaning (Price, 2000). In the brain, its neural architecture exists beyond multiple sensory inputs, with a series of parallel hierarchical channels being distributed throughout the cortex (Kolb and Whishaw, 1996).

Neurological and neuropsychological investigations of language

Many of the primary cortical language areas have been identified through lesion studies. Broca (1861) reported a patient who had impaired speech expression. A postmortem investigation revealed that the patient had damage in the region of the left inferior frontal gyrus. This area, which has since been referred to as 'Broca's area', has been linked to speech output functions. Not long after, Wernicke (1874) presented a patient who had impairments in speech comprehension. These impairments resulted from damage in the left posterior temporal cortex, or Wernicke's area. This secondary zone receives auditory speech images from the nearby primary auditory cortex. Along with Lichtheim (1885), Wernicke went on to propose a model whereby an interruption in the white matter tracts that connect Broca's and Wernicke's areas (i.e., the arcuate fasciculus) resulted in a disconnection syndrome (i.e., conduction aphasia). Patients with conduction aphasia have intact speech comprehension and expression abilities, but cannot repeat what they hear because of the disconnection. Damage to the functional specialized

regions outside Broca's and Wernicke's areas can result in different variants of aphasia (e.g., a lesion outside Broca's area can cause transcortical motor aphasia). While damage that compromises most or all key regions in the left perisylvian area can result in global aphasia, involving significant impairments to all aspects of language (Alexander, 1997).

Classical deficits have also been identified with respect to reading (i.e., alexia). Two well-known syndromes are alexia with- and without- agraphia (Déjerine, 1891, 1892). Patients who have alexia with agraphia have deficits in reading and writing that result from damage in the region of the left angular gyrus. In contrast, patients who have alexia without agraphia (or pure alexia) have deficits in reading, but writing ability remains intact (e.g., an individual can write their own name, but will not be able to read it). The latter syndrome is associated with lesions in the left occipital lobe and splenium of the corpus callosum, giving rise to a disconnection between perceptual information and the visual word form system (Binder and Mohr, 1992; Damasio and Damasio, 1983). In addition to alexia, a number of other dyslexic syndromes exist (e.g., surface, deep, and phonological), all of which are characterized by the specific nature of impairments in reading (Coslett, 1997). Surface dyslexia is a disorder characterized best by the inability to read irregular (or exception) words in which the pronunciation cannot be derived through phonological strategies (e.g., yacht). Deep dyslexia is defined predominately on the basis of hallmark semantic errors (e.g., reading 'castle' as 'knight'). Phonological dyslexia is characterized by an inability to convert print to sound (i.e., grapheme-to-phoneme conversion).

Along with the traditional language regions identified above, there exist several other areas that have been shown to have important contributions. For example, comprehension deficits have been associated with a variety of left temporal-parietal lesions that extend well outside the classically identified areas. Furthermore, while the left hemisphere is thought to be the dominant hemisphere in language, the right hemisphere has been implicated in language comprehension, along with the right inferior frontal area being involved in fluency and prosody (Kolb and Whishaw, 1996). However, these lesions studies have been limited with respect to the interpretations that can be made. The limitations arise largely from the lack of anatomical precision, non-reproducibility, and the difficulty associated with attributing the cognitive deficits to either lesion area or the disconnection of undamaged regions (cf. Price, 2000). Accordingly, it is essential that the language models developed primarily on the basis of aphasiology be revised and enhanced using contemporary imaging measures (Démonet and Thierry, 2001).

Cognitive processes in speech and reading

Investigations of language must contend with the fact it is not a unitary phenomenon (D'Arcy, 1996). Instead, the cognitive processes that support language are dependent on the stimulus input and sensory modality. For instance, speech comprehension is temporally constrained by the sequential nature of the input (D'Arcy, Connolly, and Crocker, 2000). According to Marslen-Wilson (1984), in order to process speech, acoustic-phonetic information must be linked to a number of potential phonological word representations within the mental lexicon. Differences in relative

activation levels allow for the selection of a particular lexical item from the different candidates, a process which is temporally dependent on the incoming speech input. These activated lexical word representations must then be integrated into their semantic, syntactic, and grammatical context in order to derive meaningful information. The activated processes in reading contrast with those of speech perception. During reading, visual-perceptual analysis is necessary for word recognition. In order to process written words, the comprehension process is reliant on a complex interaction between orthographic analysis, phonological analysis, working memory (WM), semantic analysis, syntactic analysis, and morphological analysis (Caplan and Hildebrandt, 1988; Van Orden, Pennington, and Stone, 1990). Also, reading comprehension is not temporally constrained in the same manner as speech input, with many of the processes commencing shortly after the visual information reaches the cortex.

A traditional manipulation used in cognitive studies of language is semantic priming. In broad terms, the semantic priming effect refers to the observation that during the presentation of word pairs, processing of the second word is faster and more accurate if it is semantically related (Meyer and Schvaneveldt, 1971). Neely (1991) reviewed the different mechanisms that are thought to account for semantic priming. These mechanisms include automatic spreading of activation, whereby activation of the prime node spreads to the nodes of other semantically related targets. There is also expectancy-based priming, in which the prime generates an 'expectancy set' of semantically related target items. Finally, it has been proposed that post-lexical priming mechanisms exist. Post-lexical mechanisms could influence the selection of a target after it has been entered

into a lexical set, utilize information from both the prime and the target in order to access memory, or exert their influences during the output stage (e.g., response processing). Most research on these mechanisms has focused on single-word semantic priming paradigms, and it is likely that all three mechanisms contribute (to varying degrees) to semantic priming in sentence comprehension. The critical issue involves the fact that knowledge of semantic priming has provided a fundamental tool to be used in tightly controlled experiments in order to study the complex processes that support language (Neely, 1991).

One of the ways that semantic knowledge can be primed is through the utilization of hierarchical structure in semantic memory. Cognitive studies have demonstrated that superordinate and subordinate categories exist with these semantic hierarchies (Kintsch, 1977; Loftus, Freedman, and Loftus, 1970; Waters, 1978). The basic findings have shown that recall performance for members of a superordinate category is greater than that for a subordinate proposition (Waters, 1978). Although Loftus et al. (1970) found that reaction times did not vary as a function of category membership. The important point of this work concerns the fact that it established an organized taxonomy in semantic memory, with retrieval of superordinate categories being more probable than that of subordinate words. Any chronometric differences in mental processing that may contribute to the superordinate-subordinate relationship remain to be explored.

Neuroimaging: ERPs and fMRI

Among the various non-invasive imaging techniques, high-resolution event-related brain potentials (ERPs) and functional magnetic resonance (fMRI) represent two

of the predominate measures used for spatiotemporal investigations of information processing. It has also become increasingly evident that no single technique is sufficient; instead it is essential to adopt a multimodal imaging approach (Démonet and Thierry, 2001; McCarthy, 1999). The primary rationale for this approach stems from the inherent strengths and weaknesses of electromagnetic measures (e.g., ERPs and magnetoencephalography, MEG) and hemodynamic measures (e.g., fMRI and positron emission tomography, PET). Many of the technical issues concerning differences in the techniques are discussed in greater detail in the chapters that follow. This section provides a basic overview of ERPs and fMRI.

An ERP is an electrical change that is recorded from the scalp in association with stimulus processing in the brain. It may be 'evoked' by an external stimulus (sensory) or 'emitted' as a result of subsequent information processing (cognitive). The major advantage of these recordings is the on-line recording of stimulus processing in time. The nomenclature for ERPs is typically based on the polarity and latency of the peak or component in question. For instance, a negative going peak that occurs in the 100 ms range may be referred to as a N100. However, the latencies tend to vary somewhat within and between individuals depending on the recording circumstances, so these terms commonly refer to the prototypical situation (cf. Picton, Lins, and Scherg, 1995).

ERPs are derived from electroencephalographic (EEG) recordings. The neural activity recorded by EEG stems from various intracranial neuronal generators distributed throughout the brain. The major limitation of scalp electromagnetic recordings is the uncertainty with respect to the location of sources (Knight, 1997). The sources result

primarily from post-synaptic potentials (excitatory and inhibitory) in an open-field configuration (extracellular fields sum and can be recorded at a distance). Neurons in open-field geometry include primarily pyramidal cells in the laminar structure of the cortex or hippocampus (Hämäläinen, Hari, Ilmoniemi, Knuutila, and Lounasmaa 1993; Knight, 1997; Picton et al., 1995). The distance of these active sources determines the strength of the signal recorded at the scalp (near or far field), with dipolar synaptic current flow, which decrease in signal strength more slowly than quadrupolar axonal current flow, being the primary source[1]. In order to extract the ERP signals buried in ongoing EEG, the time-locked activity must be averaged over multiple trials. Because the background EEG is random with respect to the stimulus onset, it averages to zero (or near zero). The signal-to-noise ratio (SNR) provides a measure of the ability to identify the ERP signal in background noise (the SNR is proportional to the square root of the number of stimulus repetitions). Typically, cortical ERPs (near field) are acquired with trial numbers on the order of 20 to 40, whereas a brainstem auditory evoked potential (BAEP; far field) requires more than 1000 trials (Knight, 1997).

In fMRI, magnetic signals are detected through changes in blood flow in order to localize active brain areas. Neural activity affects the degree to which a region is saturated with oxygen. Deoxyhemoglobin acts as a paramagnetic contrast agent that alters magnetic

---

[1] If r is equal to the distance from the source, dipolar current flow decrease as $1/r^2$ and quadrupolar current flow decreases as $1/r^3$ (Hämäläinen et al., 1993). Given their short duration and restricted spatial extent, action potentials are an unlikely source of the extracranial signals recorded by EEG.

susceptibility. Local activation leads to an increase in blood flow, which changes the oxy-/deoxyhemoglobin ratio, which in turn alters the magnetic susceptibility in the local area. These magnetic fluctuations give rise to blood-oxygen level-dependent (BOLD) contrast imaging. Similar to ERPs, BOLD effects can be induced by the presentation of an external stimulus or arise from ensuing higher-level processes.

The primary advantage of fMRI is its superior spatial resolution (< 1mm). For instance, a number of studies have demonstrated that it is possible to image activity in ocular dominance columns (e.g., Menon and Goodyear, 1999) as well as the various layers in the lamina of the cortex (e.g., Kim, Duong, and Kim, 2000). While this represents currently the highest resolution for non-invasive techniques (there are ~10^5 pyramidal cells in 1mm^2 of cortex; Hämäläinen et al., 1993), the majority of studies, particularly cognitive studies, use lower spatial resolutions (~ 5mm) in order to scan the whole brain. The primary limitation of fMRI is its temporal resolution, which by definition is restricted to the time constants of hemodynamics (~ secs). However, image acquisition capabilities have improved (well within the ms range) and recent investigations have demonstrated that it is possible to gain valuable chronometric information, primarily through the use of more sophisticated experimental designs (Menon and Kim, 1999; Thierry, Boulanouar, Kherif, Ranjeva, and Démonet, 1999).

Thesis objectives

This research was directed at understanding the neuroanatomical architecture that supports cognitive processes that are fundamental to language. The cognitive processes of particular interest included phonological processing, semantic analysis, and verbal WM.

With respect to neuroimaging, the spatiotemporal nature of these cognitive processes was investigated using both ERPs and fMRI. The various experiments shared a central focus on neural correlates of semantic comprehension, as they exist across sensory modalities and measurement techniques. In the second chapter, cortical potentials that reflect phonological and semantic processing in speech were investigated using ERPs. It was predicted that distinct neural generators could be identified for phonological and semantic analysis. Preliminary evidence for verbal WM involvement was also expected. In the third chapter, the effects of increased WM load on semantic processing were studied. The principle aim was to determine whether increased WM load would affect the timing of semantic neural systems during reading. If these effects were present, then the question was whether they could be imaged by virtue of the activation of intracranial generators? Following two independent demonstrations of semantic neural sources in speech and reading, the goal of the fourth chapter was to determine whether or not the electromagnetic activity that was linked to semantic processing was sufficient to invoke hemodynamic correlates that could be localized using fMRI. Provided that the BOLD responses were sensitive to similar experimental manipulations, these finding could provide the neuroanatomical backdrop for the semantic neural response. In the fifth chapter, the various findings are integrated and the central issues raised by this work are discussed in greater detail.

Chapter Two

Phonology and semantics in a visual-auditory word priming task:

A high-resolution event-related brain potential study

Chapter Two - Summary

Electrophysiological correlates of phonological and semantic analysis were studied using high-resolution event-related brain potentials (ERPs). The first objective was to demonstrate the efficacy of a novel speech perception task in eliciting these potentials. The second and third objectives were to evaluate the effects of lexical candidate activation and to examine the spatiotemporal characteristics of the potentials, respectively. In the task, participants were presented first with a visual sentence to study (e.g., The man is in the classroom). They were instructed to anticipate the superordinate terminal word (e.g., school), operationally defined as any word that describes a location higher in the semantic hierarchy than the prime word. Following the prime, a digitized spoken sentence was presented that ended with either a congruent or an incongruent terminal word (e.g., The man is in the... school/barn). The incongruent terminal words mismatched expectation in terms of both the initial phonological (unexpected sounds) and semantic content (unexpected meaning). The unexpected words elicited the phonological mismatch negativity (PMN) and N400 responses. The sentence stimuli were divided on the basis of number of possible congruent alternatives, providing two levels of lexical candidate activation (i.e., high and low). Interestingly, a small PMN but no N400 was observed to congruent words in the high lexical candidate condition, supporting the role of phonological processing in lexical access. Brain mapping and source analysis techniques demonstrated that the PMN and N400 represented *distinct* neural processes, localized to *different* cortical regions. The findings provide temporally resolved evidence for the inter-relationship between phonological and semantic neural systems during the formulation and evaluation of lexical candidate lists in speech perception.

Chapter Two - Introduction

The functional neuroanatomy of language is being established largely through behavioural studies of healthy and brain-damaged individuals as well as recent advances in non-invasive brain imaging techniques (Caplan, Carr, Gould, and Martin, 1999; Démonet and Thierry, 2001; Goodglass, 1993). With respect to the latter, brain imaging studies are providing critical information about the temporal and spatial characteristics of the neural architecture that supports language. Event-related brain potentials (ERPs) and magnetoencephaolography (MEG) have become two of the prominent electromagnetic techniques used to provide an on-line record of the neurocognitive processes.

I. Event-related brain potentials

Similar to evoked potentials (Chiappa, 1997), ERPs are derived from an electroencephalogram (EEG) and provide a highly resolved temporal record of the brain's reception of and response to stimuli (Knight, 1997). While the main strength of ERPs stems from the fact that they can be used to dissect the time course of cognitive processes, it is also possible to obtain valuable spatial information about the particular processes being studied (Picton, Lins, and Scherg, 1995; Scherg and Picton, 1991). The spatial information (which is better resolved by high-density arrays of electrodes) can include detailed topographical maps (i.e., brain mapping) of the scalp-recorded activity and estimates of the relevant intracranial dipoles (i.e., source analysis). The source of the activity is thought to arise from summed excitatory and inhibitory post-synaptic potentials (EPSPs and IPSPs) at the soma and dendrites of active neurons. Specifically, the electromagnetic potentials that are recorded by EEG at the scalp stem from oriented, synchronous activity (i.e., open fields), predominately arising from pyramidal cells within

the lamina of the cerebral cortex. Pyramidal neurons are relatively large cells and tend to be oriented perpendicular to the cortical surface. Because these neurons guide the flow of current, the current flowing in the dendrites tends also to be perpendicular to the cortical surface (Hämäläinen, Hari, Ilmoniemi, Knuutila, and Lounasmaa, 1993; Nunez, 1981; Picton, Lins, and Scherg, 1995).

II. The N400 response

A number of ERP studies have investigated reading and speech perception in language, with many focusing on the well-known N400 response (Kutas and Van Petten, 1994; Kutas, 1997; Segalowitz and Chevalier, 1998). The N400 was initially demonstrated to occur to the onset of semantically incongruent terminal words in contextually constrained sentences (Kutas and Hillyard, 1980). It is a late negative-going waveform, which peaks at approximately 400 ms post-stimulus, and is typically associated with a centro-parietal scalp topography. Although the N400 was originally observed following the presentation of visual sentence stimuli (in a rapid-serial-visual-presentation format), it has since been obtained in a variety of language-related tasks that use different forms of stimuli (e.g., text, speech, and pictures).

In the auditory modality, the N400 has been elicited to digitized speech stimuli that, similar to their visual counterparts, contained incongruent terminal words (Connolly and Phillips, 1994; Connolly, Stewart, and Phillips 1990; Connolly, Phillips, Stewart, and Brake, 1992; Holcomb and Neville, 1990). It has also been shown in cross-modal paradigms, supporting the existence of an amodal semantic-conceptual system (Connolly, Byrne, and Dywan, 1995a; Ganis, Kutas, and Sereno, 1996; Nigam, Hoffman, and Simons, 1992). Further, the N400 has been obtained in tasks that involve semantically

related word pairs (Bentin, McCarthy, and Wood, 1985; Brown and Hagoort, 1993). It has also shown promise in shedding light on semantic deficits secondary to diseases such as Alzeimer's Disease (Schwartz, Kutas, Butters, Paulsen, and Salmon, 1996) and neurotrauma such as stroke (D'Arcy et al., 2002).

III. The PMN response

Phonological analysis has been linked to a component that precedes the N400 during speech comprehension only (Connolly, Phillips, and Forbes, 1995b). In the early studies, it was proposed that a negative-going response, termed the phonological mismatch negativity (PMN), might have reflected the acoustic-phonetic process in the phonological stage of word processing (Connolly et al., 1990; Connolly et al., 1992). Connolly and Phillips (1994) subsequently used contextually constrained spoken sentences to determine whether the PMN varied independently from the N400.

In order to demonstrate that the PMN was linked to phonological analysis and was independent from the N400, Connolly and Phillips (1994) manipulated both the phonological and semantic features of the terminal words and recorded ERPs to the onset of these words. The study included four experimental conditions. In the *probable* condition, the highest Cloze probability ending was used (Bloom and Fischler, 1980). Thus, the terminal word had an expected initial phoneme and was semantically congruent (e.g., The piano was out of... tune). In the *phonological* condition, the terminal word had an expected initial phoneme, but was semantically incongruent (e.g., The gambler had a streak of bad... luggage/luck). In the *rare* condition, a low Cloze probability word was used that had an unexpected initial phoneme, but was nonetheless semantically congruent (e.g., The pigs wallowed in the... pen/mud). The *anomalous* condition was characterized

by an unexpected initial phoneme and was semantically incongruent (e.g., Joan fed her baby some warm... nose/milk). The results showed that the PMN could be double dissociated from the N400. That is, the PMN occurred in both the anomalous and rare conditions (which contained unexpected initial phonemes), but was reduced in the probable and phonological conditions. In contrast, the N400 was elicited in both the anomalous and phonological conditions (which were semantically incongruent), but not the probable and rare conditions. The authors concluded that the PMN (which peaked between 270 ms to 300 ms) was independent of the N400 and reflected phonological processing during spoken word recognition.

The PMN has since been replicated by our group (Connolly et al., 1995a; Connolly, Service, D'Arcy, Kujala, and Alho, 2001) and others (Dehaene-Lambertz, Dupoux, and Gout, 2000; Hagoort and Brown, 2000; Praamstra and Stegeman, 1993; van Den Brink, Brown, and Hagoort, 2000). It has also been used to evaluate language functions for patients with neurological disease (Connolly et al., 1995a; Revonsuo, Portin, Juottonen, and Rinne, 1998). Connolly et al. (2001) reported the use of high-resolution ERPs to identify the spatiotemporal characteristics of the PMN using a priming paradigm that involved a phonological auditory image/word-matching task. Subjects studied a visual word/non-word followed by a brief presentation of a prime letter (e.g., House, M). They were instructed to anticipate the word/non-word formed by substituting the visual word's initial letter with the prime letter. Subsequently, the subjects heard an auditory target word/non-word that either matched or mismatched their expectations (e.g., Mouse/Table). ERPs were recorded to the onset of the auditory words/non-words and the results showed that incongruities elicited a significant PMN. Importantly, there

was no difference between the PMN in the word and non-word conditions, supporting the role of phonological processing independent of the contextual influence derived from top-down lexical selection processes. The scalp topography of the PMN was characterized by a frontal, right asymmetrical distribution. Further analysis, using spatial de-blurring (with current source density maps), suggesting that the distribution resulted, in part, from an active left anterior generator. The authors concluded that the PMN represented a phonological marker essential to speech processing and stressed the importance of future work directed at localizing the PMN and N400 sources and characterizing their respective contributions to speech processing.

IV. Objectives and hypotheses

There were three main objectives in the current study: 1) to investigate the PMN and N400 using a novel visual-auditory sentence matching paradigm; 2) to determine whether the number of active lexical candidates affected the PMN or the N400; and 3) to localize the PMN and N400 generators. These objectives are addressed in more detail below.

Objective 1: The task used in this study differed from those used in prior experiments. Prior work has employed contextually constrained sentences in which the ending was predictable (i.e., creating a semantic expectation). In the present experiment, the goal was to present the contextual information using a prime sentence in order to create semantic expectation. The task isolated contextual information within the initial sentence of a sentence pair. The sentence pairs used semantic hierarchical relationships (Loftus, Freedman, and Loftus, 1970) that required participants to form expectations (phonological and semantic) and maintain those expectations in memory for subsequent

evaluation. In contrast to previous studies in which half of the contextually constrained sentences had incongruent endings (i.e., they were not sensible), the target sentences in this experiment could only have been judged as incongruent in relation to the preceding prime sentence. In isolation, all of the target sentences made sense, it was only with reference to the prime sentence that the endings were incongruent. Thus, evaluation was conducted on the basis of knowledge maintained within semantic memory. It is noteworthy that the structure of this paradigm is well suited to delineating some of the critical factors that may interact with components like the PMN and N400 (e.g., working memory and contextual information). However, this information would only be amenable to investigation if the stimuli successfully elicited large, robust PMN and N400 responses (Hypothesis 1).

Objective 2: During the design of this task, it was possible to divide the stimuli on the basis of the number of active lexical candidates. The superordinate terminal words were selected on the basis of normative data (i.e., individuals were surveyed in order to select the candidate words). As expected, the calculated probability values for these words varied based on the number of possible alternatives for each item. For example, 'cockpit' has fewer superordinate alternatives (like airplane or helicopter) than 'closet' (like house, school, office, apartment, store, et cetera). Therefore, a split-half procedure (high and low) was used to test whether the number of active lexical candidates would selectively influence either the PMN or N400 amplitudes. It is important to note that this experimental condition differed from previous work using high and low Cloze probability words. Cloze probability is calculated on the basis of the percentage of subjects using a word to complete a particular sentence (Bloom and Fischler, 1980). The low Cloze words

used by Connolly and Phillips (1994) were alternative endings with lower probability values. In contrast, the split-half process used in this study involved selecting all the words with the highest exemplar-category probability values (which were calculated in the same manner as Cloze probability) and dividing them based on the degree of consensus. This procedure made it possible to predict that effects of high and low lexical candidate activation would be evident in the ERPs (Hypothesis 2).

Objective 3: Spatial information about the PMN and N400 is critically important to understanding the neural basis of these responses. The present investigation represents the initial attempt to localize PMN dipoles. Moreover, while there has been some work examining N400 dipoles, the majority of studies have localized the visual N400 (e.g., Helenius, Samelin, Service, and Connolly, 1998). The location of auditory N400 dipoles (and their relationship to the corresponding visual dipoles) remains to be determined. Accordingly, high-resolution ERPs (128 channels) were used to replicate prior PMN mapping results (Connolly et al., 2001) and determine whether the PMN and N400 generators are localized to *distinct* cortical regions, with *different* time courses of activation. In addition, because the current task also involved working memory (WM) processes and there has been speculation recently about the involvement of WM in the PMN (Connolly et al., 2001), it was predicted that the spatial analysis would uncover phonological, semantic, *and* WM activation (Hypothesis 3).

Chapter Two - Methods

I. Participants

Ten English-speaking participants (6 females and 4 males) volunteered for a study on language. Their mean age was 26 years ($SD = 4.6$) and their mean level of education was 16.8 years ($SD = 2.4$). All were given the Edinburgh Handedness Inventory (Oldfield, 1971) and were dextral (LQ range = 54.5 to 100). The participants had normal or corrected-to-normal vision and were screened with a self-report measure for a history for audiological, psychiatric, and/or neurological problems. Informed consent was obtained and all participants were told that the study duration was approximately three hours. Upon completion of the experiment, all participants were debriefed fully and any questions were answered. This study had ethical committee approval.

II. Experimental Paradigm

The paradigm was designed to investigate ERP responses to the phonological (PMN) and semantic (N400) features of spoken words. It involved a cross-modal priming task using sentence pairs. For each sentence pair, the first sentence (prime sentence) was presented visually and primed a superordinate word. The superordinate word was to be anticipated as the terminal word in the second sentence (target sentence), which was presented in the auditory modality. For example, the visual prime sentence "The man is teaching in the classroom" was followed by the auditory target sentence "The man is in the... school." Each prime sentence contained a subject (man, woman, boy, or girl), a verb, and a prepositional phrase expressing a location. All visual prime sentences were constructed to establish an expectancy, to be evaluated subsequently within the context of the target sentences. All auditory target sentences contained a brief, natural pause prior to

the terminal word onset (i.e., normal prosody). Both the phonological and semantic features of the terminal words in the target sentences were manipulated to match or mismatch expectation.

In order to determine the congruent terminal words used to complete the target sentences, the exemplar-subordinate probability for the terminal words in each sentence pair was calculated (cf. Bloom and Fischler, 1980). One hundred sentence pairs were constructed and given as a normative survey to 58 individuals. All individuals (43 females and 15 males) were fluent in English, the mean age was 26.1 years (SD = 8.5), and the mean level of education was 16.7 years (SD = 3.1). The exemplar-subordinate probability was calculated on the basis of the most frequent terminal words used to complete the target sentence. Only answers that sensibly completed the sentence were accepted. If the percentage of unacceptable responses was greater than 33% for any given sentence pair, then the item was not included (there were only four sentence pairs rejected).

On the basis of the exemplar-subordinate probabilities for remaining 96 sentence pairs (calculated for all responses), the stimuli were divided into two groups (High and Low). Sentence pairs with exemplar-subordinate probabilities above/below .655 were labeled as High/Low, respectively. For the High group (48 sentences), the mean probability was .869 (SD = .099) and for the Low group (48 sentences), the mean probability was .546 (SD = .133) (calculated for acceptable responses only). Half of the sentence pairs in the High and Low groups were assigned randomly to either the Congruent or Incongruent conditions. In the Congruent condition, the terminal word was selected on the basis of the normative data. In the Incongruent condition, semantically

unrelated alternate terminal words with initial phonemes that did not match any of the normative responses were selected from the normative data to replace the original words. These words were selected from the normative responses in order to control for word frequency effects. The probabilities and word lengths were also evaluated and no difference was found between the experimental conditions.

There were four experimental conditions. The High Congruent condition contained 24 sentence pairs with high probability congruent terminal words in the second sentence (e.g., The boy is swimming in the shallow end. "The boy is in the... pool."). The Low Congruent condition contained 24 sentence pairs with low probability congruent words (e.g., The woman is swimming in the sunken ship. "The woman is in the... ocean."). The High Incongruent condition contained 24 sentence pairs with high probability incongruent terminal words (e.g., The girl is sitting in the cockpit. "The girl is in the... church."). The Low Incongruent condition contained 24 sentence pairs with low probability incongruent words (e.g., The man is entering through the swinging doors. "The man is in the... marsh."). A full list of the stimuli used in the experiment is provided in Appendix 1.

The prime sentences were presented visually on a 14-inch computer screen in yellow letters on a black background (36-font size). The mean width of the sentence stimuli was 20.15 cm ($SD = 1.87$) and the mean height was 3.08 cm ($SD = 0.51$). The sentence stimuli subtended a visual angle of approximately 1.76 degrees. The target sentences were presented in the auditory modality and were recorded using a female voice with the NeuroScan Incorporated™ stimulus software package (i.e., natural speech). The sentences were recorded at 100 dB within a fixed 3 s sample duration. The speech

was sampled digitally at 20,000 Hz with the low pass filter at 10,000 Hz (low pass slope = 24 dB/octave). The stimulus onset was defined as the beginning of the terminal words in the target sentences, and was marked by a stimulus trigger that was manually positioned at the onset of the sound spectrum for each word. ERPs were recorded from the beginning of the stimulus trigger.

III. Procedures

The experiment began with a practice phase, comprising the task instructions and three sample trials. Participants were given a description of the sentence pairs and instructed to anticipate the superordinate word for each target sentence. For an individual trial, the prime sentence was presented for 10 s on a computer screen. Immediately following the prime sentence, the target sentence was presented binaurally using audiometric quality insert earphones. Participants were instructed to indicate, with a button press, whether the terminal word matched or mismatched the superordinate word that they had anticipated. They were told to respond as accurately as possible and that the speed of their response was not important (i.e., the instructions emphasized accuracy only). Their response hand (left or right) was counterbalanced. The stimulus onset asynchrony (SOA) between the target sentences and the beginning of the next trial was 6 s, providing approximately a 3 s response window. The sentence pairs were presented in a fixed pseudo-random order ('pseudo' = no greater than three repetitions of the same condition). Due to the sensitivity of EEG recordings, participants were instructed to remain as still as possible. Furthermore, they were told to try to restrict their blinks to the 10 s period during the prime sentences and not to blink during the presentation of the auditory target sentences, particularly during or after the terminal words. While listening

to the target sentences, they were instructed to fixate on a cross-hatch positioned in the centre of the computer screen.

EEG activity was recorded using a 128-channel NeuroScan Synamps™ system with all electrodes referenced to an electrode on the nose (a common reference was derived for the spatial analyses, below). The electrodes were fitted within a NeuroScan Quik-Cap™ using an extension (American Electroencephalographic Society, 1991) of the International 10/20 System (Jasper, 1958). An electro-oculogram (EOG) recorded vertical and horizontal eye movements, as well as blinks. EOG activity was recorded by electrodes placed above, below, and on the outer canthi of both eyes. The ground electrode was at the AFz site. All electrodes were Ag/AgCl and impedances were maintained at or below 10 KΩ. The continuous EEG recordings were obtained with a bandpass of 0.05 to 30 Hz (digitally sampled at 500 Hz). The continuous recordings were then epoched off-line beginning –100 ms before the stimulus onset and ending 1000 ms after the stimulus onset (550 data points). Trials contaminated with EOG activity greater than ±75 μV (-100 ms to 750 ms) were excluded from the analysis. The mean percentage of trials rejected from the analysis was 8.0 (SD = 8.5). The remaining trials were averaged by experimental condition, taking behavioural performance into account (i.e., only trials in which the individual provided a correct response were included in the average). The mean percentage of correct responses was 98.9 (SD = 0.88), indicating that the participants' behavioural performance was near perfect. Averaging across the High and Low Incongruent conditions and subtracting the High Congruent condition derived the difference waveforms used for the analyses. The rationale for this subtraction procedure was based on the results of the standard waveform analysis (described below).

Grand average waveforms for the experimental conditions and the subtraction were derived from the averages of the individual waveforms.

In order to reduce the number of statistical comparisons across electrode sites, a linear derivation was used to compute waveforms for nine scalp regions. The regions were divided into left (L), midline (M), and right (R) sectors as well as frontal (F), central (C), and posterior (P) sectors (LF, MF, RF, LC, MC, RC, LP, MP, and RP). The waveform for each region was derived from ten electrode sites in the specified sector and electrode selection for each region was uniform across all participants (Figure 1). In all, the data were derived from 90 representative sites, excluding peripheral sites (which were susceptible to artifacts). These data were used in the statistical analyses and grand average waveforms were also recomputed (spatial analyses were not restricted to 90 sites, below). Two statistical analyses were conducted: one on the standard waveforms and the other on the difference waveforms. The analyses were done using a repeated measures analysis of variance (ANOVA) with conservative degrees of freedom (Greenhouse and Geisser, 1959). The analysis of the PMN and the N400 included Condition (4 levels), Time (4 levels), and Region (9 levels) as factors. Significant main effects and interactions were submitted to additional post-hoc analyses using the Tukey Honestly Significant Difference (HSD) test. An alpha level of $p < 0.05$ was required for statistical significance in all ANOVAs and post-hoc analyses.

The data from all channels were evaluated for subsequent topographical mapping and source analysis (Picton, Lins, and Scherg, 1995; Scherg and Picton, 1991). The channel labels and theta (azimuth angle with the z-axis) and phi (latitude angle with the

Figure 1 - Caption

The nine regions, comprising ten electrodes per region, were selected from the 128-channel montage. The regions are left frontal (LF, light green), midline frontal (MF, light red), right frontal (RF, dark blue), left central (LC, yellow), midline central (MC, orange), right central (RC, pink), left posterior (LP, light blue), midline posterior (MP, dark green), and right posterior (RP, dark red). Peripheral sites were excluded, as these sites were most susceptible to artifact contamination (e.g., cardiac interference).

Figure 1

Electrode Map and Regional Sectors

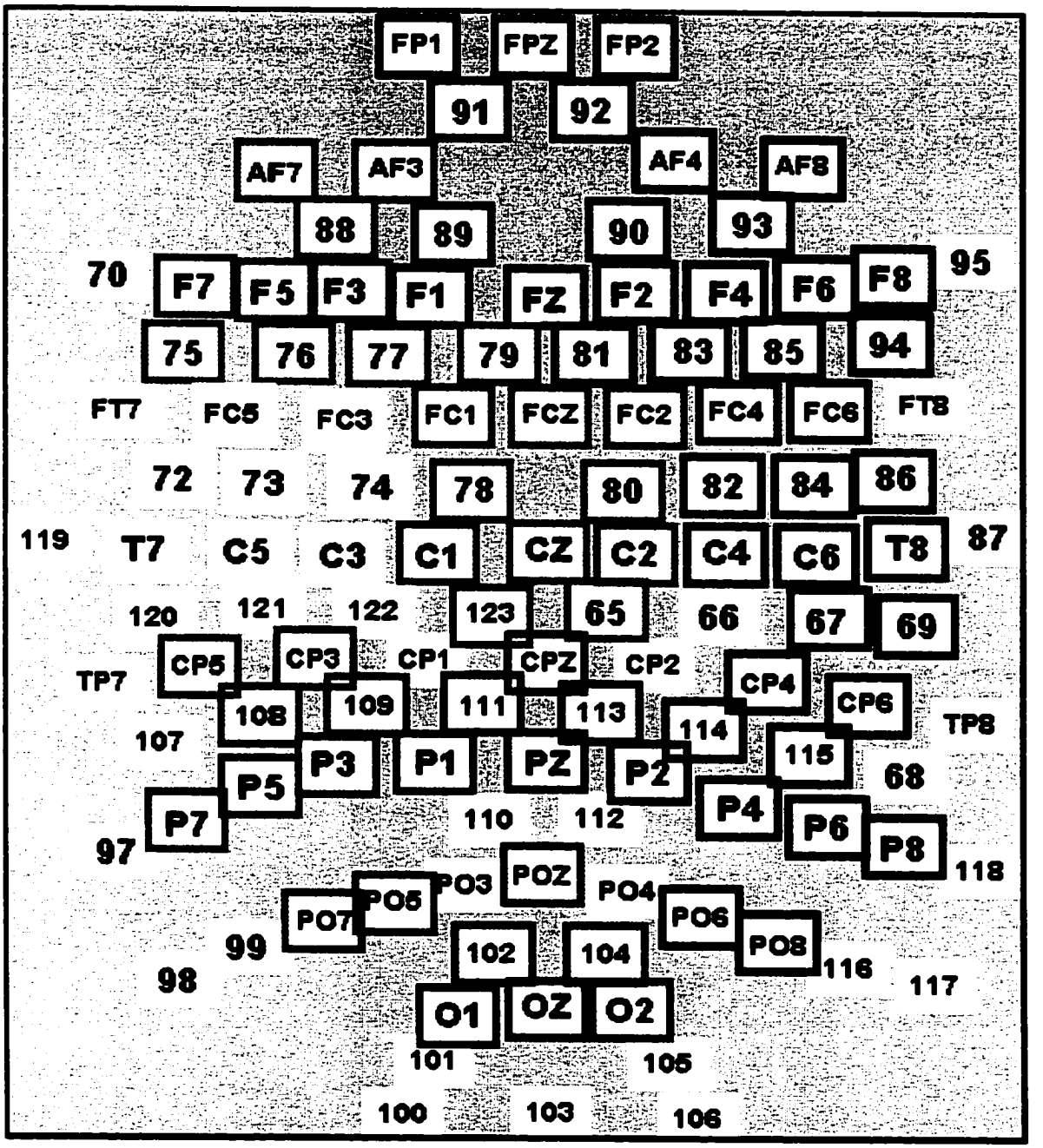

x-y plane) positional values were imported into BESA (Brain Electromagnetic Source Analysis, MEGIS version 3.0), with the additional electrode locations being determined on the basis of the 10/10 system electrode location landmarks. In order to minimize the ocular activity, a more conservative artifact rejection procedure (-100 ms to 1000 ms) was used. The mean percentage of trials rejected was 16.4 (SD = 16.1). The averaged data (artifacts rejected; 0 ms to 1000 ms) were re-filtered to optimize the signal for source analysis (10 Hz low pass). Difference waveforms were used to isolate the PMN and N400 activity (and their underlying sources)[2]. Visual inspection of the individual waveforms revealed that the PMN and N400 peaks were present in all ten waveforms. Artifact channels and electrodes contaminated with artifacts (e.g., electrodes over the ears) were excluded from the analysis.

Spherical spline and current source density (CSD) maps were derived using the grand average waveforms. The spherical spline maps show the distribution of the scalp potential using isocontour lines (with the zero contour line suppressed). The CSD maps use a spatial de-blurring technique (Laplacian) in order to compensate for the smearing of electrical activity due to inhomogeneities in volume conduction (e.g., skull).

Source analysis was conducted to model the dipoles for the PMN and the N400. Source analysis of ERP data is necessarily an approximation. Dipole modeling involves multiple iterations and is inherently time-consuming. Because of the intensive nature of the analysis, dipoles were localized using the grand average waveform (Scherg, Vajsar,

---

[2] While differences in source locations between standard and difference waveforms cannot be overlooked (cf. Démonet and Thierry, 2001), difference waveforms were selected in order to limit the number of dipoles in the source analysis. The additional PMN model provided a means of confirming these source locations through replication.

and Picton, 1989). The grand average models provided a global estimate of active regions across subjects. However, inter-individual variance undoubtedly exists and must always be considered (Haan, Streb, Bien, and Rösler, 2000). Therefore, the model was empirically validated using the individual waveforms in order to determine whether the fit was reliable. A description of the modeling procedure is provided below.

The analysis was conducted using a 4-shell spherical head model with conductivities estimated for the cerebrospinal fluid (1.0), skull (0.0042), and scalp (0.33). A principal component analysis (PCA) was used to estimate the number of sources and it was assumed that the decomposed source activities were not orthogonal (i.e., the PCA waveforms may represent more than one process). Using a regional source strategy (Scherg, Vajsar, and Picton, 1989), the analysis goal was to determine whether the PMN and N400 are generated by different sources, characterized by different activation time courses (or source waveforms). The modeling procedure comprised two steps: 1) formation of the initial model to identify the general areas of activity; and 2) development of the advanced model to fit the location and orientation of individual dipoles. Location and source waveforms were the primary parameters of interest. However, the orientation parameter was used in combination with a photographic atlas (DeArmond, Fusco, and Dewey, 1989) to obtain neuroanatomical estimates. Brodmann's areas (BAs) are reported in combination with anatomical descriptions. BAs were selected for integration with other neuroimaging studies and, because they are based on differences in cytoarchitectonic structure and connectivity, may also represent differences in function (Cabeza and Nyberg, 2000).

The validity of the model was evaluated primarily on the basis of goodness-of-fit/residual variance (RV) between the projected waveforms and the actual data (253 ms to 475 ms interval-of-interest), with RV = 10% (or > 90% of the variance) being specified *a priori* as an appropriate cut-off. Projected spline maps were also examined in order to verify that an overlap in topography also existed. Lastly, the dipole locations were evaluated on the basis of existing physiological and anatomical evidence.

Chapter Two - Results

I. Standard waveforms analysis

The objective of the standard waveform analysis was to determine whether there were differences in the waveforms during the PMN and N400 time intervals. Figure 2 shows grand average waveforms for all four experimental conditions at nine regions. The PMN was defined as the peak occurring in the 250 ms to 350 ms post-stimulus interval and the N400 was defined as the peak occurring in the 350 ms to 550 ms post-stimulus interval. Within the pre-determined PMN time interval, average amplitudes were calculated for successive 50 ms epochs. Within the pre-determined N400 time interval, average amplitudes were calculated for successive 100 ms epochs. The intervals for the N400 were larger because this component was characterized by broader peak morphology. A repeated measures ANOVA was conducted with Condition (High Congruent, Low Congruent, High Incongruent, and Low Incongruent), Time (250 ms to 300 ms, 300 ms to 350 ms, 350 ms to 450 ms, and 450 ms to 550 ms), and Region (LF, MF, RF, LC, MC, RC, LP, MP, and RP) as factors (Table 1).

The analysis yielded a significant main effect of Condition, $F(3,27) = 36.38$, $p < 0.0001$, $\varepsilon = 0.74$. Subsequent post hoc analyses revealed that the amplitudes in the High Incongruent condition ($\underline{M} = -1.35$ μV, $SE = 1.18$) and the Low Incongruent condition ($\underline{M} = -0.42$ μV, $SE = 1.01$) were different than those in both the High Congruent ($\underline{M} = 7.14$ μV, $SE = 1.15$) and Low Congruent ($\underline{M} = 3.68$ μV, $SE = 0.91$) conditions. The amplitudes in the Low Congruent condition were also different than the amplitudes in the High Congruent condition providing support for a PMN in the Low Congruent condition.

Figure 2 - Caption

Grand average ERPs (N = 10) to terminal words in the High Congruent (— — —), Low Congruent (- - - -), High Incongruent (————), and Low Incongruent (— - —) conditions for all nine regions. EOG sites (HEOG, LVEOG, and RVEOG) were artifact free (data not shown). A PMN (*) and a N400 (†) were elicited in the High and Low Incongruent conditions and a PMN was elicited in the Low Congruent condition. Time (ms) is on the x-axis and Voltage (μV) is on the y-axis (negative is up).

Figure 2

Grand Average Waveforms (N=10), Nine Regions

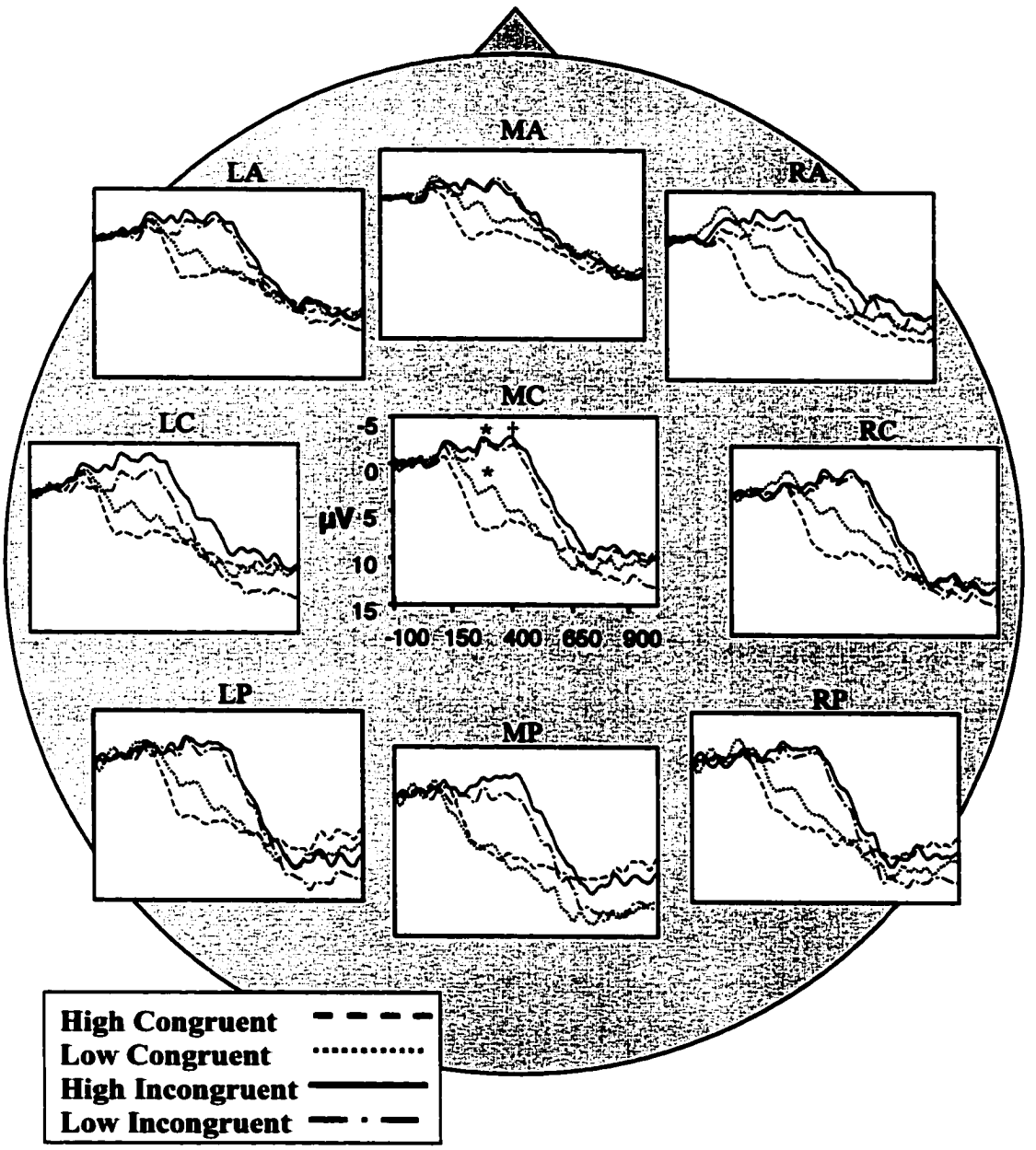

Table 1

Repeated Measures ANOVA for the PMN and N400

Analysis	Factor	*F*	df	*p* <
PMN and N400				
	Condition	36.38	3,27	0.0001
	Time	6.31	3,27	0.028
	Region	2.92	8,72	0.054
	C X T	4.86	9,81	0.001
	C X R	1.45	24,216	0.253
	T X R	4.24	24,216	0.006
	C X T X R	1.27	72,648	0.290

There was also a significant main effect of Time, $F(3,27) = 6.31$, $p < 0.05$, $\varepsilon = 0.37$. Post hoc analyses showed that the amplitudes at Time 4 (450 ms to 550 ms) were more positive than those in all preceding time intervals, likely reflecting the late positive-going response that is commonly observed upon sentence completion (Table 2). While the main effect of Region was not significant, the p value of 0.054 suggested that distribution effects might exist.

The data are best interpreted within the significant two-way Condition X Time interaction, $F(9,81) = 4.86$, $p < 0.005$, $\varepsilon = 0.57$. Post hoc analyses on this interaction demonstrated that the negative amplitudes in both Incongruent conditions were similarly enhanced, relative to the amplitudes in the High Congruent condition, across all time intervals (Table 3). Further, in the Incongruent conditions, the negative amplitudes were sustained across Times 1 to 3 (indicating the presence of both the PMN and N400) and were attenuated at Time 4. The negative amplitudes in the Low Incongruent condition were characterized by a more pronounced attenuation at Time 4. The negative amplitudes in the Low Congruent condition also differed from those in the High Congruent condition, there was a prominent peak at Times 1 and 2, with response attenuation at Times 3 and 4. While the peak was smaller than those in the Incongruent conditions, it nonetheless confirmed the existence of a PMN (and not a N400) in the Low Congruent condition (Fig. 2). The amplitudes in the High Congruent condition remained stable across Times 1 to 3 and became more positive at Time 4.

There was a significant two-way Time X Region interaction ($F(24,216) = 4.24$, $p < 0.01$, $\varepsilon = 0.17$) and post hoc analyses confirmed that there were more positive

Table 2

Mean Amplitudes (in μV) and Standard Error of the PMN and N400 responses for Time

Time Interval	Mean Amplitude	Standard Error
250-300	1.35	0.97
300-350	1.59	0.87
350-450	2.01	0.93
450-550	4.11	1.23

Table 3

Mean Amplitudes (in μV) and Standard Error of the PMN and N400 responses for Condition and Time

Condition Time Interval	Mean Amplitude	Standard Error
High Congruent		
250-300	6.94	1.25
300-350	6.95	1.16
350-450	6.98	1.20
450-550	7.71	1.39
Low Congruent		
250-300	2.36	0.96
300-350	2.37	0.90
350-450	4.23	1.12
450-550	5.75	1.11
High Incongruent		
250-300	-2.36	1.23
300-350	-1.87	1.05
350-450	-1.98	1.18
450-550	0.82	1.60

Table 3 continued...

Mean Amplitudes (in μV) and Standard Error of the PMN and N400 responses for Condition and Time

Condition	**Mean Amplitude**	**Standard Error**
Time Interval		
Low Incongruent		
250-300	-1.52	1.04
300-350	-1.10	0.99
350-450	-1.20	1.04
450-550	2.16	1.44

amplitudes in Time 4. Because this result reflected the positive-going response, it provides minimal information about the PMN and N400 distributions. The two-way Condition X Region interaction and the three-way Condition X Time X Region interaction were not significant. Given the preliminary indication of a Region main effect, difference waveforms were derived in order to characterize better the PMN and N400 topographies.

II. Difference waveforms analysis

The results of the standard waveforms analysis showed that there was a PMN in the Low Congruent condition, but not in the High Congruent condition. There were no major differences between the High Incongruent and Low Incongruent conditions (Fig. 2). Therefore, the two Incongruent conditions were averaged together and only the High Congruent condition was subtracted (i.e., Incongruent minus High Congruent). For each individual difference waveform, the maximal peak latencies for the PMN (within the 200 ms to 350 ms interval) and the N400 (within the 350 ms to 600 ms interval) were identified. The latencies for each peak were then averaged and an amplitude interval (50 ms, centered at the peak) was calculated for all individual difference waveforms. The purpose of this 'latency fitting' procedure was to focus the analysis specifically on the PMN and N400 peaks. Thus, the average amplitude values accounted for individual variation in PMN and N400 peak latencies. The average peak latency for the PMN and N400 was 287 ms (SD = 17.8) and 424 ms (SD = 61.5), respectively.

The objective of the difference waveform analysis was to determine whether there was a significant Region effect following compensation for peak latency variance. Figure 3 depicts the grand average difference waveforms for the nine regions. A repeated

Figure 3 - Caption

Grand average difference waveforms derived by subtracting the High Congruent condition from the Incongruent condition (i.e., High and Low combined). Nine regions show the broad central, right asymmetrical distribution of the PMN and N400. The PMN peaked at approximately 287 ms and the N400 peaked at approximately 424 ms. Because the difference waveforms isolated both components, they were used in the mapping and source analysis. All other details as for Fig. 2.

Figure 3

Grand Average Difference Waveforms (N=10), Nine Regions

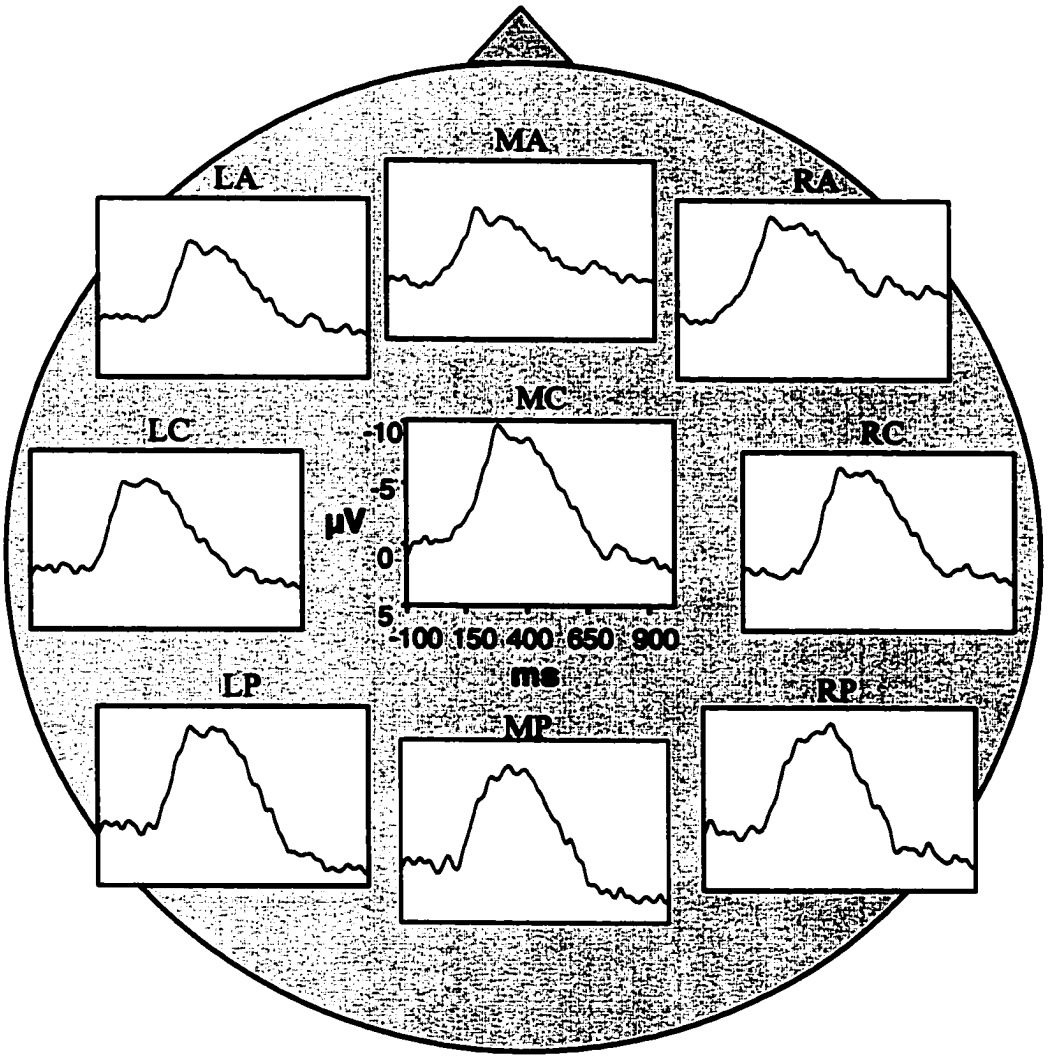

Table 4

Repeated Measures ANOVA for the PMN and N400 - Difference Waveforms

Analysis	Factor	*F*	df	*p* <
PMN and N400				
Difference waveforms				
	Time	0.04	1,9	0.842
	Region	2.92	8,72	0.044
	T X R	1.12	8,72	0.362

measures ANOVA was conducted with Time (PMN Interval and N400 Interval) and Region (LF, MF, RF, LC, MC, RC, LP, MP, and RP) as factors (Table 4). The main effect of Time was not significant ($F<1.0$). However, there was a significant main effect of Region ($F(8,72) = 2.92$, $p < 0.05$, $\varepsilon = 0.4$) and post hoc analyses revealed that, while broadly distributed, the PMN and N400 were largest at the MC and RC regions (Table 5). The two-way Time X Region interaction was not significant. Because there were no meaningful interactions involving the Region factor, the data were not submitted to additional normalization procedures (McCarthy and Wood, 1985).

III. Scalp distribution maps

Figure 4 presents the scalp distribution maps for the PMN and N400 (i.e., spline and current source density maps, see Methods section). On the basis of the prior difference waveforms analysis, the PMN time range was set to 212 ms to 333 ms (~ 30 ms intervals) and the N400 time range was set to 364 ms to 556 ms (~ 50 ms intervals)[3]. The spline maps (Fig. 4 a,c) show that the PMN and N400 were characterized by a broadly distributed central topography. However, slight differences between the two components existed. The PMN had a central peak distribution (see 273 ms map), while the N400 was characterized by a centro-parietal distribution (see 414 ms map). The CSD maps (Fig. 4 b,d) provide more detailed topographical information, with activation in multiple areas. The central, right asymmetrical distribution in the spline maps and the activation in left anterior region of the CSD maps replicated prior PMN mapping results (Connolly et al., 2001). While the maps provide valuable information about the general

[3] The minor variations in the time interval ranges selected resulted from importing the data into BESA (i.e., the sampling rate and corresponding number of time points were reduced to minimize the computational processing during source fitting iterations).

Table 5

Mean Amplitudes (in μV) and Standard Error of the PMN and N400 responses for Region

Region	Mean Amplitude	Standard Error
LF	-7.57	1.14
MF	-6.88	0.87
RF	-9.74	1.50
LC	-9.10	1.37
MC	-10.75	1.08
RC	-10.37	1.29
LP	-10.27	1.44
MP	-8.86	0.99
RP	-9.59	1.12

Figure 4 - Caption

Scalp distribution maps of the PMN and N400. The iso-contour lines are separated by 2 μV and grey regions represent negative activation. **A.** Spline maps for the PMN time range (212 ms to 333 ms) in ~ 30 ms intervals. The maps confirm that the PMN is broadly distributed over the central region. **B.** The CSD maps for the PMN time interval show a distributed activation pattern, with one of the prominent areas being in the left anterior region (see 273 ms map). **C.** Spline maps for the N400 time range (364 ms to 556 ms) in ~ 50 ms intervals. The N400 is also characterized by a central topography, but the activation extends into the parietal regions (see 414 ms map). **D.** The CSD maps for the N400 time interval reveal distributed activation (similar to the PMN), with close agreement between the active areas and source analysis (see Figs. 5 and 6).

Figure 4

Scalp distribution maps for the PMN and N400

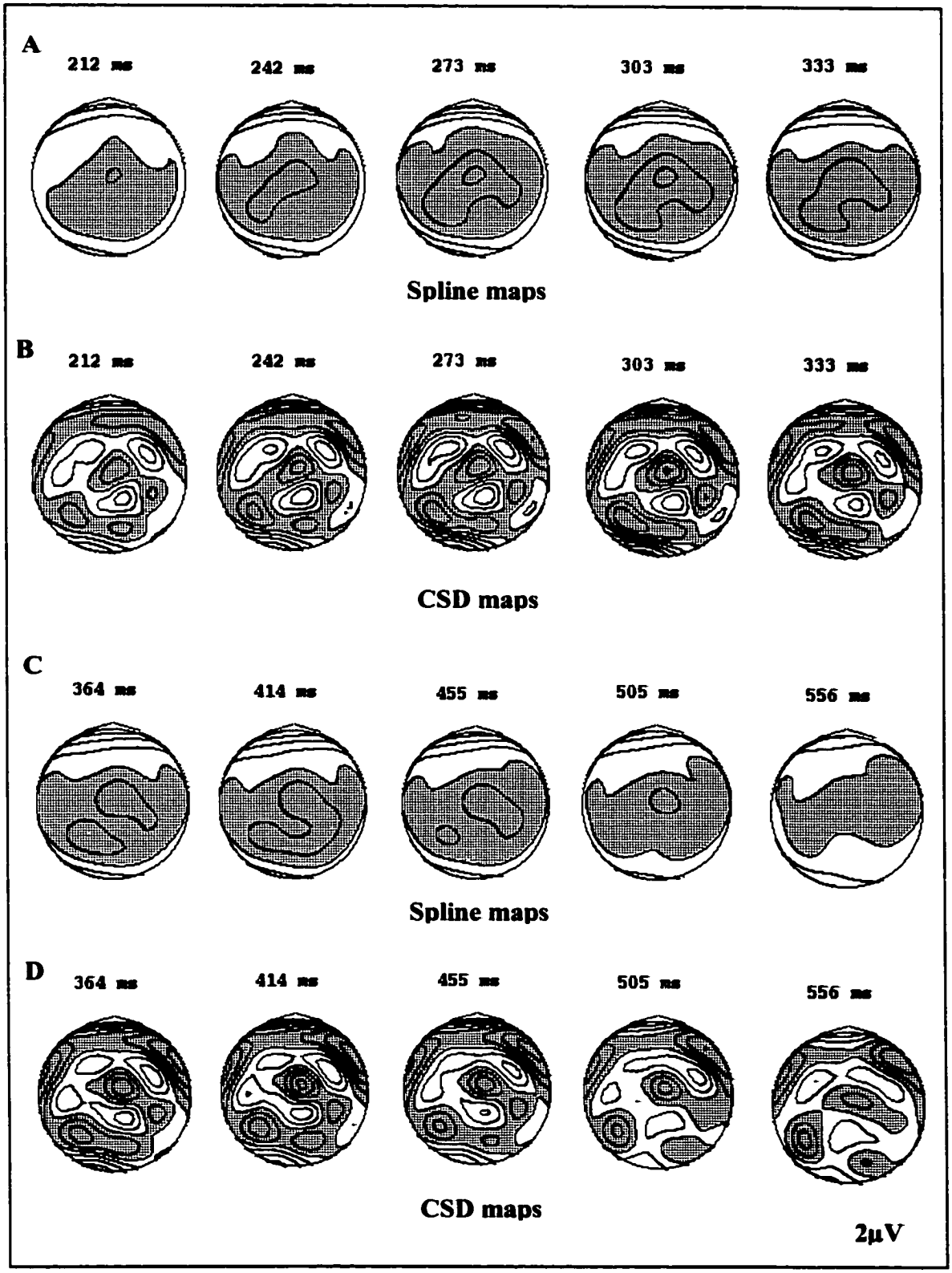

areas that are involved in generating the PMN and N400, it is necessary to model the equivalent current dipoles in order to identify neuroanatomical generators (Picton et al., 1995).

IV. Source analysis

A standard modeling process was used in the source analysis. A PCA (0 ms to 1000 ms) was done to estimate that a minimum of eight sources accounted for over 99% of the variance, but as these may have bilateral representations, the upper limit was set to 16. The initial model determined the general areas of activation using regional sources. A regional source is comprised of three dipoles in the same location, but oriented in orthogonal planes (i.e., orientation-independent). To localize the sources, the simplest possible assumptions were made, with levels of complexity being added only when necessary (Berg, Kakigi, Scherg, Dobel, and Zobel, 1999). Symmetry constraints were used for bilateral sources and solutions in which the dipoles interacted were avoided. That is, the Energy criterion was set at 20% to ensure that large amplitude in one dipole was not compensated by large amplitude in a second dipole, giving rise to a small potential on the scalp. In the advanced model, the regional source constraints were released and location and orientation parameters were fitted separately and together until stability was achieved. Additional constraints were used during the final fitting procedure because it was assumed that activation was concentrated in a particular time range (Variance 50%). The interval-of-interest for the PMN and N400 was 253 ms to 475 ms.

Initial model: Figure 5 depicts the localization of the regional sources and the spatial mapping comparisons for the PMN and N400. As one of the recommended procedures in BESA, a single source was localized to the midline region at the eyes to

Figure 5 - Caption

Brain electromagnetic source analysis (BESA) showing an initial model with regional sources used to localize active regions. **A.** Sagittal and axial views depicting dipoles associated with the speech perception, visual, and response-related task demands. Bilateral inferior frontal (BAs 44/45), bilateral posterior superior temporal (BA 22), and left polymodal (temporal-parietal-occipital) sources (BA 37) accounted for PMN and N400 activity. Sources in the ocular and occipital regions (BAs 17/18) accounted for activation associated with eye movements and visual fixation, respectively. The bilateral sources in the central sulcus region explained response-related activation. **B.** A comparison of the projected spline maps with the actual spline maps for PMN and N400 times. The projected maps derived from the initial model are remarkably similar to the actual scalp distribution for both the PMN and N400. **C.** The goodness-of-fit (solid line) and global field power (dashed line) for the full epoch (0 ms to 1000 ms). The residual variance was 9.59% for the 253 ms to 475 ms interval-of-interest.

Figure 5

PMN and N400 Active Regions

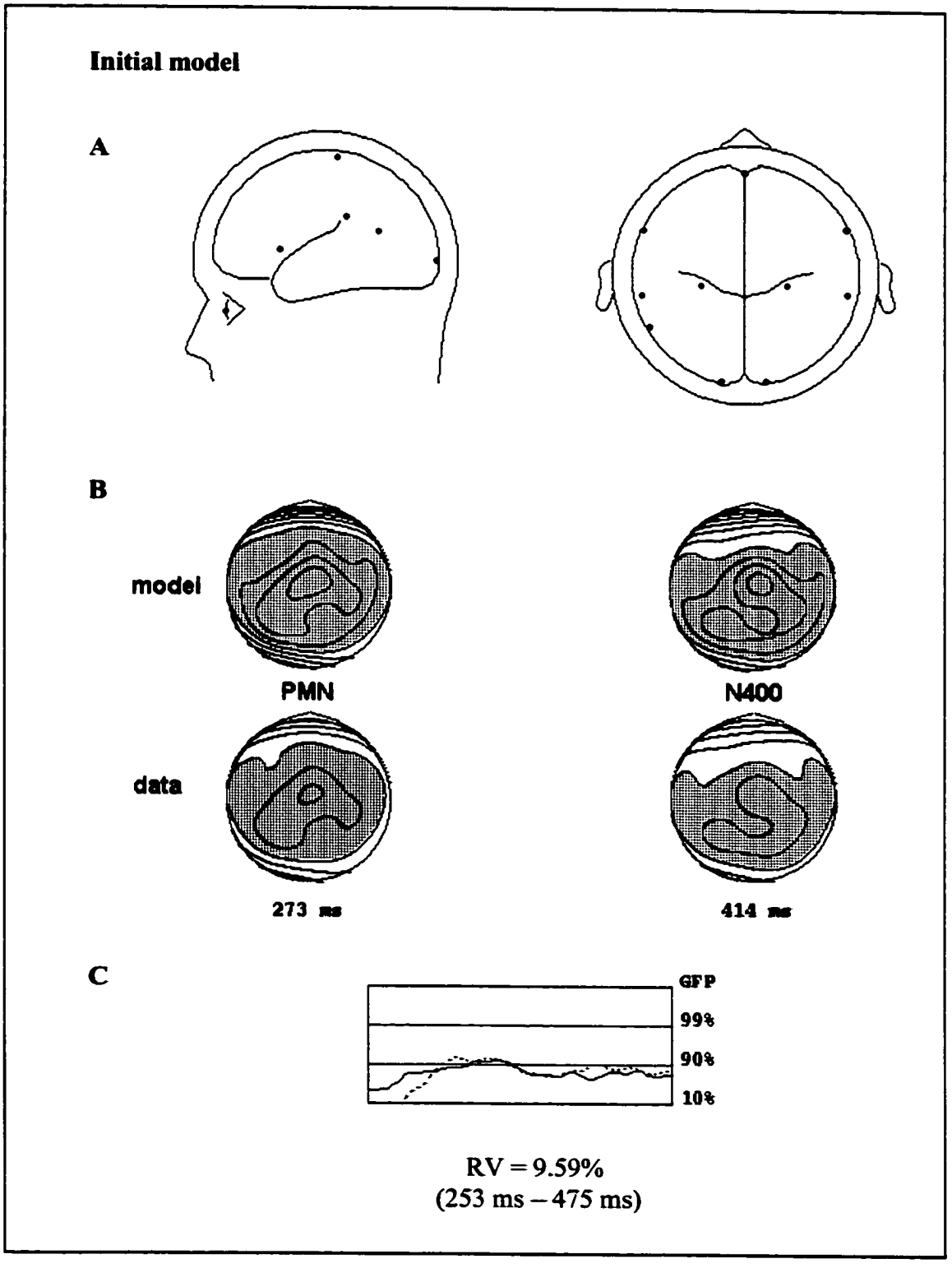

account for residual ocular activity. All additional sources were localized within the cortex and accounted for activation due to task-related requirements.

A number of possible PMN and N400 sources were identified (Fig. 5a). Bilateral symmetrical sources were localized to the posterior superior temporal gyri (pSTG, BA 22) bordering the parietal lobes, with the left source located in Wernicke's area. These were characterized by maximal activation in the N400 time range and a strong left hemisphere activation asymmetry. Also, two bilateral symmetrical sources were also localized to the inferior frontal regions (BAs 44/45) matching activation in the CSD maps. Again, there was a strong left hemisphere activation asymmetry, with the source in Broca's area peaking in the PMN time range. While the modeled dipoles provided a reasonable fit between the projected waveforms and the data, there was a small deflection in the PMN time range that suggested an additional source was required. An extra source modeled the time interval more accurately. The second source was localized to the left polymodal (temporal-parietal-occipital) region (BA 37), showing activity in both the PMN and N400 time ranges.

Two pairs of bilateral symmetric sources were associated with the visual and response-related task demands. Bilateral sources were localized to the occipital lobe (BAs 17/18) and accounted for posterior occipital activation in the CSD maps. The occipital sources likely resulted from visual cortex activation due to the visual fixation requirement. Because the participants were also required to make behavioural responses (counterbalanced left and right), bilateral sources were localized to the central sulcus region. The visual and response-related sources provided strong evidence for the physiological validity of the model (Fig. 5a).

The modeled spline maps were similar to the data spline maps, indicating that the localization of the sources provided a reasonable solution (Fig. 5b). As Figure 5c shows, the goodness-of-fit for the 253 to 475 ms interval-of-interest was above 90% (RV = 9.59%). Adding another test source evaluated the source model. The test source did not reduce notably the RV and the source waveforms depicted only noise. While neuroanatomical regions with *known* involvement in speech processing had been localized in the initial model, it was necessary to characterize better the sources (and corresponding source waveforms) in the left posterior temporal and inferior parietal areas. Accordingly, the regional source constraints were released and an advanced model was formed on the basis of individual dipoles.

Advanced model: Figure 6 depicts the advanced model. Releasing the regional source constraints and fitting the orientation and location parameters of individual dipoles derived the advanced model. The dipoles were fitted using the peak activation in the source waveforms. Sources with symmetrical constraints were fitted initially with the constraints maintained and then re-adjusted with the constraints released. The visual and response-related dipoles remained in the same location (BAs 17/18), with response-related dipoles being modeled bilaterally in the pre- and post- central gyri (BAs 3/4). Bilateral location constraints were maintained for the motor and sensory response-related dipoles in order to maximize the model's stability. The primary focus of the advanced model was on the PMN and N400 source, with source locations and source waveforms being the major parameters of interest.

The two bilateral sources remained localized to the pSTG, with a prominent left hemisphere asymmetry. The source waveform for the left N400 dipole in Wernicke's

Figure 6 - Caption

The final model in BESA using single dipoles (instead of regional sources) to characterize better the intracranial generators for the PMN and N400. **A.** Left sagittal, axial, and right sagittal views depicting the location of PMN, N400, and 'response-hand' dipoles. PMN dipoles were located in Broca's area (PMN_{S1}: BAs 44/45) and the homologous area of the right hemisphere. There was also a PMN dipole in the left inferior parietal lobe (PMN_{S2}: BAs 39/40). The N400 dipoles were located in the posterior superior temporal gyrus (pSTG, bilaterally), with activation predominating in the Wernicke's area ($N400_{S1}$: BA 22). A second N400 dipole was localized, anterior to $N400_{S1}$, in the left supratemporal plane (STP) of the superior temporal gyrus ($N400_{S2}$: BA 22). A third dipole was localized to the left polymodal (temporal-parietal-occipital) region ($N400_{S3}$: BA 37). Dipoles linked to 'response-hand' were localized to the primary motor and primary sensory hand/finger regions (BAs 3/4) in both hemispheres (not shown are the ocular and occipital sources). **B.** Source waveforms reflecting the contributions of dipoles to the scalp recorded activity. The PMN source waveforms (PMN_{S1} and PMN_{S2}) reveal a prominent peak at 283 ms (*) followed by sustained activation. Two N400 source waveforms ($N400_{S1}$ and $N400_{S2}$) show peak activation at 404 ms (†) and the remaining N400 source waveform ($N400_{S3}$) shows a similar peak and a slow wave in the later time range. **C.** The actual (solid line) and projected waveforms (dashed line) for a single electrode. The goodness-of-fit (solid line) and global field power (dashed line) for the full epoch (0 ms to 1000 ms). The residual variance was 7.82% for the 253 ms to 475 ms interval-of-interest.

Figure 6

PMN and N400 Source Locations and Waveforms

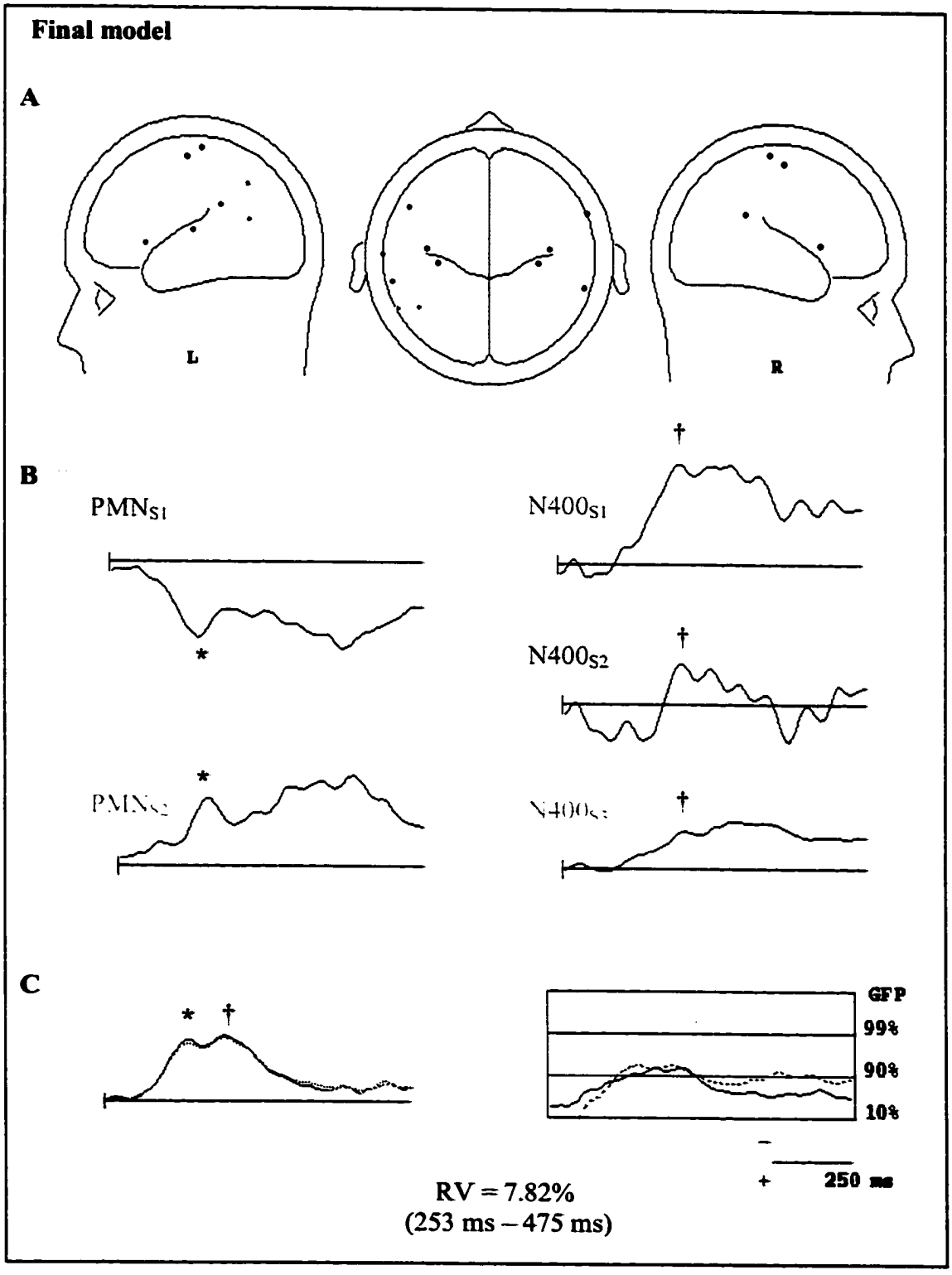

area ($N400_{S1}$: BA 22) was characterized by a peak activation at 404 ms, and the morphology was comparable to the recorded scalp N400. A second N400 dipole ($N400_{S2}$: BA 22) was localized to the left supratemporal plane (STP) of the superior temporal gyrus, anterior to $N400_{S1}$. The $N400_{S2}$ source waveform was remarkably similar to the $N400_{S1}$ source waveform, also peaking at 404 ms. A third N400 dipole was localized to the left polymodal (temporal-parietal-occipital) region ($N400_{S3}$: BA 37). While there was a similar peak in the $N400_{S3}$ source waveform, it was also characterized by a slow wave in the later time range (possibly a secondary generator). The peaks in the N400 source waveforms occurred ~ 20 ms earlier than the peak in the corresponding scalp recorded N400. However, small differences between the scalp waveforms and the source waveforms were expected *a priori* (Scherg and Picton, 1991).

Two bilateral anterior sources remained in the inferior frontal regions (Fig. 6a). There was a PMN component observable in the left dipole localized to Broca's area (PMN_{S1}: BAs 44/45), with the peak occurring at 283 ms in the source waveform. A second PMN dipole was localized in the left inferior parietal lobe (PMN_{S2}: BAs 39/40). The source waveform for PMN_{S2} was remarkably similar to that observed for PMN_{S1}, with the peak at ~ 283 ms (Fig. 6b left). The PMN_{S2} dipole accounted for the deflections in the residual variance observed previously in the initial model. The peaks in the PMN source waveforms corresponded with those in the scalp recorded PMN[4]. Importantly, the PMN sources remained relatively active for the remainder of the epoch, indicating that the phonological processing continued well after the PMN peak (i.e., activation

[4] The latencies in BESA are measured in 10 ms intervals, accounting for the ~ 4 ms difference between the source waveforms and scalp recorded peaks.

associated with verbal WM).

In order to verify that the PMN sources were reliable, difference waveforms were subsequently obtained for the Low Congruent condition (Low Congruent - High Congruent), using the same parameters as in the PMN and N400 source analysis described previously. Recall that the Low Congruent waveforms contained *only* a PMN, with no (or little) N400 activation. If N400 activity was genuinely absent, then it should only be possible to model the PMN sources. Accordingly, the PMN source models in this condition addressed two critical issues: 1) whether or not the PMN dipole locations were replicated; and 2) whether or not N400 dipoles could be modeled. The interval-of-interest for the PMN alone was 253 ms to 354 ms (i.e., centered in the PMN time range).

Figure 7 presents the model for the PMN in the Low Congruent difference waveform. Source analysis of the PMN alone shows that the location of the dipoles were remarkably similar to those obtained when it was modeled simultaneously with the N400 (Fig. 7a). Specifically, there were two bilateral sources in the inferior frontal regions, with the source activation showing a strong left asymmetry. The PMN_{S1} was again localized to Broca's area (BAs 44/45). There was also a left hemisphere source in the inferior parietal lobe (PMN_{S2}: BAs 39/40). Interestingly, the source waveform activation for these dipoles showed more sustained activation in the PMN time range (Fig. 7b). In addition, it was not possible to model a N400 dipole. Indeed, when bilateral probe dipoles were placed in the N400 regions and fitting procedures were conducted, these sources were localized to the dorsolateral prefrontal cortices (DLPFC; BAs 8/9), in the vicinity of the middle frontal gyri. The involvement of the DLPFC provides evidence of WM

Figure 7 - Caption

Final model for the PMN only in the Low Congruent condition. The objective of this analysis was to determine whether PMN dipole locations were replicated and whether N400 dipoles could be modeled. **A.** Left sagittal, axial, and right sagittal views depicting the location of PMN dipoles (visual and 'response-related dipoles' were modeled, but not shown). PMN dipoles were located in Broca's area (PMN_{S1}: BAs 44/45) and the homologous area of the right hemisphere (left asymmetrical). There was also a PMN dipole in the left inferior parietal lobe (PMN_{S2}: BAs 39/40). No N400 dipole could be modeled, but bilateral probe dipoles were localized to the vicinity of the dorsolateral prefrontal cortices (DLPFC: BAs 8/9). **B.** Spline maps for the PMN *in isolation*. Projected spline maps (left) match the actual spline maps (right). **C.** Source waveforms reflecting the contributions of PMN dipoles to the scalp recorded activity. The source waveforms (PMN_{S1} and PMN_{S2}) reveal prolonged activation, peaking at 283 ms (*). The goodness-of-fit (solid line) and global field power (dashed line) for the full epoch (0 ms to 1000 ms). The residual variance was 10% for the 253 ms to 354 ms interval-of-interest.

Figure 7

PMN Source Locations and Waveforms - Replication

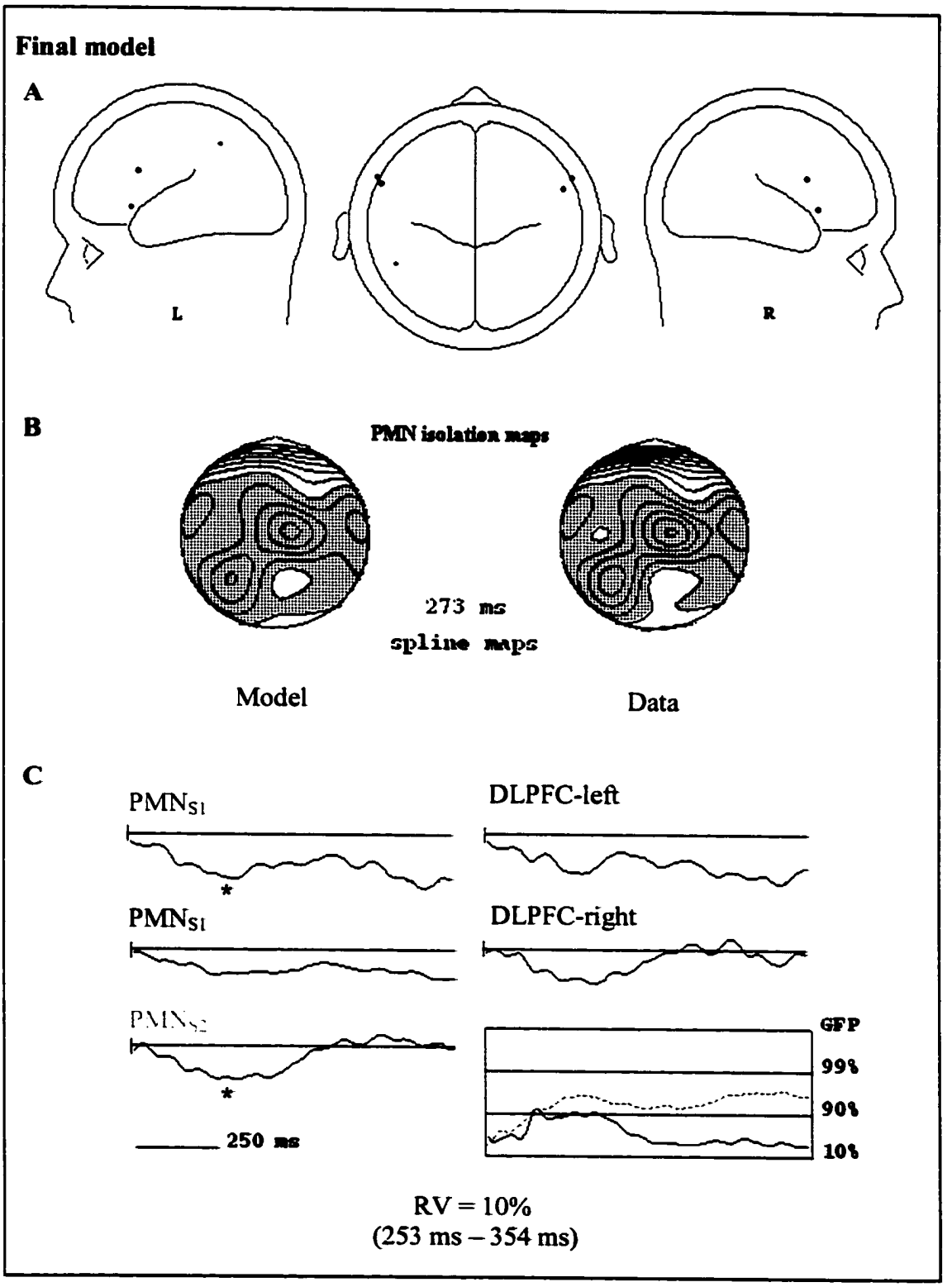

activation related to increased lexical candidate activation. It is also important to note that these PMN spline maps provide an excellent estimate of the component's *actual* topography, in the absence of the N400 (Fig. 7b).

The source analysis successfully disentangled the PMN and N400. For waveforms with both the PMN and N400 (advanced solution), the RV was 7.82% for the 253 ms to 475 ms interval-of-interest. For waveforms with only the PMN (advanced solution), the RV was 10% for the 253 ms to 354 ms interval-of-interest. However, it should be noted that a discrepancy between the global field power and the goodness-of-fit remained for the PMN time range. This suggests that not all sources for the PMN have been resolved fully.

V. Individual reliability analysis

In order to determine whether the source locations were representative across individuals, the initial model was subsequently applied to the individual waveforms (Fig. 5). Regional sources were selected because the reliability analysis was concerned with the general areas of activation. Difference waveforms for all ten participants were imported into BESA, using the same methods applied for the grand average difference waveform and the response hand source that did not correspond with the participant's response hand was excluded (either left or right). The RV for the 253 ms to 475 ms interval-of-interest was then recorded for each individual to evaluate the model's reliability. The global source locations identified in the initial model fit reliably the individual waveform data. The mean RV was 13.35 ($SD = 3.61$, range 8.9 to 18.3) demonstrating that on average the initial model accounted for more than 85% of the variance.

Chapter Two - Discussion

The findings demonstrated that the incongruent terminal words elicited both the PMN and N400 responses (Fig. 2). Prior work has linked the PMN to heightened phonological processing and the N400 to semantic analysis during speech perception (e.g., Connolly and Phillips, 1994). The current results show that these responses can be elicited by naturalistic spoken sentences that are *by themselves* completely sensible, but violate expectations formed by reading preceding sentences. These results provided the initial validation for the experimental paradigm (Hypothesis 1).

There were no significant differences between the High Incongruent and Low Incongruent conditions. However, there was a small PMN and no N400 in the Low Congruent condition (Fig. 2). The High Congruent condition differed from the Low Congruent condition as a function of the possible number of acceptable lexical candidates, with the latter being characterized by a greater number of alternatives. The sensitivity of the PMN to the number of active lexical candidates provides strong evidence for a functional interpretation that stresses lexical search processes during the formulation of a candidate list - on the basis of the incoming phonological information (Connolly et al., 2001). Thus, the results demonstrated that increased lexical candidate activation has a selective effect on the PMN (Hypothesis 2).

Statistical analysis of the difference waveforms revealed that the PMN and the N400 were distributed over the central region with a slight right asymmetry (Fig. 3). The spline maps showed that the PMN peaked in the central region (Fig. 4a), while the N400 peaked in the centro-parietal region (Fig. 4c). The results were similar to those reported in the Connolly et al. (2001) study, confirming the PMN distribution. Indeed, the spline

maps for the PMN only matched this central profile and provided possibly the best window into the PMN topography (Fig. 7b). The CSD maps showed a number of active regions. Importantly, there was activation in the left anterior region during the PMN time range, which also replicated prior CSD results (Connolly et al., 2001).

I. Localization of the PMN and N400

Source analysis revealed areas of activation related to the task demands and the overall areas of activation were fairly reliable across individual data sets. With respect to language-related activation, there was a pronounced left hemisphere asymmetry. The hypothesis that the PMN and the N400 resulted from distinct neuroanatomical generators with different time courses of activation was clearly supported. The PMN and N400 were localized reliably to key regions that are known to be involved in language processing, and examination of the source waveforms revealed that they represent physiologically different processes (Hypothesis 3).

Specifically, a N400 dipole ($N400_{S1}$) was localized to the pSTG (Wernicke's area), with similar but reduced activation in the homologous area of the right hemisphere. A second N400 dipole ($N400_{S2}$) was localized, anterior to $N400_{S1}$, to the left STP (supra-temporal plane). A third ($N400_{S3}$) was localized to the left polymodal (temporal-parietal-occipital) region. The source waveforms for all three dipoles were comparable with major peaks being centered in the N400 time range. The $N400_{S1}$ and $N400_{S2}$ were characterized by similar activation patterns with an overall morphology that resembled closely the scalp recorded N400. The activation pattern for $N400_{S3}$ was characterized by a slow wave in the later time range, and was likely a secondary generator (Fig. 6a,b right).

PMN sources were localized to the left inferior frontal region (PMN_{S1}; in Broca's area) and the left inferior parietal lobe (PMN_{S2}). Some activation was also observed in the homologous inferior frontal area of the right hemisphere (Fig. 6a). The source waveforms for both PMN dipoles revealed similar time courses with a pronounced peak at 283 ms (Fig. 6b left). This timing fits well with the scalp-recorded peak at 287 ms. Critically important is the fact that PMN dipoles in the Low Congruent condition were localized to the same regions as those in the difference waveforms, with no active regions for the N400. The location of PMN_{S2}, the sustained source activation profile, and the novel activation in the dorsolateral prefrontal region for the Low Congruent condition provided clear evidence of verbal WM involvement (see discussion below).

Additional physiological confirmation of the model's validity was derived from evidence of sensory activation. Dipoles associated with visual and response-related activation were identified in the occipital region (activation from visual fixation) and the primary motor/sensory regions (activation from behavioural responses), respectively (Figs. 5a and 6a). This activation was completely consistent with the task demands and provided evidence similar to that utilized frequently in other functional neuroimaging studies. For instance, in functional magnetic resonance imaging (fMRI) studies, activation in anatomical areas required for, but not the focus of, the processing in question is expected (e.g., activation in visual cortex during reading, see Chapter Four).

II. The speech perception network

Perhaps the most striking finding is that the neuroanatomical regions identified in the current experiment fit remarkably well with a recently proposed network for speech perception. Hickock and Poeppel (2000) have developed a model in which the posterior-

superior temporal lobe (bilaterally) is the primary substrate for constructing sound-based speech representations. They suggested that while both hemispheres contribute to speech perception, there is a left hemisphere asymmetry. Two functional neuroanatomical pathways are thought to diverge from the left posterior-superior temporal lobe. The first pathway involves sound based representations of speech, assembled in the bilateral posterior STP and posterior STG, which interface with amodal semantic-conceptual representations of the mental lexicon in the left temporo-parietal junction. The second pathway involves accessing sub-lexical speech segments and possibly verbal working memory. In this pathway, the left inferior frontal region and the left inferior parietal lobe (e.g., supramarginal region) may support an auditory-motor interaction during the process of sub-vocal articulation. Sub-vocal articulation is assumed to provide a temporary storage system for acoustic or speech-based information, which fades away within seconds unless otherwise maintained by rehearsal (Baddeley, 1996).

The current results implicate the involvement of all of the above regions during spoken sentence processing. In addition, the functional independence of the PMN and N400 provide clarification about which aspects of the speech stimulus are responsible for producing activation in a particular region, corroborating the results of less temporally-resolved functional imaging studies (Démonet et al., 1992; Démonet, Price, Wise, and Frackowiak, 1994; Hickock and Poeppel, 2000). Indeed, the *interface* between the two pathways that enables the construction of speech representations seems to involve phonological input, as reflected in the PMN.

The functional role of the left perisylvian regions, particularly in the vicinity of the left STP (e.g., $N400_{S2}$), is also being refined. All of the N400 sources were localized

to the left perisylvian region. Most functional interpretations of the N400 stress the evaluation of a word's semantic content as it relates to the sentential context and semantic memory structure (Federmeier and Kutas, 1999; Kutas and Van Petten, 1994). It is noteworthy that the peak activations of the N400 dipoles occurred beyond the time period for which spoken word identification occurs (Marslen-Wilson, 1984; Zwitserlood, 1989). Moreover, similar temporal regions have been identified for visual N400 dipoles using ERPs and MEG (Chapter Three; Helenius et al., 1998; Simos, Basile, and Papanicolaou, 1997) as well as a recent MEG study on auditory N400 dipoles (Helenius et al., 2002), all of which supports the notion that the left perisylvian region may be centrally involved in supporting a distributed amodel semantic-conceptual system[5]. These findings concur with the results from both positron emission tomography (PET) and fMRI studies (Cabeza and Nyberg, 2000; Price, 2000). In light of the converging evidence, the functional role of the superior (and middle) temporal cortex may include the evaluation of the semantic content, independent of sensory modality. However, the notion of amodal semantic integration as one of the functions subsumed by the left perisylvian region remains speculative and will require further empirical support.

III. Working memory influences in speech perception

Functional imaging evidence for the neural correlates of working memory in speech perception is mounting. D'Arcy, Connolly, and Crocker (2000) reported a N2b component elicited by phonological deviations from a cognitive template maintained in working memory. Thierry, Boulanouar, Kherif, Ranjeva, and Démonet (1999)

---

[5] Separate studies on the visual N400 have also identified anterior medial temporal activation (Chapter Three; McCarthy, Nobre, Bentin, and Spencer, 1995; Nobre and McCarthy, 1995), suggesting that other neural structures may be involved in this system.

investigated phonological processing in a fMRI study and reported evidence of working memory involvement. They found activation consistent with the well-known contribution of Broca's area and Wernicke's area, and in particular, activation in the left supramarginal region. They conducted a temporal analysis of the hemodynamic responses and revealed segregation between sensory and association speech regions during phoneme monitoring, but not during fast repetition. The temporal uncoupling was hypothesized to reflect sustained, delayed processing consistent with the functional model of the phonological loop (Baddeley, 1992, 1996). In the Connolly et al. (2001) study, a later negativity was observed following the PMN. We speculated that the later negativity reflected sustained activation associated with continued phonological processing and the influences of working memory. The findings in the current experiment substantiate the view that, in fact, phonological processing continues well beyond the early peak activation of the PMN. The sustained activation for PMN sources in Broca's area and the left inferior parietal region is consistent with other neuroimaging results supporting the conceptualization of a phonological loop (Démonet et al., 1992; Démonet et al., 1994; Paulesu, Frith, and Frackowiak, 1993; Thierry et al., 1999).

In summary, evidence has confirmed that physiological signs of working memory influences in speech perception exist. The left inferior parietal region appears to be one of the primary cortical substrates of verbal working memory (Cabeza and Nyberg, 2000; Miyake and Shah, 1999). However, the precise role of this region in WM (e.g., as a phonological store) remains to be determined (Becker, MacAndrew, and Fiez, 1999).

Chapter Two - Conclusion

PMN activation arose mainly from the left inferior frontal and the left inferior parietal regions and reflected phonological analysis and elements of working memory during speech perception. PMN activity may also reflect processes associated with the development of candidate lists, providing the necessary input for semantic analysis (as indexed by the N400). Semantic neural systems involved in generating the N400 during speech perception include, but may not be limited to, cortical zones in the left perisylvian region. The experimental paradigm used in this study provides an ideal framework in which to investigate processes that interact with prominent components like the N400. Accordingly, the following chapter presents an investigation into whether or not WM influences on the N400 can be detected.

Chapter Three

The influences of increased working memory load on semantic neural systems: A high-resolution event-related brain potential study

Chapter Three - Summary

The effects of working memory (WM) on the semantic N400 response were studied using high-resolution event-related brain potentials (ERPs). Participants were presented with sentence pairs that related to each other within a semantic hierarchy. Terminal word congruence in the second sentence was varied in order to elicit the N400. A modified fan procedure (Anderson, 1974, 1983) was used in which the sentence pair stimuli were divided into two separate levels of WM load. ERPs were recorded to the onset of the terminal word (Congruent and Incongruent) for sentence pairs in both WM levels (Load 1 and Load 2). Analysis of the behavioural data provided confirmation of the fan-effect. Incongruent terminal words elicited a N400 response for all sentence pairs. Increased WM load resulted in a reduction in N400 amplitude (i.e., a smaller congruency effect). Importantly, there was also a significant N400 peak latency delay as a result of increased WM (~50 ms on average), which appeared to be related to individual WM capacity. Source analysis revealed active intracranial generators in brain regions known to be involved in language, semantic retrieval, and working memory. Increased WM load led to novel N400 activation in the left inferior parietal region as well as enhanced activation in anterior temporal regions. The activation changes were consistent with the functional roles typically ascribed to these areas. The WM effects were interpreted as delaying semantic integration and retrieval processes at the interface between WM and long-term memory.

Chapter Three - Introduction

Working memory (WM) and semantic comprehension have been the central focus of numerous studies in cognitive neuroscience. However, the manner in which these cognitive processes interact and the neural systems that support these interactions remains to be characterized fully. Behavioural studies, particularly those that use sophisticated experimental designs, have contributed a great deal to the development of theories concerning the inter-relationship of different cognitive processes. In addition, advances in neuroimaging have allowed for the structure and function of the neurocognitive architectures that support behavioural outcomes to be identified. Ultimately, a combination of both approaches will provide the information essential to disentangling higher-order cognitive processes. In the current study, WM load and semantic congruence were varied systematically in order to investigate corresponding interactions in brain activity.

I. Spatiotemporal investigations of neurocognitive processes

Event-related brain potentials (ERPs) represent a non-invasive brain imaging technique that is ideally suited for neurocognitive investigations. As discussed in Chapter Two, ERPs provide an on-line measure of the brain's information processing. They are derived from scalp recorded electroencephalographic (EEG) activity and are obtained through a signal averaging process in which the EEG activity is time-locked to the onset of a series of stimuli and then averaged to extract the non-random electrical activity (Knight, 1997). The main strength of ERPs lies in their exquisite temporal resolution. Evidence of this temporal resolution was observed in the fractionation of processes that underlie the PMN and N400 in Chapter Two. In addition, it was demonstrated that spatial

estimates of these components could be derived from the scalp recorded electrical activity. These estimates utilized high density electrode arrays (128 channels), making it possible to obtain detailed topographical information about the distribution of electrical potentials and to model the active equivalent current dipoles using source analysis techniques (Picton, Lins, and Scherg, 1995; Scherg and Picton, 1991).

However, the spatial data obtained from ERPs (and magnetoencephalography, MEG) must be integrated with existing findings from hemodynamic measures like positron emission tomography (PET) and functional magnetic resonance imaging (fMRI). This goal is particularly relevant to the current study because a number of PET and fMRI studies on WM and semantic comprehension exist (Cabeza and Nyberg, 2000). Unfortunately, it is not possible to assume *a priori* that a direct correspondence exists between ERP/MEG findings and PET/fMRI findings. In fact, the nature of the intricate relationship between neural activity and cerebral metabolism remains to be understood fully (Jueptner and Weiller, 1995; Magistretti and Pellerin, 1996; Orrison, Lewine, Sanders, and Hartshorne, 1995). An additional difficulty arises from limits associated with source analysis that are necessarily imposed due to the inverse problem (Hämäläinen, Hari, Ilmoniemi, Knuutila, and Lounasmaa 1993; Nunez, 1981; Picton, Lins, and Scherg, 1995). While dipole modeling provides powerful insight into functional neuroanatomy, the solutions are not unique. Given these methodological challenges, the initial step must involve straightforward comparisons between electromagnetic dipole models and hemodynamic activation maps. The preliminary evidence for some form of correspondence is encouraging, with overall convergence of co-localized activation in a variety of tasks that activate different neurocognitive architectures (e.g., Dale et al., 2000;

McCarthy, 1999; Puce, Allison, Spencer, Spencer, and McCarthy, 1997; Thierry, Doyon, and Démonet, 1998). Ultimately, the integration of results from multiple imaging modalities will assist greatly in identifying the functional connectivity of a given network (Friston, 1994).

II. Semantic analysis and the N400 response

Similar to the previous chapter, the majority of ERP studies on language processing have focused on the N400. From its initial discovery, the N400 has been regarded as being highly sensitive to the semantic features of a word (Kutas and Hillyard, 1980). The prototypical N400 is elicited to semantically incongruent terminal words of visually presented contextually constrained sentences (e.g., "She takes her coffee with cream and *dog*", when 'sugar' is expected). The results of Chapter Two showed that it can also be elicited using semantically-related sentence pairs, in which the terminal word in the second (or target) sentence was incongruent with expectation. In both of these cases, the incongruent words elicited a late negative-going peak (at approximately 400 ms), which is distributed in the centro-parietal regions (Kutas and Van Petten, 1994).

Indeed, there is a good deal of evidence that suggests the N400 can be elicited in a variety of different circumstances - all of which share a common emphasis on semantic evaluation. The N400 has been observed using word pair stimuli (Bentin et al., 1985; Brown and Hagoort, 1993). Also, the component has been observed in numerous studies that use speech stimuli, proving that it is not specific to the visual modality (Chapter Two; Connolly and Phillips, 1994; Holcomb and Neville, 1990). The N400 has also been observed when using paradigms that combine text and speech (Chapter Two), pictures and speech (Connolly, Byrne, and Dywan, 1995a), and text and pictures (Ganis, Kutas,

and Sereno, 1996; Nigam, Hoffman, and Simons, 1992). In sum, the common finding of a N400 reported in these and other investigations suggest that it is linked to an amodel semantic conceptual system.

With respect to the functional interpretation, there is evidence that the N400 reflects controlled post-lexical semantic integration processes. Holcomb (1993) reported that degraded stimuli delayed the latency of the N400 regardless of whether the words were primed or unprimed (i.e., if the N400 reflects pre-lexical processing, then this processing will be less affected by stimulus degradation). The failure to obtain an interaction between priming and stimulus degradation was taken as evidence of post-lexical processing. Brown and Hagoort (1993) used masked and unmasked primes and found that the relatedness of the prime influenced the amplitude of the N400 only in the unmasked condition (i.e., if the N400 processes are pre-lexical, then preventing the stimulus from reaching conscious perception will not affect the response). They found that the primes modulated the N400 amplitude only when they were consciously perceived, again highlighting its role in semantic integration. However, the role of pre-lexical automatic processes in the N400 cannot be discounted yet, as contradictory evidence for this claim exists (Deacon, Hewitt, Yang, and Nagata, 2000).

Electromagnetic studies (ERPs and MEG) that localize N400 sources (in visual and auditory modalities) have begun to reach a general consensus with respect to some of the key brain areas. The middle and superior portions of the left temporal lobe, particularly in the posterior regions, provide major contributions to N400 scalp recorded activity (Chapter Two; Haan, Streb, Bien, and Röesler, 2000, Helenius, Salmelin, Service, and Connolly, 1998; Helenius et al., 2002; Simos, Basile, and Papanicolaou,

1997). In addition, homologous temporal areas in the right hemisphere, as well as polymodal regions in the left temporal-parietal-occipital region (BA 37) have also been implicated (Chapter Two; Haan, Streb, Bien, and Rösler, 2000; Helenius, Samelin, Service, and Connolly, 1998).

The anterior-medial temporal lobe (AMTL) has been identified as another major contributor to N400 activity. McCarthy, Nobre, Bentin, and Spencer (1995) and Nobre and McCarthy (1995) used intracranial electrodes in different brain areas and found N400 generators in the AMLT (includes the inferior temporal neocortex, the anterior fusiform and parahippocampal gyri). Simos, Basile, and Pananicolaou (1997) replicated these results using MEG, localizing N400 sources in the vicinity of hippocampus and parahippocampal gyrus. While the converging evidence is promising, it is still not possible to assume a single neural architecture for the N400. A recent high-density ERP study by Haan et al. (2000) used current density reconstruction algorithms (i.e., CURRY) and found a broad and scattered distribution of active locations in the cortex. In addition, they reported the existence of inter-individual differences in topographies and cortical current source estimates. These results indicated that it is important to consider the variance in the location of N400 source within and between individuals.

III. WM and ERPs

Working memory (WM) is thought to be a system involved in maintaining newly acquired and re-activating stored verbal and non-verbal information in order to make it available for processing (Baddeley, 1992, 1996; Baddeley and Hitch, 1974). Multiple theories about WM exist, all of which address the relationship between WM and complex

cognitive processes. In an attempt to unify the phenomenon, Miyake and Shah (1999) have recently provided the following comprehensive definition of WM:

> "Working memory is those mechanisms or processes that are involved in the control, regulation, and active maintenance of task-relevant information in the service of complex cognition, including novel as well as familiar, skilled tasks. It consists of a set of processes and mechanisms and is not a fixed "place" or "box" in the cognitive architecture. It is not a completely unitary system in the sense that it involves multiple representational codes and/or different subsystems. Its capacity limits reflect multiple factors and may even be an emergent property of the multiple processes and mechanisms involved. Working memory is closely linked to LTM, and its contents consist primarily of currently activated LTM representations, but can also extend to LTM representations that are closely linked to activated retrieval cues and, hence, can be quickly reactivated." (pp. 450)

A significant proportion of research on the relationship between WM and complex cognitive processes has focused on semantic comprehension. Evidence obtained in behavioural studies demonstrated the involvement of WM in comprehension abilities. Daneman and Carpenter (1980), among others, have reported that individual differences in reading comprehension abilities correlate with WM capacity (as measured by a reading-span task). King and Just (1991) used object-relative and subject-relative sentences to show that individual differences in syntactic processing were also related to differences in WM capacity. A number of studies done by Engle and his colleagues have examined the relationship between individual WM capacity and reading comprehension ability using the so-called fan procedure (Engle, 1996).

Anderson (1974, 1983) originally used the fan procedure to demonstrate that the speed and accuracy of retrieving information from long-term memory (LTM) depends on the number of items to be retrieved. Figure 8 shows the general structure of the fan

Figure 8 - Caption

The fan procedure showing the relationship between SUBJECT and PLACE terms (adapted from Cantor and Engle, 1993). The fan set sizes were one, three, and four. Participants studied the Target sentences (left column) and were then presented with items from either the Target or Foil groups (.5 probability). Reaction times and error rates increased as fan set size increased (i.e., the fan-effect).

Figure 8

The Fan Procedure

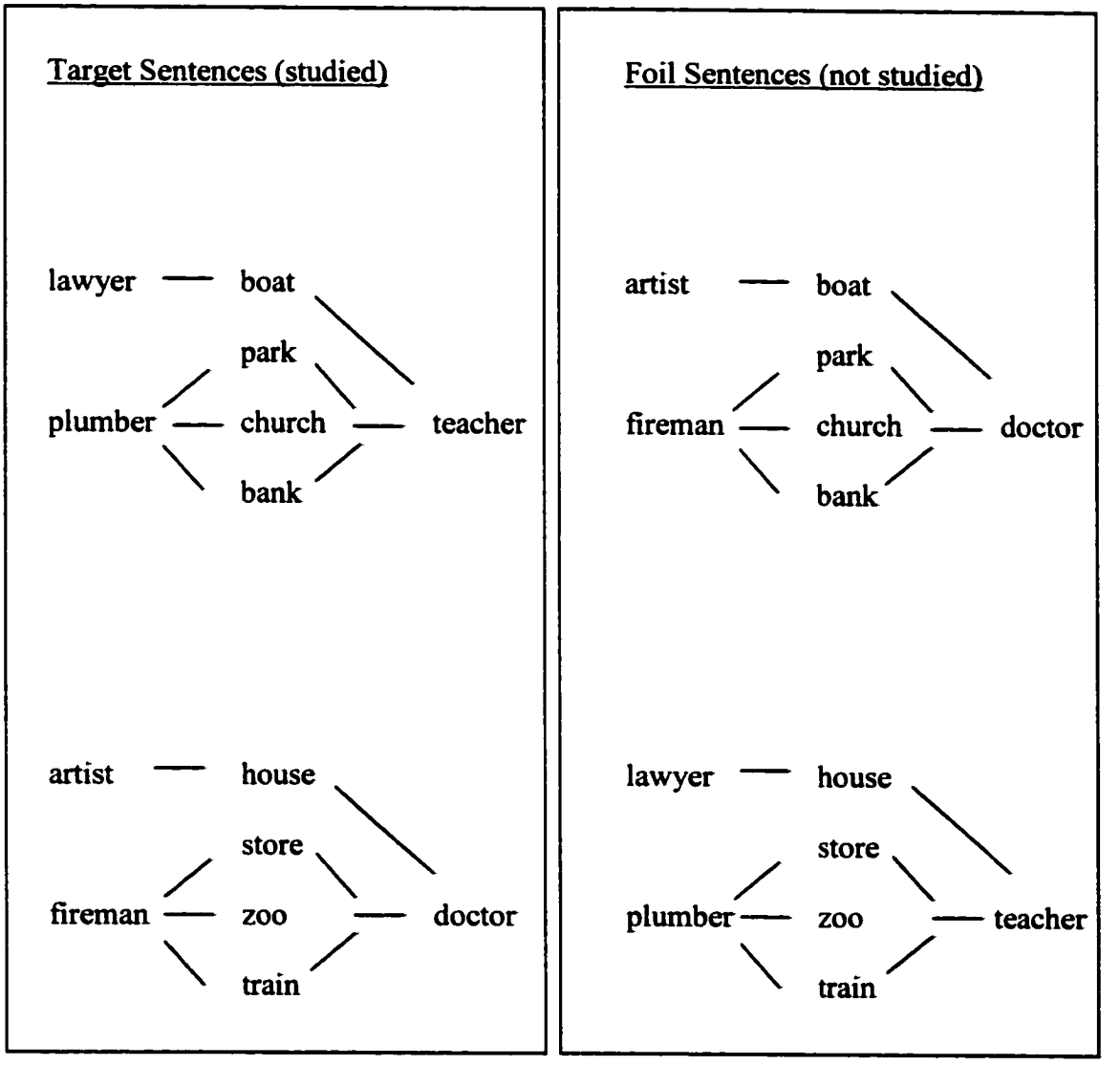

procedure. In this task, participants study a set of propositions, with each proposition comprising a subject and an object (e.g., "The lawyer is in the boat"). The number of shared concepts for these propositions is varied to increase the memory set size (i.e., propositional fan size). Once participants learn all of the sentences, they are given a speeded verification task containing both the studied sentences and foils. The basic finding was that reaction times (RTs) and error rates increased as the fan size increased (Anderson, 1974, 1983). These results were thought to reflect processes related to the spread of activation among concepts in LTM, with greater propositional sets requiring more active concepts, which in turn led to longer retrieval times (ACT* model, e.g., Anderson, 1983).

Using a similar procedure, Cantor and Engle (1993) studied individual differences in memory capacity and sentence reading ability. They demonstrated that individuals who had low WM capacities also had larger fan-effects (i.e., longer RTs and higher error rates) than individuals who had high WM capacities. This work demonstrated that WM capacity interacts in some manner with the activation of conceptual knowledge units in LTM. The ambient level of activation across these conceptual knowledge units was proposed to be limited, with individuals varying in the total amount of activation that was available within their system. The interpretation of the interaction between individual differences in WM capacity and sentence reading ability has been described within the framework of the General Capacity Theory, which highlights a controlled and effortful retrieval process (Cantor, and Engle, 1993; Engle, 1996, Engle, Cantor, and Carullo, 1992).

General Capacity Theory attempts to explain the mechanisms that mediate the relationship between WM and complex cognitive functions (Engle, 1996). It assumes that WM is more extensive than short-term memory, and involves activating knowledge units in LTM above a certain threshold. The total amount of activation in the system is limited and differs between individuals. WM activation allows for a temporary shift of attention away from a given task while maintaining the ability to recover the relevant information at a later point. The General Capacity Theory predicts that individual WM capacity is important for both the acquisition of new information and the retrieval of well-learned information.

Some insight into the relationship between WM and cognitive processes has been provided by ERP studies. While several ERP memory studies have been done, much of this work has examined the P300 component as it related to recognition memory (Polich and Kok, 1995) or memory in general (Rugg, 1995). The influence of WM in particular has been reported for the Mismatch Negativity or MMN (Cowan, Winkler, Teder, and Näätänen, 1993) as well as negative slow wave potentials (Rösler, Heil, and Glowalla, 1993). The latter study is of interest because the authors used the fan procedure with concrete nouns to investigate tonic voltage changes in ERPs (which were thought to reflect the excitability of the underlying cortical tissue). Rösler et al. (1993) found that memory probes elicited DC-like negative potentials, particularly over the left anterior region, and increases in fan size produced potential changes over the frontal and parietal sites for negative probes (i.e., items not in the memory set).

Using a semantic memory search task, Mecklinger, Kramer, and Strayer (1993) had participants learn memory sets that were semantically unrelated and then recorded

ERPs during the presentations of words in subsequent probe trials (set sizes 2, 4, and 6). While the main findings showed that the P300 amplitude reduced with increasing memory load, Mecklinger et al. (1993) also observed that a negative-going waveform increased in amplitude as a function of memory load. They proposed that the negativity reflected either attentional processes associated with the N2b (Pritchard, Shappell, and Brandt, 1991) or semantic analysis linked to a N400-like response. Upon consideration of the larger amplitudes to negative probes (which were interpreted as being similar to semantic mismatches and/or unprimed words), the authors suggested that the phenomenon might have been a N400. However, the degree to which this early negativity represented a N400 is not clear. The amplitude difference between the positive and negative probes was small (Set size 2 = 2.3 μV; Set size 4 = -0.1 μV; and Set size 6 = 0.3 μV) and it was not characterized by the typical central parietal topography (being largest at Fz). Indeed, the negativity seems consistent with a N200 elicited by increased attentional demands associated with processing larger set sizes (see Discussion section).

Arguably, one of the most comprehensive studies on WM and the N400 to date has examined the effects of aging on these processes. Gunter, Jackson, and Mulder (1995) used memory-demanding sentences to examine ERPs in younger and middle-aged participants. They utilized syntactic sentence structure (cf. King and Just, 1991) to create sentences that varied in terms of working memory load and terminal word congruence. In order to increase WM load, the authors used sentences in which the subordinate clause was embedded within the main clause (instead of following the main clause, see below). Additionally, Gunter et al. (1995) also varied the thematic relatedness within each of the sentences (i.e., sentence context). Examples of thematic/non-thematic sentences in

Low/High WM load (Dutch translated word-by-word into English) are: 1) Low load thematic - "While a large crowd stood towards to look, the small (drowning person) by the hero *saved/understood*"; 2) High load thematic - "The small (drowning person) was by the hero, while a large crowd stood towards to look, *saved/understood*"; 3) Low load non-thematic - "While on the Berlin exchange the (dollar rate) dropped, was the small (drowning person) by the hero *saved/understood*"; and 4) High load non-thematic - The small (drowning person) was by the hero, while on the Berlin exchange the (dollar rate) dropped, *saved/understood*". Individual WM capacity was evaluated through the administration of standard behavioural measures (e.g., word span, forward and backward digit span, and an auditory-sentence dual task paradigm).

The main objective of the Gunter et al. (1995) study was to examine age difference in sentence processing as a function of WM capacity. They found that the older participants had lower scores on the measure of WM (although there were no differences in word and digit span scores). As expected, the N400 amplitude was reduced and the latency was delayed in the older subject group. Distinctive ERP effects of memory load were also reported in both age groups. Specifically, the authors reported that high WM load reduced the amplitude of the N400. In the younger sample, N400 congruency effects occurred in both low and high WM conditions, but were reduced in the High condition. In the older sample, a N400 congruency effect was present only for the low WM condition and disappeared in the high condition. In young subjects, the most notable effect of theme was to further reduce the congruency effect in the high WM load condition for non-thematic sentences. The authors also examined positive and negative shifts in the waveforms that were proposed to reflect on-line memory storage and

retrieval processes, respectively. They proposed that while both storage and retrieval processes depend on WM capacity, semantic processes (as indexed by the N400) modulated only retrieval processes. Gunter et al. (1995) concluded that most ERP-effects were dependent on WM capacity. Moreover, with respect to aging, they proposed that individual WM capacity, rather than age itself explained differences in sentence processing.

IV. Objectives and hypotheses

In order to characterize the specific influences of WM on semantic processing and the N400, the present study used a more direct and well-established manipulation of WM load in a sample of university students. The paradigm incorporated a modification of the fan procedure in a sentence verification task (Anderson, 1974, 1983; Fig. 8). It was predicted that the behavioural fan-effect would be present in the RT data using the modified fan procedure (Hypothesis 1). While WM-induced variations in the N400 amplitude were expected, it was predicted that increased WM load would delay the N400 latency for individual subjects (Hypothesis 2). N400 latency delays were examined because, if they occurred, the results would correspond directly to the behavioural WM findings (i.e., RT delays)[6]. By evaluating whether similar timing effects exist for the N400, it would be possible to obtain direct physiological evidence for the influence of WM on semantic integration and retrieval of information from LTM. In order to explore this idea further, the relationship between N400 latencies and individual WM capacity

---

[6] Very few N400 studies have shown within-subjects latency delays using *cognitive* manipulations. To our knowledge, N400 latency has been delayed previously only by presenting phonologically expected, but semantically incongruent terminal words in the auditory modality (e.g., "The gambler had a streak of bad... *luggage*"; Connolly and Phillips, 1994).

was also examined to determine whether individual differences were a relevant factor (Engle, 1996). Finally, high-resolution ERPs were used to localize the N400 generators. In particular, this analysis focused directly on phasic activation in the N400 time range. These spatial findings were integrated with prior N400 localization data as well as with PET and fMRI findings on WM. Once the key regions were identified, the source waveforms were also examined in order to determine whether WM load influenced source activation. By comparing source waveforms as WM load was increased, it would be possible to dynamically image mnemonic changes, which were predicted to exist within the semantic neural architecture (Hypothesis 3).

Chapter Three - Methods

I. Participants

Sixteen university students (10 females and 6 males) volunteered to participate in a study on language and memory (some received course credit where applicable). One additional participant was tested, but the data were not included in the study due to self-reported reading difficulties. All 16 participants were fluent in English, their mean age was 22.1 years (*SD* = 2.5), and their mean level of education was 15.9 years (*SD* = 1.3). The Edinburgh Handedness Inventory (Oldfield, 1971) was used to assess handedness and all participants were dextral (LQ range = 39.1 to 100). All had normal or corrected-to-normal vision and were screened using a self-report measure for audiological, psychiatric, and/or neurological history. The participants were told that the study duration was approximately three hours. The study had ethical committee approval and informed consent was obtained before the experiment proceeded. Upon completion, each participant was debriefed and all questions were answered.

The participants' WM capacities were assessed using the Digit Span (Forward, Backward, and Total) from the Wechsler Memory Scale – Revised (WMS-R; Wechsler, 1987). Their mean scores for Total, Forward, and Backward were 17.2/24 (*SD* = 3.1, range = 12 to 24), 10.1/12 (*SD* = 1.5, range = 7 to 12), 7.1/12 (*SD* = 2.2, range = 4 to 12), respectively. On the basis of the normative data (20 to 24 age range), the mean Forward scores were in the 82nd percentile (range = 99 to 18) and the mean Backward scores were in the 52nd percentile (range = 99 to 14). Using a split-half procedure, High and Low groups were derived using the Total scores. The mean score for the High group was 19.5 (*SD* = 2.3) and the mean score for the Low group was 14.9 (*SD* = 1.8).

II. Experimental Paradigm

The paradigm was adapted from a previous visual-to-auditory sentence-matching task used to investigate speech perception (Chapter Two). The modified paradigm used a visual-to-visual sentence-matching task. The sentence pairs contained prime and target sentences that were characterized by an exemplar-superordinate semantic hierarchical relationship. For example, for the prime sentence "The man is climbing into the *cockpit*," the target sentence was "The man is in the *airplane*." The prime sentences comprised a subject (man, woman, boy, or girl), a verb, and a subordinate noun phrase. They were constructed to establish an expectancy, which was evaluated subsequently within the context in following target sentences. The semantic congruence of the terminal words in the target sentences was manipulated to match or mismatch expectation (e.g., airplane/office). Appendix 2 provides a full list of the experimental stimuli.

The congruent terminal words were selected to complete the target sentence by using the highest probability word for each sentence pair (Bloom and Fischler, 1980). Two hundred sentence pairs were constructed in the form "The SUBJECT is VERB in the PLACE" "The SUBJECT is in the... ?". The sentence pairs were then given as a normative survey to 108 individuals, who were instructed to complete the second sentence with the most appropriate superordinate ending. The normative data from Chapter Two were combined with additional data obtained for this study (Chapter Two: N = 58 and Chapter Three: N = 50). The overall normative sample (72 females and 36 males; all fluent in English) was characterized by a mean age of 27.5 years (*SD* = 10.2) and a mean level of education of 17.1 years (*SD* = 3.3). From the 200 sentence pairs, a subset of 180 sentence pairs was selected. Any items with error rates greater than 33% or

repeat words and sentences were excluded. The incongruent terminal words were semantically unrelated words with initial phonemes that did not match any of the normative responses. The incongruent words were selected from alternate words in the normative data set for comparable word frequency. The stimuli in all conditions were also equal with respect to calculated probabilities and word lengths. The ERP data for high and low probability trials were checked for probability-related differences, but no probability effect was found. Therefore, this experimental manipulation was not investigated further (i.e., the experimental conditions were collapsed across exemplar-subordinate probability).

The 180 sentence pairs were divided into two levels of WM Load[7] (Load 1: 60 pairs and Load 2: 120 pairs). Load 1 contained a single prime and target sentence (e.g., Prime: The woman is riding on the underground train. Target: The woman is in the subway / church). Load 1 replicated the Chapter Two findings, using new sentence stimuli in the visual modality. WM Load was increased in Load 2 by using a second unrelated sentence in the prime[8]. Thus, Load 2 required participants to anticipate and remember the superordinate endings for *two* sentences (e.g., Prime: The boy is sitting on the witness stand. The boy is standing at the grave.). After the prime, participants were presented with a single target sentence with either a congruent or incongruent ending (Target: The boy is in the courtroom / laboratory / cemetery). There were 60 trials in both

---

[7] 'WM Load' refers to the statistical factor, whereas, 'WM load' refers to the theoretical concept.

[8] All sentences were unrelated in order to obtain the typical fan-effect. This was done because previous work by Cantor and Engle (1993) has shown that when thematic relations characterize the propositional fan, it is possible to form mental models on the basis of semantic relatedness and subsequently show a negative fan-effect (particularly in high span participants).

Load 1 and Load 2 with 30 congruent and 30 incongruent trials in each WM Load. The stimuli were presented in a fixed pseudo-random and counterbalanced order (Load 1 - Load 2 and Load 2 - Load 1). Given the high trial numbers that were required for signal averaging (which increased exponentially with memory set size), the current study was limited to set sizes of one and two propositions.

Both the prime and target sentences were presented visually on a 14-inch computer screen positioned 1 m from the participant's nasion. The text stimuli were presented in yellow letters on a black background (36-font size). For Load 1, a single prime sentence was presented in the center of the computer screen. For Load 2, two prime sentences were presented simultaneously in the top and bottom half of the screen. The Load 1 prime sentences had a mean width of 19.76 cm (SD = 2.13) and mean height of 3.00 cm (SD = 0.62). The Load 2 prime sentences had a mean width of 20.83 cm (SD = 1.87) and a mean height of 11.02 cm (SD = 0.55). The prime sentence stimuli subtended a maximum visual angle of approximately 14.3 degrees. Each prime sentence was presented in its entirety for the participants to study. Following the prime, each target sentence was presented in rapid-serial-visual-presentation (RSVP) format in order to minimize ocular artifact. The target sentence words subtended a maximum visual angle of approximately 5.7 degrees. The stimulus onset was defined as the beginning of the terminal words in the target sentences. ERPs were recorded from the stimulus onset.

III. Procedures

Prior to the experiment, Digit Span (Forward and Backward) from the Wechsler Memory Scale – Revised (WMS-R; Wechsler, 1987) was administered to all participants. The Digit Span was selected to provide a standardized measure of WM and the scores

were correlated with the ERP data. Digit Span Total and Backward scores were taken as the best measures of WM.

The ERP experiment began with a practice phase, comprising the task instructions and sample trials containing examples (both Load 1 and Load 2). Participants were given a description of the sentence pairs and instructed to anticipate the superordinate words for the target sentences. Each prime sentence was presented for a 10 s duration. Immediately after the prime sentence, the target sentence was given, with a 0.5 s duration/word and 0 s specified for the inter-stimulus interval (ISI). A 6 s stimulus onset asynchrony (SOA) defined the time between the terminal word in the target sentences and the onset of the next trial (with a 3 s behavioural response window).

All participants were instructed to make a button press in order to indicate whether the terminal words matched or mismatched expectation. They were told to respond as quickly and as accurately as possible (i.e., speed/accuracy trade-off instructions) and their response hand (left or right) was counterbalanced. During the recording session, participants were told to remain as still as possible because of the sensitivity of EEG recordings. They were also instructed to restrict their blinks to the 10 s period during prime sentence(s) presentation and to try not to blink during the target sentences, particularly around the time of terminal word presentation.

EEG activity was recorded using a 128-channel NeuroScan Synamps™ system. The electrodes were embedded in a NeuroScan Quik-Cap™, positioned on the basis of an extension (American Electroencephalographic Society, 1991) of the International 10/20 System (Jasper, 1958). Vertical and horizontal eye movements as well as blinks were recorded using an electro-oculogram (EOG), with electrodes above, below, and on the

outer canthi of both eyes. The impedances were maintained at or below 10 KΩ and AFz served as a ground electrode. All electrodes were Ag/AgCl and an electrode located on the nose served as the reference. The continuous EEG recordings (bandpass: 0.05 to 30 Hz, digitally sampled at 500 Hz) were epoched off-line (–100 ms to 1000 ms) and digitally low pass filtered at 20 Hz. Any trials with EOG artifacts greater than ±75 μV (-100 ms to 750 ms) were excluded from the analysis. The mean percentage of trials accepted in the analysis was 96.5 (SD = 4.3) for Load 1 and 91.1 (SD = 8.8) for Load 2. The remaining trials were averaged by experimental condition and only trials in which the individual provided a correct response were included in the average. The mean percentage of correct responses for Load 1 and Load 2 combined was 94 (SD = 9.5). Subtracting the Congruent condition from the Incongruent condition derived difference waveforms. Difference waveforms were used to isolate N400 activity (i.e., the congruency effect). Individual waveforms were averaged together to create grand average waveforms for both the experimental conditions and the difference waveforms.

Statistical analyses were conducted on both the behavioural and electrophysiological data. The behavioural and the electrophysiological analyses were conducted using a repeated measures analysis of variance (ANOVA) with conservative degrees of freedom (Greenhouse and Geisser, 1959). Significant main effects and interactions were submitted to additional post-hoc analyses using the Tukey Honestly Significant Difference (HSD) test. An alpha level of $p < 0.05$ was required for statistical significance.

Accuracy and reaction time (RT) data were analyzed separately, with the factors being Order (2 levels), WM Load (2 levels), and Congruency (2 levels). Before deriving

the individual mean RTs, trials with values greater than 2 s, outliers (±2 *SD*), and errors were excluded from the analysis. The main ERP factors were Order (2 levels), WM Load (2 levels), Congruence (2 levels), and Region (9 levels). Any interactions (using peak scoring) involving the factor Region were subjected to additional normalization procedures (McCarthy and Wood, 1985). The number of statistical comparisons across electrode sites was reduced to nine scalp regions using a linear derivation to re-compute the waveforms. The electrodes were separated laterally into left (L), midline (M), and right (R) sectors. The sectors were then subdivided into frontal (F), central (C), and posterior (P) sectors to obtain the nine regions (LF, MF, RF, LC, MC, RC, LP, MP, and RP). Ten electrode sites were used to compute the waveform for each region. For two individuals (S02 and S13), the MP and MF sections (respectively) contained data from only nine electrodes because noisy electrodes were excluded.

Source analysis was conducted using BESA (Brain Electromagnetic Source Analysis, MEGIS version 3.0) and is necessarily an approximation. Difference waveforms were examined to isolate N400 activity and limit the number of dipoles in the solution. Load 1 and Load 2 were modeled separately because it was assumed that active brain regions might change as WM Load increased. Due to the intensive nature of the analysis, solutions were obtained using grand average waveforms (Picton et al., 1995; Scherg and Picton, 1991; Scherg, Vajsar, and Picton, 1989). An advantage of grand average models is that they provide a global estimate of the active regions across individual data sets. However, inter-individual variance was considered as a factor in source localization (Haan et al., 2000). The regional source models were empirically

evaluated using individual data in order to determine whether the fit was reliable. An overview of the modeling procedure is provided below.

Channel labels as well as the theta (azimuth angle with the z-axis) and phi (latitude angle with the x-y plane) positional values were imported into BESA. Additional electrode locations were determined using the 10/10 system electrode landmarks. The data were pre-processed further using a more conservative artifact rejection procedure to minimize ocular artifacts (-100 ms to 1000 ms; Load 1 accepted trials $\underline{M} = 91.0\%$, $SD = 14.9$; Load 2 accepted trials $\underline{M} = 85.1\%$, $SD = 14.8$). As a standard procedure in BESA, the averaged data (0 ms to 1000 ms) were also re-filtered with the low pass setting at 10 Hz and residual EOG artifact activity was accounted for by using an ocular regional source. Artifact channels and electrodes contaminated with noise (e.g., electrodes over the ears) were excluded from the analysis.

A principal component analysis (PCA) was used to estimate the number of sources, assuming that the decomposed source activities were not independent. A regional source strategy was selected to localize the dipoles and identify the source waveforms (Scherg, Vajsar, and Picton, 1989). In the initial model, regional sources (comprising three orthogonally oriented dipoles in the same location) were used to identify active areas of current flow. To begin, sources were placed in established N400 regions (see Introduction section). Additional sources were added if required and the locations were fitted separately and together until the model achieved stability. Once active regions were identified, releasing the regional constraints and fitting the individual dipoles (separately and together) formed an advanced model. Bilateral location constraints were used throughout the fitting procedure because releasing them reduced

the RV by less than 0.5%. An Energy criterion (20%) was used in the fitting procedures in order to minimize source interactions (i.e., linear dependency, see Chapter Two).

The validity of the model was evaluated using goodness-of fit/residual variance (RV), the projected spline maps, and prior physiological and anatomical evidence. Response-related dipoles were included within the model for additional physiological validation. The Load 1 and Load 2 models were also evaluated using individual data sets. Regional sources were selected to test the number and location of the sources, independent of the orientation. Difference waveforms for all participants were imported into BESA using the same parameters applied to the grand average waveforms. Only the response hand source that matched the individual's response hand was active (e.g., right hand – left source). The RV for the 303 ms to 505 ms interval-of-interest was then recorded to evaluate the model's goodness of fit (for both grand average and individual data).

Chapter Three - Results

I. Behavioural analysis

The objective of the behavioural analysis was to evaluate the hypothesis that the fan-effect would be replicated. The accuracy data were analyzed using a repeated measures ANOVA with Order (2 levels), Congruency (2 levels), WM Load (2 levels) as factors (Table 6). There was a significant main effect of Congruency, $F(1,14) = 5.70$, $p < 0.05$, indicating that the participants' performance was better for Incongruent words ($\underline{M}$ = 95.2 % correct, $SE = 1.6$) than for Congruent words ($\underline{M}$ = 92.6 % correct, $SE = 2.1$). There were no other significant main effects or interactions.

The RT data were analyzed using a repeated measures ANOVA with the same factors (Table 6). There was a significant main effect of Order, $F(1,14) = 5.21$, $p < 0.05$, with shorter RTs in the Load 1 - Load 2 Order ($\underline{M}$ = 740 ms, $SE = 71$) and longer RTs in the Load 2 - Load 1 Order ($\underline{M}$ = 970 ms, $SE = 71$). The main effect of Congruency factor was also significant ($F(1, 14) = 30.28$, $p < 0.0001$) with shorter RTs in the Incongruent condition ($\underline{M}$ = 840 ms, $SE = 50$) and longer RTs in the Congruent condition ($\underline{M}$ = 870 ms, $SE = 51$). Importantly, there was a significant main effect of WM Load, $F(1,14) = 10.55$, $p < 0.01$, indicating that the RTs in Load 1 ($\underline{M}$ = 781 ms, $SE = 49$) were shorter than those in Load 2 ($\underline{M}$ = 929 ms, $SE = 61$).

There was also a significant interaction between the Congruency and WM Load factors, $F(1,14) = 5.91$, $p < 0.05$. Subsequent post hoc analyses revealed that Load 1 RTs were shorter than Load 2 RTs, with the Incongruent condition showing the maximum difference between Load 1 and Load 2 (~168 ms delay) (Table 7). At Load 1, there were significant Congruency differences (Incongruent < Congruent; ~ 50 ms), but no

Table 6

Behavioural Analyses: Performance and RTs

Analysis	Factor	*F*	df	*p* <
Performance				
	Order	0.39	1,14	0.542
	Congruency	5.70	1,14	0.032
	WM Load	3.15	1,14	0.098
	O X C	2.64	1,14	0.127
	O X WM	3.68	1,14	0.076
	C X WM	0.13	1,14	0.721
	O X C X WM	1.19	1,14	0.293
RT				
	Order	5.21	1,14	0.039
	Congruency	30.28	1,14	0.0001
	WM Load	10.55	1,14	0.006
	O X C	3.09	1,14	0.100
	O X WM	1.94	1,14	0.185
	C X WM	5.91	1,14	0.029
	O X C X WM	0.02	1,14	0.881

Table 7

Mean RTs (in ms) and Standard Error for Congruence and WM Load

Congruence WM Load	Mean RT	Standard Error
Congruent		
Load 1	806	49
Load 2	934	61
Incongruent		
Load 1	756	50
Load 2	924	61

differences existed at Load 2 (~ 10 ms difference). All other interactions were not significant.

In order to determine whether differences in the fan-effect existed between the High and Low groups, the data were reanalyzed using the between-subjects factor WM Group (High and Low groups, see Methods section) instead of the Order factor. The same within-subjects main effects and interaction were again significant following the reanalysis (i.e., Congruency, WM Load, and Congruency X WM Load; all $F > 5.0$ and $p < 0.05$; replicating the prior result). In addition, there was a significant WM Group X WM Load interaction, $F(1,14) = 5.46$, $p < 0.05$. Post hoc analyses revealed that the fan-effect for the Low group was larger than that of the High group (Table 8). The Congruency X WM Load and WM Group X WM Load interactions are depicted in Figure 9.

II. Electrophysiological analysis

The main objective of the ERP analysis was to evaluate the effects of Congruency and WM Load on the N400. Figure 10 presents grand average waveforms for the Congruent and Incongruent conditions at Load 1 and Load 2. The initial analysis examined the standard waveforms with Order (Load 1 - Load 2 and Load 2 - Load 1), Congruency (Congruent and Incongruent), WM Load (Load 1 and Load 2), and Region (LF, MF, RF, LC, MC, RC, LP, MP, and RP) as factors. Follow-up analyses examined more closely the effects of WM on the amplitude and latency characteristics of the N400 using difference waveforms. Examination of the data (Fig. 10) revealed that, as expected, the experimental effects were observed primarily in the N400 component. However, the N200 component was also analyzed in order to determine whether it was sensitive to

Table 8

Mean RTs (in ms) and Standard Error for WM Group and WM Load

WM Group	Mean Amplitude	Standard Error
WM Load		
High		
Load 1	742	75
Load 2	987	100
Low		
Load 1	820	75
Load 2	871	100

Figure 9 - Caption

The figure shows a replication of the fan-effect. **A.** Mean RT data for Congruent (- - -) and Incongruent (——) conditions at the two levels of WM Load (Load 1 and Load 2). Increased WM Load resulted on longer RTs in both the Congruent and Incongruent conditions. RT differences between Congruent and Incongruent were significant only at Load 1. **B.** Mean RTs for the High (——) and Low (- - -) groups (WM span) at the two levels of WM Load. The Low group has a larger fan-effect than the High group (see text for details). WM Load is on the x-axis and RT (ms) is on the y-axis. Note that the scales are set to the separate RT ranges.

Figure 9

The Fan-Effect Replication of RT Findings

A.

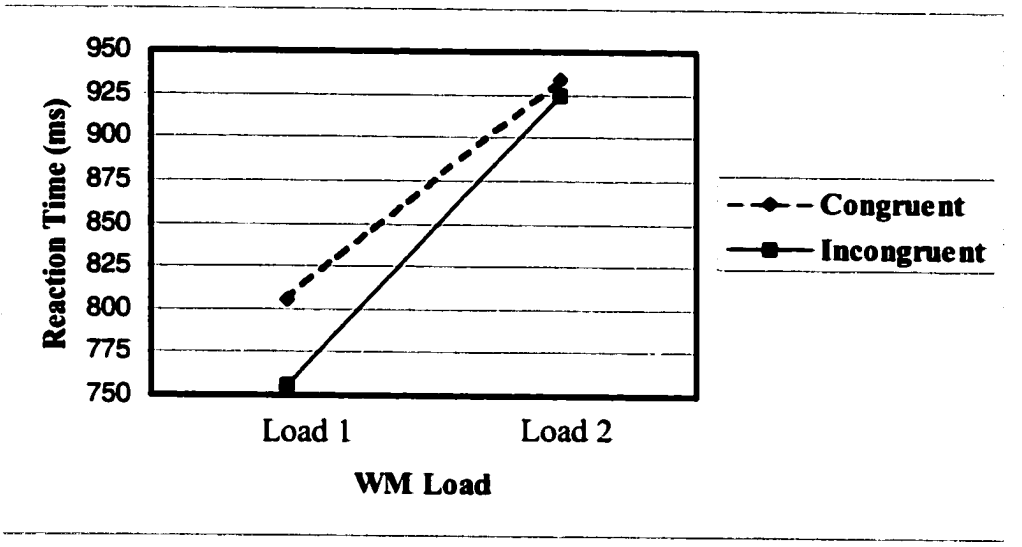

B.

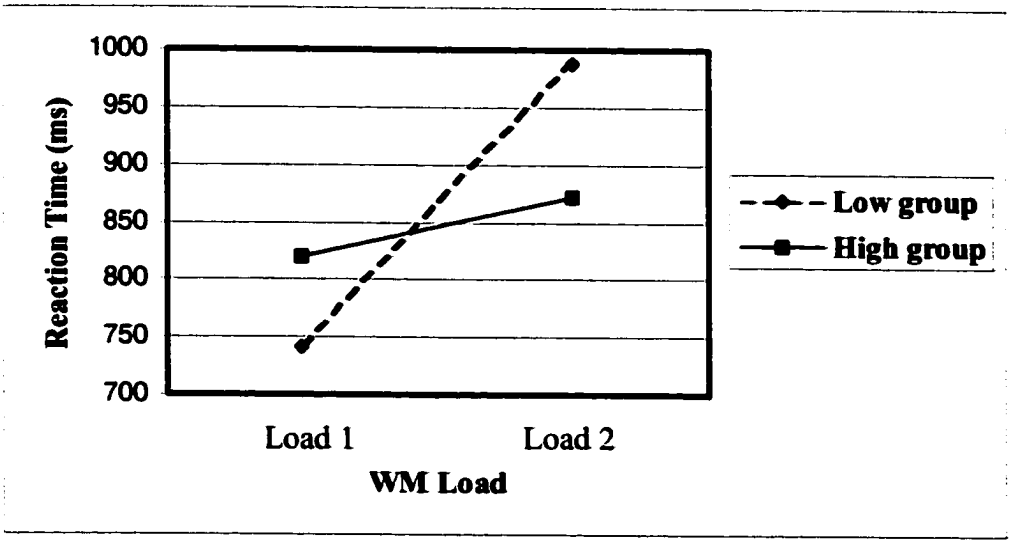

Figure 10 - Caption

Grand average ERPs (N = 16) to terminal words in the Congruent Load 1 (— — —), the Congruent Load 2 (- - - -), the Incongruent Load 1 (————), and the Incongruent Load 2 (— - —) conditions. Nine regions (ten electrodes per region, from a 128 channel system) across the scalp are presented. EOG sites (HEOG, LVEOG, and RVEOG) were artifact free (data not shown). A N400 component was elicited in both Incongruent Load 1 and Load 2 conditions. The N400 in the Load 2 condition was reduced in relative peak amplitude and delayed in peak latency. Time (ms) is on the x-axis and Voltage (μV) is on the y-axis (negative is up).

Figure 10

Grand Average Waveforms (N=16), Nine Regions

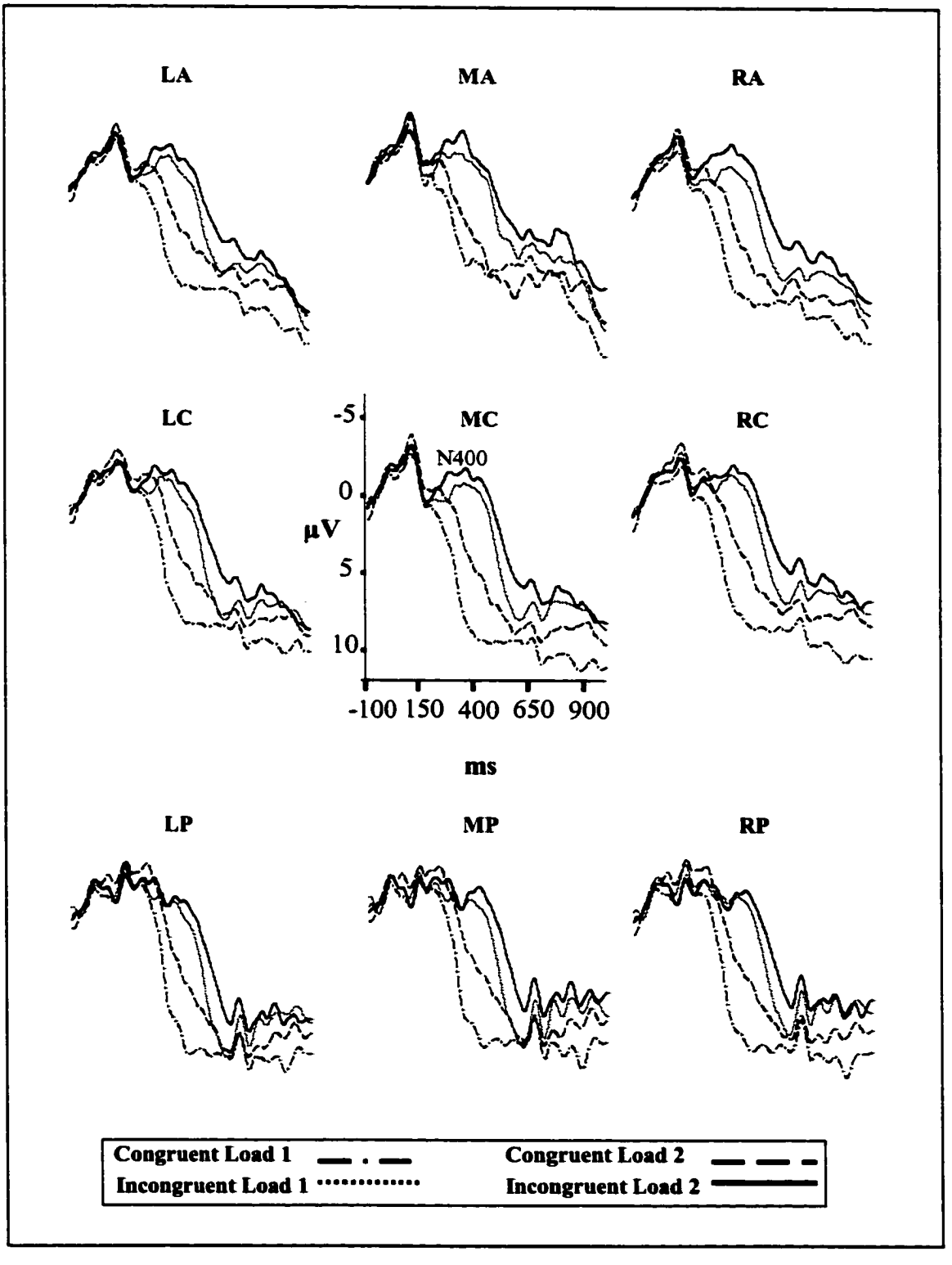

attentional effects resulting from the Order factor (cf. Prichard et al., 1991).

N400 standard waveform analysis: As stated previously, the N400 was the primary component of interest. The initial ANOVA was conducted on the 350-450 ms time interval (average amplitude method) (Table 9). There was a significant main effect of Congruency ($F(1,14) = 107.73$, $p < 0.0001$) with larger negative-going amplitudes in the Incongruent condition ($\underline{M} = -0.59$, $SE = 1.09$) compared to those in the Congruent condition ($\underline{M} = 5.99$, $SE = 1.35$). There was also a significant main effect of WM Load ($F(1,14) = 24.60$, $p < 0.0001$) resulting from more positive amplitudes in Load 1 ($\underline{M} = 3.86$, $SE = 1.15$) as compared to Load 2 ($\underline{M} = 1.54$, $SE = 1.26$). This result reflected the smaller positive-going response in the Congruent condition. There were no other significant main effects.

The Congruency X WM Load interaction was significant, $F(1,14) = 11.49$, $p < 0.005$. Subsequent post-hoc analyses revealed that the difference between the Incongruent and Congruent conditions was reduced as WM Load increased (~ 3.76 μV) (Table 10). While the amplitudes in the Incongruent condition did not differ between Load 1 and Load 2, the positive amplitudes in the Congruent condition at Load 1 were significantly reduced at Load 2. This interaction was consistent with the interpretation that the WM Load main effect reduced the positive-going response in the Congruent condition. All other interactions were not significant.

N400 difference waveform analysis: Follow-up analyses were directed specifically at WM influences on the amplitude and latency characteristics of the N400. In order to examine more closely the effects of WM Load on the N400, difference waveforms were derived by subtracting the Congruent condition from the Incongruent

Table 9

Repeated Measures ANOVA for the N400:

Standard Waveforms Analysis

Analysis	Factor	*F*	df	*p* <
N400				
	Order	3.02	1,14	0.104
	Congruency	107.73	1,14	0.0001
	WM Load	24.60	1,14	0.0001
	Region	2.24	8,112	0.107
	O X C	1.88	1,14	0.192
	O X WM	4.29	1,14	0.057
	O X R	0.59	8,112	0.603
	C X WM	11.49	1,14	0.004
	C X R	2.12	8,112	0.128
	WM X R	2.48	8,112	0.079
	O X C X WM	0.19	1,14	0.667
	C X R X O	0.44	8,112	0.684
	O X WM X R	0.93	8,112	0.430
	C X WM X R	1.34	8,112	0.277
	C X WM X R X O	0.30	8,112	0.687

Table 10

Mean Amplitudes (in μV) and Standard Error of the N400 response for Congruence and WM Load

Congruence WM Load	Mean Amplitude	Standard Error
Congruent		
Load 1	7.87	1.34
Load 2	4.11	1.44
Incongruent		
Load 1	-0.15	1.14
Load 2	-1.04	1.12

condition. Peak amplitude and latency values were obtained for the most negative-going peak occurring in the 300 ms to 600 ms time period (peak scoring method). Separate ANOVAs were conducted on the amplitude and latency data variables (both with WM Load (2 levels) and Region (9 levels) as factors) (Table 11).

Figure 11 depicts the N400 in difference waveforms for Load 1 and Load 2 at all nine regions. In the amplitude analysis, there was a significant main effect of WM Load ($F(1,15) = 9.2$, $p < 0.01$), indicating that the N400 amplitudes were larger in Load 1 ($\underline{M}$ = -10.45, $SE = 0.89$) than in Load 2 ($\underline{M}$ = -8.15, $SE = 0.63$). The main effect of WM Load was consistent with the significant Congruency X WM Load interaction in the previous standard waveform analysis. There was also a significant main effect of Region ($F(8,120) = 2.74$, $p < 0.05$, $\varepsilon = 0.469$) and subsequent post hoc analyses revealed that the N400 peak was largest in the MC region (Table 12). The WM Load X Region interaction was not significant ($F < 1.0$).

With respect to peak latency, there was a significant main effect of WM Load, $F(1,15) = 11.21$, $p < 0.005$. The peak latencies for Load 1 ($\underline{M}$ = 397.6 ms, $SE = 10.35$) were shorter than peak latencies for Load 2 ($\underline{M}$ = 448.4 ms, $SE = 11.24$), demonstrating a significant N400 latency delay resulting from increased WM Load (~50.8 ms). Neither the Region main effect nor the WM Load X Region interaction was significant ($F < 1.0$).

Individual N400 peak latency delay: Because individual differences in WM capacity have proven to be important in behavioural work (Engle, 1996), the relationship between individual WM differences and N400 peak latency delays was explored further. The objective of this analysis was to evaluate whether the latency delays would correlate significantly with WM capacity. For each participant, the N400 peak latencies were

Table 11

Repeated Measures ANOVA for the N400:

Difference Waveforms Analyses

Analysis	Factor	*F*	df	*p* <
Amplitude				
	WM Load	9.20	1,15	0.008
	Region	2.74	8,120	0.040
	WM X R	0.95	8,120	0.392
Latency				
	WM Load	11.21	1,15	0.004
	Region	0.29	8,120	0.851
	WM X R	0.50	8,120	0.629

Figure 11 - Caption

Grand average difference waveforms derived by subtracting the Congruent conditions from the Incongruent conditions. The difference waveforms depict the changes in amplitude and latency as a function of WM Load. There was a reduction in peak amplitude and a delay in peak latency. Nine regions show the Midline Central (MC) distribution of the N400. The N400 peaked around the 400 ms range. All other details as for Fig. 10.

Figure 11

Grand Average Difference Waveforms (N=16), Nine Regions

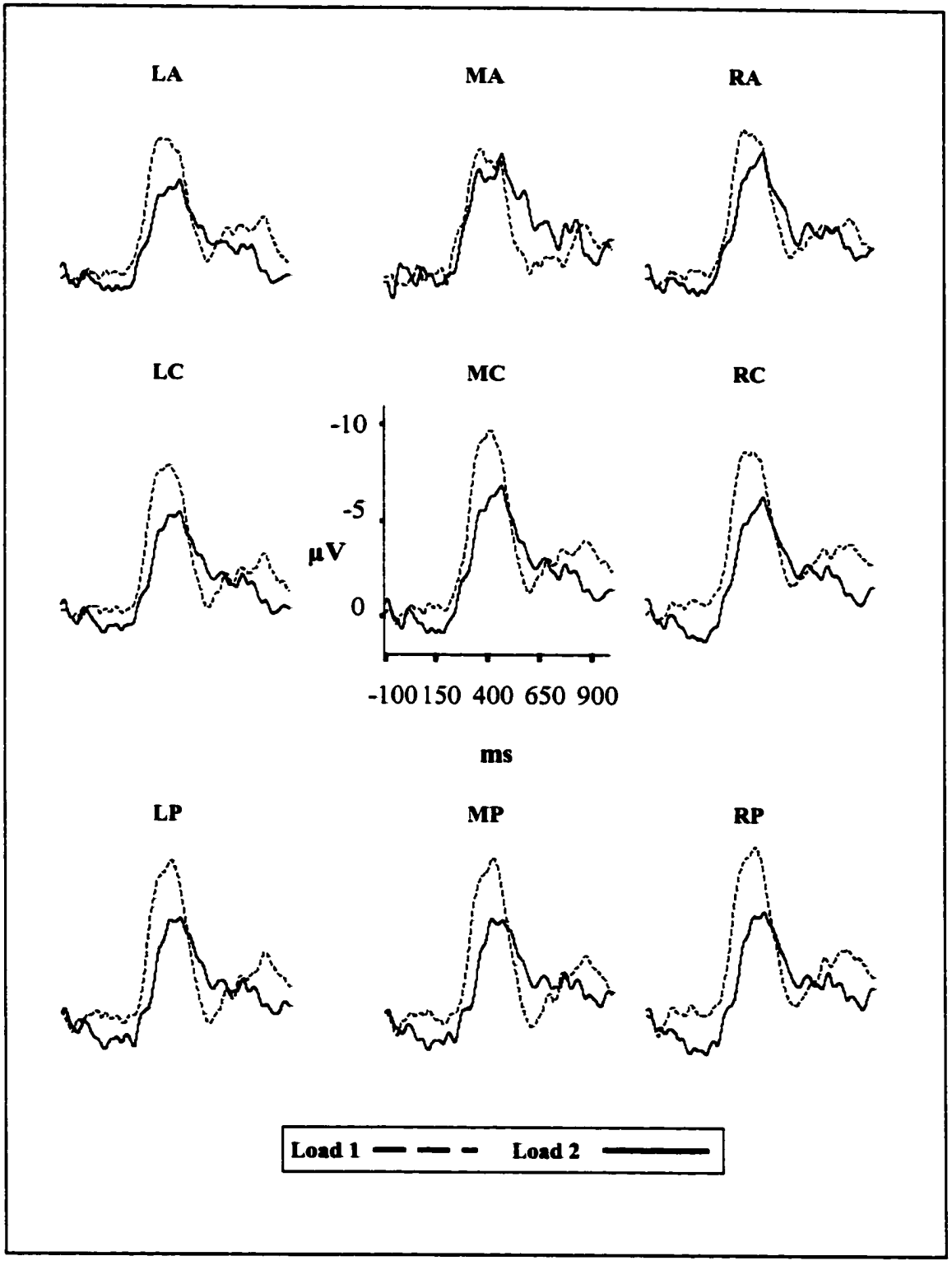

Table 12

Mean Amplitudes (in μV) and Standard Error of the N400 response for Region

Region	Mean Amplitude	Standard Error
LF	-8.30	0.72
MF	-9.53	0.79
RF	-9.39	0.87
LC	-8.79	0.76
MC	-10.45	0.77
RC	-9.34	0.66
LP	-9.10	0.79
MP	-9.23	0.72
RP	-9.56	0.64

obtained for Load 1 and Load 2 using the MC regions from both the difference and standard waveforms. Subtracting the latency values at Load 2 from those at Load 1 derived the peak latency delay.

Examination of the latency delays using difference waveforms revealed no significant correlations with individual WM capacity. However, a correlation analysis of latency delays in the standard waveforms revealed a significant inverse relationship (two-tailed) with performance on Digit Span. N400 peak latency delays correlated negatively with both the Total scores ($r = -.52$, $p < 0.05$) and, more importantly, they also correlated negatively with the Backward scores ($r = -.55$, $p < 0.05$). However, the latency delays did not correlate with the Forward scores ($r = -.27$, $p = 0.315$). These results provided preliminary indications that peak latency delays were sensitive to individual WM capacity.

Attentional analysis: As a result of behavioural evidence for Order effects, an additional analysis was conducted in order to determine whether a N200 component was sensitive to task-related attentional demands (Prichard et al., 1991). Specifically, the amplitude of the N200 was examined in order to determine whether it varied as a function of Order (Load 1 - Load 2 and Load 2 - Load 1). Figure 12 depicts grand average waveforms showing a pronounced N200 in *both* the Congruent and Incongruent conditions for Load 2; only when it was given first. Accordingly, a repeated measures ANOVA was conducted on the 200 to 300 ms time interval (average amplitude method) in order to evaluate the effect of Order on the N200 (Table 13). As before, the factors were Order (Load 1 - Load 2 and Load 2 - Load 1), WM Load (Load 1 and Load 2), Congruency (Congruent and Incongruent), and Region (LF, MF, RF, LC, MC, RC, LP,

Figure 12 - Caption

Grand average waveforms (Midline Posterior, MP) showing the effects of Order (of presentation) on the N200 component. Top: ERPs for participants who received Load 1 first and Load 2 second (Load 1 - Load 2). Bottom: ERPs for participants who received Load 2 first and Load 1 second (Load 2 - Load 1). Attentional effects were present, with a pronounced N200 in both Congruent and Incongruent conditions in the Load 2 condition *only* when the Order was Load 2 - Load 1. Statistical analysis showed that the N400 was relatively unaffected by the Order factor (see text for more information). All other details as for Fig. 10.

Figure 12

Attentional Analysis, N200, (N=8 per group), Nine Regions

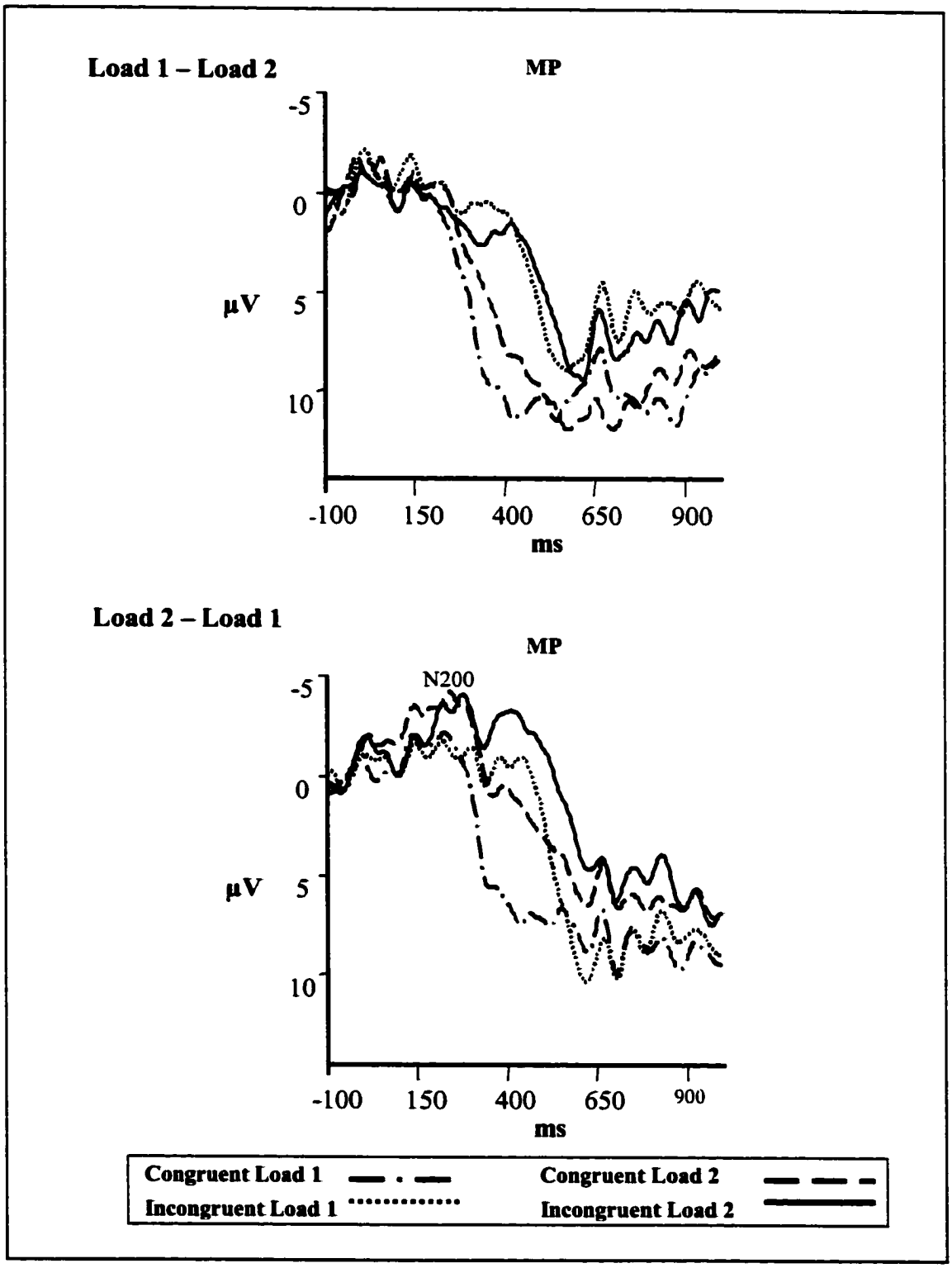

Table 13

Repeated Measures ANOVA for the N200:

Attentional Analysis

Analysis	Factor	*F*	df	*p* <
N200				
	Order	0.99	1,14	0.337
	Congruency	19.30	1,14	0.001
	WM Load	0.02	1,14	0.898
	Region	1.65	8,112	0.209
	O X C	0.82	1,14	0.380
	O X WM	6.44	1,14	0.024
	O X R	0.34	8,112	0.728
	C X WM	0.68	1,14	0.424
	C X R	7.44	8,112	0.001
	WM X R	3.19	8,112	0.037
	O X C X WM	1.32	1,14	0.271
	C X R X O	0.86	8,112	0.455
	O X WM X R	2.59	8,112	0.071
	C X WM X R	0.64	8,112	0.538
	C X WM X R X O	1.58	8,112	0.223

Table 14

Mean Amplitudes (in μV) and Standard Error of the N200 response for Order and WM Load

Order	Mean Amplitude	Standard Error
WM Load		
Load 1 - Load 2		
Load 1	0.29	1.22
Load 2	2.69	1.68
Load 2 - Load 1		
Load 1	0.71	1.22
Load 2	-1.45	1.68

MP, and RP).

There was a significant main effect of Congruency ($F(1,14) = 19.3, p < 0.005$) with more pronounced N200 in the Incongruent condition ($\underline{M} = -0.920$, $SE = 1.03$) than in the Congruent condition ($\underline{M} = 1.03$, $SE = 0.957$). Importantly, there was a significant Order X WM Load interaction ($F(1,14) = 6.44, p < 0.05$) and post hoc analyses showed that for Load 2, the N200 amplitudes in Order Load 2 - Load 1 were significantly different than those in Load 1 - Load 2 (Table 14). The results confirmed that a larger N200 component occurred in Load 2 when it was presented first (collapsed across the Congruency factor). There were also significant WM Load X Region ($F(8,112) = 3.2, p < 0.05$) and Congruency X Region ($F(8,112) = 7.44, p < 0.005$) interactions. However, evidence for the N200 distribution was not apparent in these interactions because the Order factor had been collapsed across. Interestingly, there was no Congruency X WM Load interaction (or a three-way interaction with Order) suggesting that the WM influences on sentence processing were somewhat restricted to the N400.

III. Source analysis

The objective of the source analysis was to evaluate WM effects on the N400 intracranial generators. The specific goals were to: 1) localize the N400 sources in Load 1 and Load 2 separately; and 2) examine whether differences existed between Load 1 and Load 2. Difference waveforms were used to isolate the N400 sources for both Load 1 and Load 2. Separate dipole models were derived for both levels of WM Load. Figure 13 and Figure 14 depict the source models for Load 1 and Load 2, respectively.

Initial examination revealed a remarkable overlap between the N400 sources localized for Load 1 and Load 2. The source locations for Load 1 are presented in Figure

13a. There were a number of active bilateral areas, including the lateral occipital gyri ($N400_{S1}$: BA 18), the occipital-temporal regions ($N400_{S2}$: BA 19), and the temporal poles ($N400_{S3}$: BA 38). An additional source was localized to the left superior temporal gyrus or STG ($N400_{S4}$: BA 22).

The source locations for Load 2 are presented in Figure 14a. The N400 sources were localized to the same bilateral areas: $N400_{S1}$ in the lateral occipital gyri (although slightly inferior to the sources in Load 1); $N400_{S2}$ in the occipital-temporal regions; $N400_{S3}$ in the temporal poles; and $N400_{S4}$ in the left STG. In addition, a novel source was modeled in the left inferior parietal lobe ($N400_{S5}$: BA 40). The novel activation associated with $N400_{S5}$ was consistent with the well-defined region, which has been identified as supporting verbal working memory (Cabeza and Nyberg, 2000; Miyake and Shah, 1999).

Examination of both Load 1 source waveforms (Fig. 13b) and Load 2 source waveforms (Fig. 14b) revealed clear peak activation in the N400 time range (~ 404 ms), replicating the findings in Chapter Two. Importantly, there were also identifiable differences in the activation between the two levels of WM Load. Figure 15 presents a direct comparison of the source waveforms for Load 1 and Load 2 in order to visualize better the WM-related differences. A number of sources ($N400_{S1,S2,S4}$) showed more pronounced peak activation in the N400 time range at Load 1. In contrast, the anterior temporal and left parietal sources ($N400_{S3,S5}$) were characterized by enhanced activation in Load 2. Further, a probe dipole in Load 1 for the $N400_{S5}$ region revealed no deflections in the source waveform. Overall, the changes in source activation between the two levels

Figure 13 - Caption

Brain electromagnetic source analysis (BESA) showing the N400 source model for Load 1. **A.** Sagittal and axial views depicting dipoles from N400 waveforms. Bilateral N400 sources were localized to the lateral occipital gyri (BA: 18), the occipital-temporal regions (BA: 19), and the temporal poles (BA: 38). An additional left hemisphere source was localized to the superior temporal gyrus (BA: 22). The ocular and central sulci sources explained residual EOG and behavioural 'response-related' activation, respectively. **B.** Source waveforms reflecting the contributions of dipoles to the scalp recorded activity. The N400 source waveforms revealed a prominent peak in the 400 ms time range. **C.** A comparison of the data maps (spline and CSD) with the model maps for the N400. The iso-contour lines are separated by 2 μV and grey regions represent negative activation. The projected maps are very similar to the actual scalp distribution of the N400. The goodness-of-fit (solid line) and global field power (dashed line) for the full epoch (0 ms to 1000 ms). The residual variance was 5.03% for the 303 ms to 505 ms interval-of-interest.

Figure 13

N400 Source Locations and Waveforms: Load 1

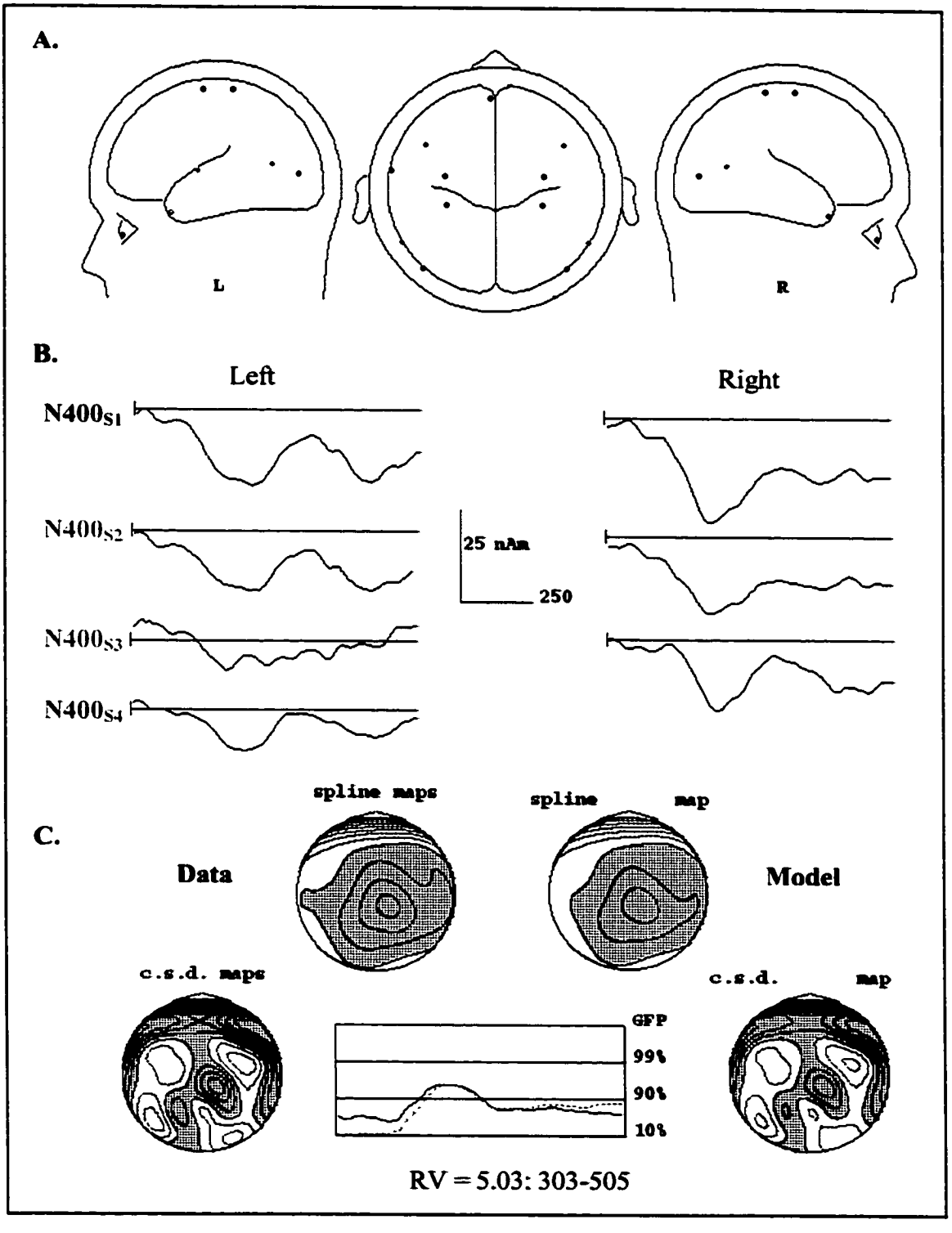

Figure 14 - Caption

BESA showing the N400 source model for Load 2. **A.** Sagittal and axial views depicting dipoles from N400 waveforms. Although separately derived the results were remarkably similar to the Load 1 model. There were bilateral N400 sources localized to the lateral occipital gyri (BA: 18), the occipital-temporal regions (BA: 19), and the temporal poles (BA: 38). There was also a left hemisphere source localized to the superior temporal gyrus (BA: 22). In addition, increased WM Load resulted in a novel source localized to the left inferior parietal lobe (BA: 40). **B.** Source waveforms that show the contributions of N400 dipoles in Load 2. The source waveforms reveal differences as a function of WM Load (see text for details). **C.** A comparison of the data maps (spline and CSD) with the model maps for the N400. The iso-contour lines are separated by 2 μV and grey regions represent negative activation. The projected maps are, again, highly similar to data maps. The goodness-of-fit (solid line) and global field power (dashed line) for the full epoch (0 ms to 1000 ms). The residual variance was 5.86% for the 303 ms to 505 ms interval-of-interest.

Figure 14

N400 Source Locations and Waveforms: Load 2

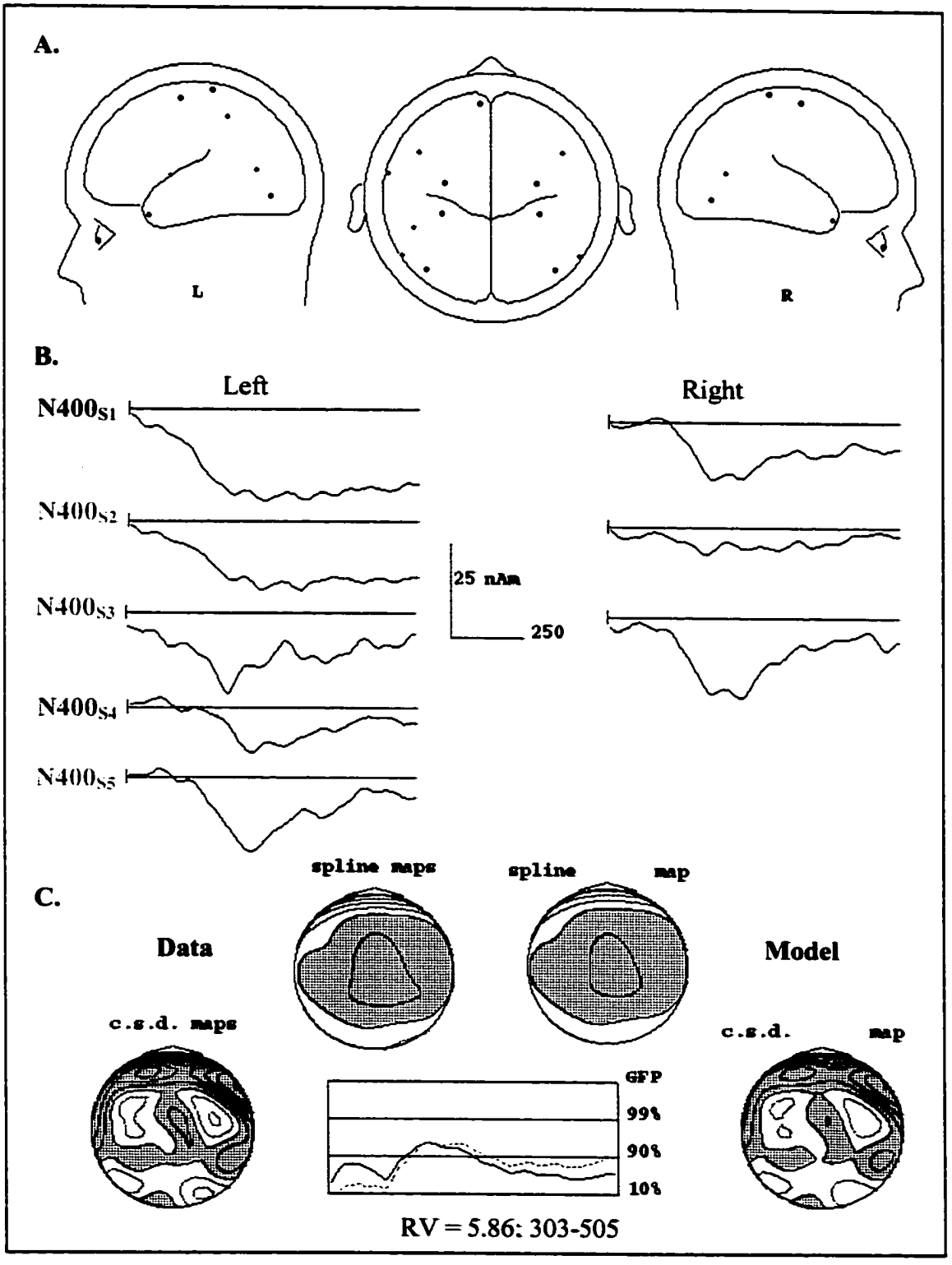

Figure 15 - Caption

The figure shows a direct comparison of the source waveform data between Load 1 and Load 2. The source waveforms are divided on the basis of the functional task requirements. Activation associated with evaluating semantic congruence is observed in the bilateral occipital, bilateral occipital-temporal, and left STG areas (top). In contrast, sources in bilateral temporal poles and left inferior parietal region reflected activation associated with the task-related memory demands. The probe source represents activation for the left parietal region at Load 1. All data are presented on a uniform scale with Time (ms) on the x-axis and Voltage (nAm) and the y-axis.

Figure 15

N400 Source Waveform Comparison: Load 1 and Load 2

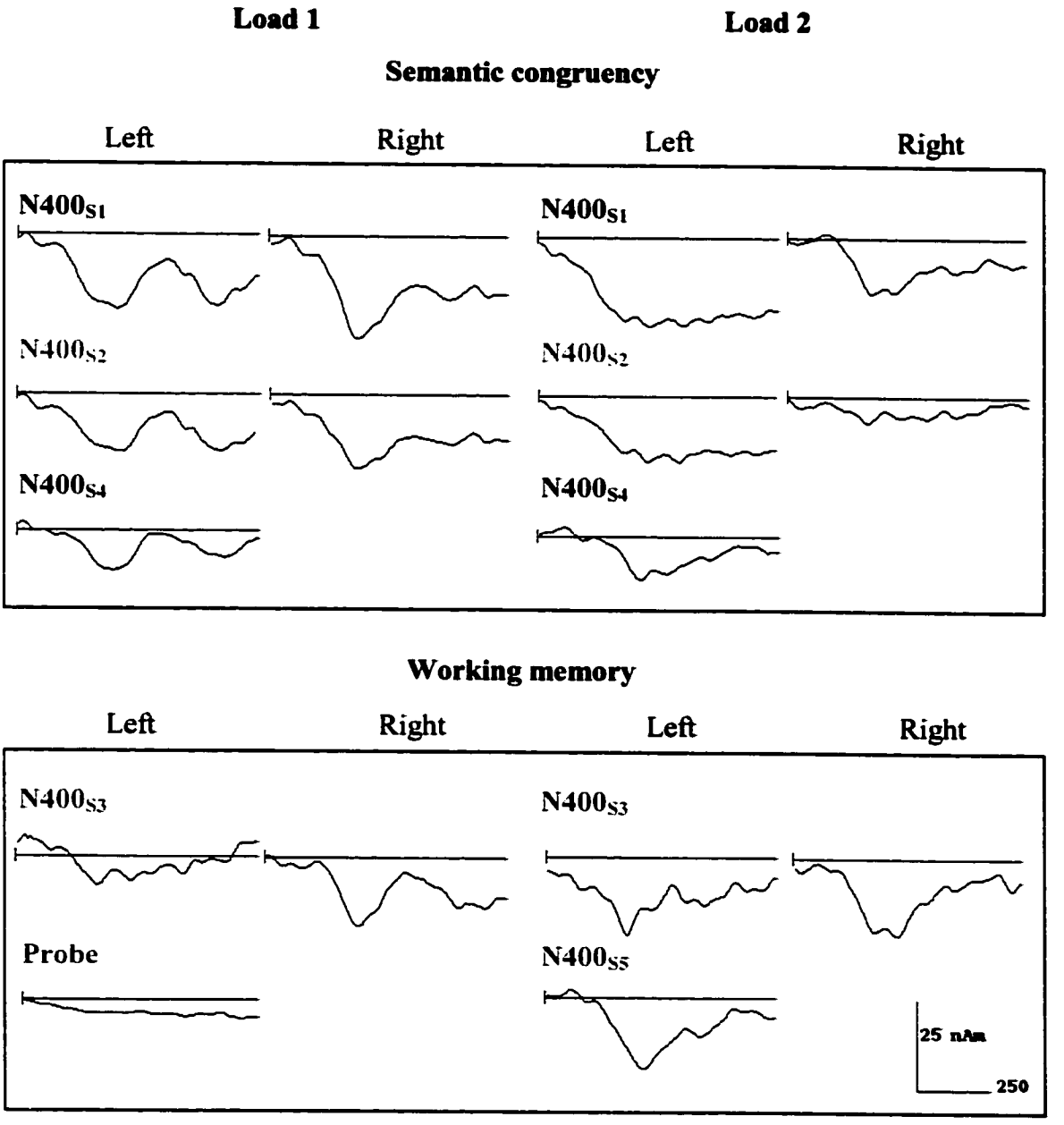

of WM Load suggested that the anterior temporal and left parietal sources were sensitive to mnemonic task requirements.

Evidence for the validity of the Load 1 and Load 2 models is presented in Figure 13c and Figure 14c, respectively. Both the Load 1 and Load 2 models accounted for more 94% of the variance in the N400 time interval-of-interest (303 ms to 505 ms). Specifically, the RV for Load 1 was 5.03% and the RV for Load 2 was 5.86%. Furthermore, the projected topographical maps for the N400 matched closely the data maps. A strong physiological validation of the models was also provided by the localization of response-hand dipoles in the primary motor and sensory cortices. Similar to previous work (Chapter Two), these sources accounted for activation associated with the participants' behavioural responses following terminal word onset.

To evaluate whether the sources localized in grand average models were representative across individuals, the Load 1 and Load 2 initial models were applied to the individual difference waveforms. The source locations for both Load 1 and Load 2 fit the individual data sets reliably. The mean RV for Load 1 was 12.2 (SE = 1.5, range 4.96 to 26.3) and the mean RV for Load 2 was 12.4 (SE = 1.1, range 7.69 to 24.2). The results showed that, on average, both the Load 1 and Load 2 models accounted for more than 87% of the variance in the N400 time interval. These results indicated that the grand average models provide a reasonable estimate of the general regions that were active across individual data sets.

Chapter Three - Discussion

In the current study WM load and semantic congruence were varied independently using a modified version of the fan procedure (Anderson, 1974, 1983). Overall, the findings demonstrated that WM influenced both the peak amplitude and latency of the N400, with the latency effects being of particular significance. Intracranial generators for the N400 were localized in brain areas associated with processing semantic congruencies and memory, with increased WM changing source activation.

I. Establishing the fan and congruency effects

Analysis of the behavioural RT data revealed the presence of a fan-effect (Hypothesis 1, Fig. 9). Specifically, the increase in WM load from Load 1 to Load 2 resulted in a corresponding increase in RTs and this effect was most pronounced in participants who had low WM capacity. It should be noted that the modified fan procedure differed from typical fan procedures in two main respects. First, participants were not required to study a propositional set prior to the experiment because the paradigm utilized semantic hierarchical associations derived from general knowledge (Chapter Two). Second, the task was limited by methodological constraints to memory set sizes of either one or two propositions (see Methods section). In contrast, traditional fan procedures have used at least three set sizes (e.g., 1, 3, and 4; Fig. 8). While the data do not provide evidence of the fan-effect beyond set sizes greater than two propositions; the preliminary results are promising. Indeed, the magnitude of the RT delays (~168 ms) falls nicely within the expected range (~150 to 200 ms) (e.g., Cantor and Engle, 1993). Thus, it is reasonable to predict similar RT trends in this task when larger propositional set sizes are used in future research.

Semantic congruency ERP effects were linked directly to the N400 response. The analyses of both the N200 and N400 confirmed that only the latter was significantly enhanced following semantically incongruent terminal words. In contrast, the N200 was sensitive to task difficulty and related attentional effects (Prichard et al., 1991). That is, when overall task difficulty was increased (by reversing the presentation order, Load 2 - Load 1), attentional effects were present in the N200[9] for *both* the Congruent and Incongruent conditions. However, there was no significant order effect observed for the N400 (Fig. 12). This finding successfully demonstrated that N400 activity is intimately linked to semantic neural systems, for which the effects of WM load can be examined in detail.

In terms of semantic comprehension, the left perisylvian region has consistently been identified as one of the primary contributors to the N400 (Figs. 13 and 14), for both visual and auditory studies, using both ERPs and MEG (Chapter Two; Helenius et al., 1998; Helenius et al., 2002; Simos et al., 1997). This result is remarkably consistent with PET and fMRI studies on language in general (Cabeza and Nyberg, 2000; Price, 2000, Démonet and Thierry, 2001). In addition, it appears that in the visual modality, N400 activity may also be extended to include posterior visual areas, possibly involving the ventral visual stream (Kolb and Whishaw, 1996; Ungerleider and Mishkin, 1982). The active visual areas included the lateral occipital gyri ($N400_{S1}$) and the occipital-temporal regions ($N400_{S2}$). These sources matched neuroimaging work that has localized

[9] These results were similar to the negativity reported by Mecklinger et al. (1993), suggesting that attentional task demands are primarily limited to the N200 and have minimal influence on the N400 (Prichard et al., 1991).

activation in similar regions during visual word form processing (e.g., Kuriki, Takeuchi, and Hirata, 1998).

II. Working memory effects on the N400

Increased WM load reduced the N400 amplitude and delayed its latency (Figs. 10 and 11). The amplitude reduction was consistent with the findings reported by Gunter et al. (1995). In fact, it is noteworthy that in the current study, semantically unrelated sentences were used in a younger sample and the results were highly comparable to the young non-thematic condition in the Gunter et al. (1995) study. Specifically, in both studies there was a prominent reduction in the congruency effect, which resulted from a smaller positive-going component in the Congruent condition as WM load increased. However, these results suggest that changes in the N400 amplitude do not directly index WM influences on semantic neural systems. There were no significant changes in the N400 peak amplitude in the Incongruent condition (Fig. 10), suggesting that the activation (i.e., uniform summation of EPSPs and/or IPSPs in cortical pyramidal neurons) elicited by semantic violations was relatively unaffected by WM load. Instead, the presence of amplitude changes in the Congruent condition (i.e., the positive-going response) may have indicated that WM demands altered recognition processes related to the evaluation of semantically *acceptable* words. This interpretation is supported by examination of the source waveform data (Figs. 13, 14, and 15). WM changes in source activation were not characterized by a dramatic reduction in source strength - in spite of the fact that the scalp recorded waveforms and spline maps clearly showed a reduction in

N400 amplitude[10] (Fig. 14). Therefore, the apparent amplitude reductions were likely due to an attenuation of phasic activation as a function of WM influences on processing acceptable sentence endings (i.e., in the positive-going response).

In contrast to the amplitude differences, the N400 latency delay (of about 50 ms) in the Incongruent condition was a direct result of increased WM load (Hypothesis 2, Fig. 11). This finding is critically important because it provides the first evidence of early delays in the temporal nature of semantic processing due to memory. It is likely that these early delays ultimately result in the behavioural fan-effect (as measured by RTs). This result also represents the first evidence for memory-based influences on the N400 latency. Interestingly, the 50 ms delay fits remarkably well within the original Sternberg (1969) estimates of the scanning slopes for active memory (36 ms for digits, 45 ms for nonsense forms, and 56 ms for faces). Given that the N400 in this study reflected processes linked to controlled post-lexical semantic integration (Federmeier and Kutas, 1999), it is possible that the latency delay results from increased demands during the retrieval of information from LTM. In support of this interpretation, there were preliminary indications that individual latency delays were related to individual WM capacities. Provided that further research confirms and elucidates this relationship, the results may shed light on theories about individual differences in WM capacity[11] and reading comprehension (Engle, 1996). In particular, it would be interesting to investigate

---

[10] From a physiological perspective, it is essential to note that the analysis (and related interpretation) assumes that congruent and incongruent stimuli were processed by, at least, partially overlapping generators (hence the use of difference waveforms). Given that there was no interaction involving the Congruency and Region factors, this assumption appears to be valid in this instance.

[11] Extensions of this work should include dual task measures that are more sensitive to WM capacity (e.g., word span, Daneman and Carpenter, 1980).

whether N400 latency-delay can be used as a physiological factor that predicts an individual's WM capacity.

III. Partitioning WM: Insights from neuroimaging data

Since its conception (Baddeley and Hitch, 1974), WM has been regarded as a mechanism or process with specialized components that include a supervisory system (the central executive), as well as temporary memory systems for storing phonological (the phonological loop) and visuospatial (the visuospatial sketch pad) information (Baddeley, 1992, 1996). Subsequently, a number of other theoretical perspectives on WM have been developed (e.g., Anderson, 1983; Cowan, 1995; Engle, 1996, Ericsson and Kintsch, 1995; Goldman-Rakic, 1990), with differences concerning the mechanisms, control, non-unitary nature, limitations, interaction with cognition, relationship to LTM, role of attention, and biological basis (Miyake and Shah, 1999). In the current investigation, the theoretical framework proposed by Baddeley (1992, 1996) has been adopted because it is the prominent model for which most neuroimaging results have been interpreted (e.g., Becker, MacAndrew, and Fiez, 1999; Thierry, Boulanouar, Kherif, Ranjeva, and Démonet, 1999; Smith and Jonides, 1998; Smith, Jonides, Marshuetz, and Koeppe, 1998). The findings show that WM influences were attributable to neurocognitive systems that support the phonological loop and, to some degree, the central executive. Evidence for this conclusion is presented below.

Examination of the source waveform data revealed sources with a clear mnemonic role (Hypothesis 3, Fig. 15). The key active areas included the bilateral temporal poles ($N400_{S3}$) and the left inferior parietal lobe ($N400_{S5}$) (Figs. 13 and 14). The anterior temporal sources may have been related to semantic memory retrieval and were

comparable to the results of intracranial studies, showing N400-like activation in the AMTL (anterior medial temporal lobe) (McCarthy et al., 1995; Nobre and McCarthy, 1995). McCarthy et al. (1995) reported that AMTL N400 potentials were located anterior to the hippocampus and near the amygdala, with similar positive field potentials located inferior and lateral to the amygdala (near the collateral sulcus). In addition, the authors reported that 'task-related' potentials were also recorded in the hippocampus. From a functional perspective, Nobre and McCarthy (1995) proposed a mnemonic role for the AMTL N400, attributing it to either activity in network of semantic representations associated with the word or post-lexical integration of the word into ongoing context. PET and fMRI reports of semantic retrieval activation in this region have been scarce, perhaps attributable to technical difficulties associated with imaging function in this region (Cabeza and Nyberg, 2000). Nonetheless, there is some recent evidence for left hippocampal and parahippocampal semantic activation in an event-related fMRI study (Newman, Pancheva, Ozawa, Neville, and Ullman, 2001).

In contrast, a number of PET and fMRI studies have identified the left parietal region as a primary contributor to verbal working memory (e.g., Paulesu, Frith, Frackowiak, 1993). ERP evidence for verbal WM activation in this region has now been revealed during speech perception (Chapter Two) and during reading (current study). Further, it has been shown that prolonged RTs in a verbal WM task were linked specifically to corresponding increases in the power of functionally active parietal regions (Honey, Bullmore, and Sharma, 2000). This pattern matches the current RT trend and activation profile. The phonological loop has been sub-divided into a passive phonological store and an active rehearsal system (Baddeley, 1992, 1996). It may

therefore be reasonable to speculate that the parietal lobe plays a central role in the phonological store.

Becker et al. (1999) have raised important concerns about the need for a finer grained analysis of the foci of the phonological store within the parietal lobe. In a review, the authors suggested that there might be different foci, none of which are fully compatible with the theory of the phonological loop. Becker et al. (1999) proposed two criteria for defining the location of the putative phonological store: 1) the locus of activation must be reliable and functionally parsimonious (i.e., appropriately located and activated by verbal WM tasks); and 2) the locus must be sensitive to a variety of tasks that may activate the store (e.g., convergence from active and passive verbal tasks), but still specific to verbal WM (i.e., not active in unrelated tasks).

Increased WM load led to N400 peak activation in BA 40 (slightly superior to the sources identified in Chapter Two). These results agree with Becker and colleagues' reliable identification of this locus (first criterion), but the authors stated that because the area is not typically identified for speech perception and has also been active in visual attention task - it does not satisfy the second criterion (i.e., sensitivity and specificity). Comparable left inferior parietal findings in Chapters Two and Three (BAs 39/40 and BA 40, respectively) may support the notion that WM activation in speech perception and reading tasks converge on a unitary store. But, it is still too early to conclude that a single locus is active across sensory modality because of limitations in the spatial resolution of BESA (and source analysis in general). Therefore, the locus of the putative phonological store remains to be determined.

Another caveat to the source imaging results exists. The source analysis focused specifically on dipoles that showed peak activation in the N400 time range (i.e., those with phasic changes of electromagnetic potentials). During the source fitting procedure, local minima (i.e., regions that accounted for waveform variance) were detected in the lateral prefrontal and parietal regions, bilaterally. Dipoles were not fitted in these regions because BESA cannot model low frequency signal accurately (Scherg and Berg, 1996). Nonetheless, this DC-like activation is reminiscent of prior work that used the fan procedure to study slow ERPs. Rösler et al. (1993) found that memory probes elicited tonic voltage changes associated with the relative excitability of underlying cortical tissue in the left anterior region as well as frontal and parietal electrode sites in general.

A number of PET and fMRI studies on WM have used *N*-back tasks[12], which are similar to the modified fan procedure with respect to WM load manipulations. *N*-back tasks involve both short-term maintenance and the central executive for attentional control. In general, regions that are commonly implicated during these tasks include (but are not limited to) the prefrontal, parietal, and cingulate areas (e.g., Braver et al., 1997; Schumacher et al., 1996; Smith, Jonides, and Koeppe, 1996; Smith, Jonides, Marshuetz, and Koeppe, 1998). Taken together, involvement of lateral prefrontal (Owen, 2000) and parietal (Honey et al., 2000) regions in central executive functions and controlled attention may also have a central influence on semantic neural systems.

---

[12] In a *N*-back task, participants indicate whether an item presented in a series of items matches one of the items that occurred one, two, or more previously in the series (i.e., WM load) (cf. Nystrom et al., 2000; Smith and Jonides, 1998).

Chapter Three - Conclusion

The current study provides definitive evidence for the interaction between WM load and semantic neural systems. The results fit remarkably well with the overall framework of functional neuroanatomy that is rapidly being defined by convergent electromagnetic and hemodynamic imaging studies. Contemporary research in multimodal imaging has related findings across imaging modalities on the basis of similarities in cognitive processing. However, there are noteworthy differences between spatial and temporal characteristics of the imaging modalities (see Chapters One, Two, and Three). In light of this fact, it is critically important to relate findings on the basis of physiological processes. The N400 has been the common reference point for both Chapters Two and Three. If a particular anatomical network supports N400 generation, then evidence for this network should be present in a fMRI investigation. Such an investigation would in turn provide valuable insight into the neuroanatomical backdrop against which electromagnetic source data can be integrated. In Chapter Four, the possibility of hemodynamic N400 correlates was evaluated using fMRI.

Chapter Four

Hemodynamic correlates of the semantic N400 response in sentence reading: An event-related functional magnetic resonance imaging study

Chapter Four - Summary

The objective of the present study was to explore whether hemodynamic correlates of the semantic N400 response can be detected using functional magnetic resonance imaging (fMRI). The N400 is an electromagnetic response that is measured using event-related brain potentials (ERPs) or magnetoencephalography (MEG). While a one-to-one correspondence between hemodynamic and electromagnetic findings cannot be assumed, it was hypothesized that a congruency contrast would yield a degree of co-localization between fMRI activity and N400 sources. A well-established N400 paradigm was adapted to an event-related fMRI design in order to obtain representative activation. Participants (N = 8) read highly contextually constrained sentences that varied with respect to terminal word congruency (e.g., The pizza was too hot to... eat/sing) and evaluated the semantic acceptability of the terminal word. Blood-oxygen level-dependent (BOLD) contrast images were obtained during stimulus presentation. Both general sentence reading activation and congruency activation were examined for individual and group data sets. Activation related to general sentence reading occurred in a number of regions known to contribute to this process (e.g., visual, ventral occipital-temporal, superior temporal/inferior parietal, and lateral frontal). Importantly, an Incongruent-weighted contrast revealed various foci that corresponded to previously identified N400 sources, but these activation patterns varied across individuals. A group analysis showed reliable activation in the left middle occipital gyrus only (BAs 38/19), reflecting robust activation from visual word form processing. The findings provide preliminary indications of hemodynamic correlates of the N400 in BOLD contrast imaging, but this activity may be at or near threshold levels.

Chapter Four - Introduction

A growing number of neuroimaging studies are focusing on the spatiotemporal characteristics of neurocognitive processing. Many of these studies have utilized hemodynamic measures, such as positron emission tomography (PET) and functional magnetic resonance imaging (fMRI), which can provide valuable spatial information as well as temporal estimates (Cabeza and Nyberg, 2000; D'Esposito, 2000; Menon and Kim, 1999). Conversely, there is a large body of research that uses electromagnetic measures like event-related brain potentials (ERPs) and magnetoencephalography (MEG) in order to obtain 'real-time' temporal measures and spatial estimates (Knight, 1997; Hämäläinen, Hari, Ilmoniemi, Knuutila, and Lounasmaa, 1993; Picton, Lins, and Scherg, 1995). However, the relationship between the hemodynamic and electromagnetic measures of brain function is not fully understood (Jueptner and Weiller, 1995; Magistretti and Pellerin, 1996; Orrison, Lewine, Sanders, and Hartshorne, 1995). Integrating the results from multiple imaging modalities will be critically important to unifying our understanding of the time course and the anatomical basis of cognitive processes (McCarthy, 1999). The studies that have started to address this issue have identified cognitive processes as the common link. It can be argued that this process must begin by first identifying physiological components that reflect the cognitive function(s) of interest. The spatiotemporal nature of these physiological components can then, in turn, be explored fully using multiple imaging modalities.

The current investigation focused on fMRI correlates of the semantic N400 response. Semantic comprehension during reading represents an ideal candidate for multimodal integration for two reasons: 1) a number of PET and fMRI studies have

provided convergent data on the functional neuroanatomy of semantic comprehension for language in general (Démonet and Thierry, 2001; Price, 2000) and reading in particular (Fiez and Petersen, 1998); 2) ERP and MEG language studies have identified and characterized a physiological response, the N400 (Kutas, 1997; Kutas and Van Petten, 1994; Segalowitz and Chevalier, 1998), which has been linked directly to semantic comprehension (Chapters Two and Three). Therefore, the explicit goal of the current investigation was to determine whether hemodynamic correlates of the N400 response could be detected using event-related fMRI. This goal is described in more detail below, but first it is useful to review relevant work on reading, semantics and the N400, and the relationship between hemodynamic and electromagnetic measures of function.

I. fMRI and PET studies of semantic comprehension in reading

Semantic comprehension in reading is a complex higher-level process that depends on multiple levels of analyses (e.g., visual word form processing, orthographic and phonological processing, lexical access, and memory processes). Fiez and Petersen (1998) have reviewed hemodynamic studies of reading and found that several 'clusters' of activation emerge from the different studies. They reported that left-lateralized foci were common in the ventral occipital-temporal cortex (fusiform and lingual gyri) and the frontal operculum. Bilateral activation occurred in the superior temporal gyrus, post-central area, basal ganglia and insular cortex, and cerebellum. There was also medial activation in the supplementary motor and cingulate areas. The outcome of this quantitative review demonstrated a promising convergence in activation patterns across a number of related studies, and the results were broadly consistent with the neurological literature. However, the authors also noted that the locations of specific foci within these

clusters varied, and not all clusters were commonly activated across different studies. Fiez and Petersen (1998) emphasized the importance of identifying the form of processing, the time course, and the nature of interactions for the various 'clusters' of activation. One approach to achieving this goal is to investigate neurophysiological responses that are linked to the cognitive processes used in reading.

II. The N400 response and related hemodynamic data

Unlike fMRI and PET studies, the functional significance of ERP components is more readily accessible. Indeed, it has been well established that the N400 response is related to semantic comprehension. Since its discovery two decades ago (Kutas and Hillyard, 1980), this negative-going waveform (peaking in the 400 ms range, post-stimulus) has been observed in numerous studies on semantic processing (Chapters Two and Three, Kutas and Van Petten, 1994; Kutas, 1997). It is typically elicited using highly contextually constrained sentences that end in either a semantically acceptable (congruent) or unacceptable (incongruent) terminal word, and has thus been referred to as the 'congruency effect' (Gunter, Jackson, and Mulder, 1995). Functionally, the N400 has been linked to controlled post-lexical integration within an amodal semantic conceptual system (Brown and Hagoort, 1993; Chapters Two and Three; Connolly, Byrne, and Dywan, 1995a; Ganis, Kutas, and Sereno, 1996; Holcomb, 1993; Nigam, Hoffman, and Simons, 1992), although this remains a matter of debate (Deacon, Hewitt, Yang, and Nagata, 2000; Federmeier and Kutas, 2001).

The evidence for the spatial distribution of N400 generators (or sources) has come from studies using source analysis or intracranial recordings, and again a convergent pattern is beginning to emerge. The primary sources appear to be localized to the

perisylvian region, predominately in the vicinity of the superior and middle temporal areas and the posterior temporal/inferior parietal regions (Chapters Two and Three; Haan, Streb, Bien, and Röesler, 2000; Helenius, Samelin, Service, and Connolly, 1998; Helenius et al., 2002). While these sources may have bilateral representations, it appears that a left hemisphere activation asymmetry exists. Additional sources, active during the N400 time period, have been localized to the anterior medial temporal lobes and the occipital-temporal areas (Chapter Three; McCarthy et al., 1995; Nobre and McCarthy, 1995; Simos, Basile, and Papanicolaou, 1997). These sources appear to be sensitive to differences in stimulus modality and/or related temporally overlapping cognitive processes (e.g., working memory; Chapter Three).

Some fMRI and PET studies have focused on semantic processing and then discussed the results in relation to the N400 literature. St George, Kutas, Martinez, and Sereno (1999) examined semantic integration during paragraph reading for comprehension. The paragraphs were presented to participants either with or without titles. Paragraphs without titles were reported to be more difficult to understand than those with titles (i.e., comprehension difficulty was manipulated). Bilateral activation was observed in the ventral occipital-temporal, the middle/superior temporal, and inferior frontal regions. In addition, the authors reported right hemisphere activation (inferior and middle temporal sulci) that was sensitive to the presence or absence of a title, with increased activation in the no-title condition. They speculated that the increased activation was related to integrative processes in the right hemisphere and was similar to activation indexed by the N400. While, the overall activation patterns reported by St George et al. (1999) fit well with other neuroimaging studies of reading (Fiez and

Petersen, 1998) as well as the location of some N400 sources, the activation associated with the title versus no-title condition was largely inconsistent with primary N400 locations in the left hemisphere.

In a separate study using dynamic statistical parametric mapping, Dale et al. (2000) examined fMRI and MEG activity during semantic processing of visually presented words that were either novel or repeated. The authors reported both fMRI activation and MEG activation (constrained by fMRI) that characterized the spatiotemporal nature of single word reading. In this study, as in the previous one, the general areas of activation corresponded with areas involved in reading, and possibly N400 sources. The authors also found that novel words elicited larger MEG responses in the N400 time range. However, the novel versus repeated word contrast highlighted activation in the prefrontal cortex, again failing to converge on the primary regions identified for the N400. It is noteworthy that the results from both of these studies overlapped with respect to the general reading-related activation patterns, but no such overlap existed with respect to the active foci that were proposed to reflect N400 sources.

A number of fMRI studies have begun to investigate modified N400 paradigms and reported activation thought to reflect *both* syntactic and semantic processes. Newman, Roumyana, Ozawa, Neville, and Ullman (2001) reviewed block task and event-related design fMRI studies that have used a combination of syntactic and semantic violations. In general, the activation in these studies highlight regions that may be involved in N400 generation (e.g., superior/middle temporal gyri, left angular gyrus, left ventral occipital-temporal cortex, inferior frontal cortex, and anterior medial temporal structures). However, the emphasis on syntax as well as semantics (rather than N400

correlates) has made it difficult to establish whether there is any consensus about activation that might reflect N400 processes (versus related downstream processing). For instance, in the Newman et al. (2001) study, participants read sentences with both syntactic and semantic violations (e.g., Syntactic: "Yesterday I cut Max's *with* apple caution" and Semantic: "Yesterday I sailed Todd's *hotel* to China"). The syntactic violations resulted in activation in the superior frontal cortex, bilaterally. The semantic activations showed greater activation in the left hippocampal/parahippocampal, the angular gyri, the right middle temporal gyrus, and the left inferior frontal sulcus. The authors concluded that semantic processing involved activation of temporal and temporal parietal regions (while syntactic processing involved greater frontal activation). The primary focus of this work was on syntactic and semantic violations, and not the N400 *per se* (nor semantic comprehension processes in isolation). The lack of evidence for activation in the left superior/middle temporal region suggests that activation from primary N400 generators was not present.

In sum, the research-to-date has not provided sufficient evidence that hemodynamic correlates of the N400 response exist. In fact, this assumption has not yet been tested explicitly. Three factors are important for establishing a correspondence between fMRI/PET and ERP/MEG results. First, the experiments must be designed specifically to investigate hemodynamic correlates of the N400 and the findings need to be integrated within the evolving N400 framework. Second, due to methodological limitations (Friston et al., 1996), block task format is not ideally suited for eliciting hemodynamic correlates of the N400. It assumes that the additional processes activated by the target condition remain unchanged across a block of stimuli grouped together, with

the average response across the entire block being examined (i.e., reducing sensitivity to the N400 effect). Instead, experiments need to use event-related methodology in order to allow for randomly intermixed stimulus presentation. Because this presentation format was adapted from ERP and MEG research, it therefore allows for a much closer methodological approximation across imaging modalities. Also, the hemodynamic responses elicited by individual stimuli can then be analyzed for spatial and temporal characteristics that are consistent with the N400 (Dale and Buckner, 1997; Menon and Kim, 1999). Third, and most importantly, the experimental manipulations must be linked directly to the N400 (i.e., the congruency effect, a fundamental characteristic of the N400). That is, if hemodynamic correlates of this effect exist, then they must be clearly demonstrable using a semantic congruency manipulation.

There is, at least, one theoretical caveat: namely, the possibility that the synaptic events which give rise to the scalp-recorded electromagnetic signals are not sufficient in magnitude to evoke reliable changes hemodynamic signals (McCarthy, 1999). Provided that some form of spatial correspondence can be shown, it is reasonable to begin by assuming that the overlap resulted from some of the same neural generator(s). It is important to note that this does not address the requirement for a temporal correspondence, which must be investigated following spatial localization.

III. Hemodynamic and electromagnetic signals

The nature of the relationship between electromagnetic responses (like the N400) and fMRI measurements, such as those obtained from Blood-Oxygen Level-Dependent (BOLD) contrast imaging (Ogawa and Lee, 1990), is particularly relevant. While ERPs and MEG provide a direct measurement of local post-synaptic electromagnetic signals

(with high temporal resolution), the spatial configuration of the intracranial sources cannot be determined uniquely (i.e., the inverse problem; Hämäläinen et al., 1993; Picton, Lins, and Scherg, 1995). However, the biological source of the activity is fairly well characterized. The electromagnetic signals are generated primarily from pyramidal cells, which are constrained anatomically (in the cerebrum) due to the fact that they are perpendicular to the cortical sheath[13] (Nunez, 1981). In contrast, fMRI and PET can be used to provide excellent spatial sampling (for fMRI; < 1 mm, Kim, Duong, and Kim, 2000; Menon and Goodyear, 1999), but the hemodynamic activity has necessarily imposed temporal limitations. The signal measured in BOLD contrast imaging results from local fluctuations in deoxyhemoglobin concentration as a result of oxidative and non-oxidative metabolism. Most functional activation is thought to reflect largely changes in oxidative metabolism that result from energy demands at the synapse (Orrison et al., 1995; Hoge and Pike, 2001; Jueptner and Weiller, 1995), but the exact neuronal (and possibly glial) sources of this activity are not known (e.g., it can reflect either excitatory or inhibitory activation).

Nonetheless, there is strong evidence of a spatial correlation between electromagnetic activity and hemodynamic fluctuations (e.g., Vanzetta and Grinvald, 1999), and the nature of the coupling is being actively investigated. With respect to the present investigation, it will be critically important to understand more about how the magnitude and timing of a hemodynamic response vary as a function of changes in the amplitude and duration of electromagnetic activity (Dale et al., 2000). To begin, it must

---

[13] MEG has better spatial resolution than EEG, but is sensitive only to tangential sources (radial sources are externally silent), which are measured primarily from the fissures of the cortex (Hämäläinen et al., 1993).

be assumed *a priori* that a one-to-one correspondence does not exist between the two modalities, but that critical cortical regions can be co-localized (McCarthy, 1999).

IV. Objectives

The aim of this study was to identify brain regions activated by an established N400 sentence-reading paradigm. The reading task was adapted from a previous study using ERPs (Connolly et al., 1995b) and has also been used in MEG research (Helenius et al., 1998). All sentences were highly contextual constrained, making the terminal word predictable, and therefore the focus of semantic analysis and integration (Bloom and Fischler, 1980). The semantic features of the terminal words were varied such that they were either congruent or incongruent. Incongruent terminal words were used to elicit the 'congruency effect'. The sentence stimuli were presented using event-related methodology (Dale and Buckner, 1997; Menon and Kim, 1999) and parametric analyses were conducted in order to determine whether hemodynamic correlates of the N400 could be detected. The initial hypothesis predicted that the Incongruent-weighted contrast would yield considerably more activation than the Congruent-weighted contrast (Hypothesis 1). It was also hypothesized that many of the regions identified by the Incongruent-weighted contrast would correspond to the location of N400 sources, but that no such relationship would exist for the Congruent-weighted contrast (Hypothesis 2). Together, support for both hypotheses was taken as preliminary evidence for correlates of the N400 in fMRI.

Chapter Four - Methods

I. Participants

Eight individuals (seven males and one female) volunteered for a MRI experiment on reading (Age: $\underline{M}$ = 27.5, SD = 3.2 years). All participants had normal reading skills (Education: $\underline{M}$ = 17.5, SD = 2.3 years), were right-handed (LQ range = 68.4 to 100; Oldfield, 1971), reported no history of neurological or psychiatric disorders, and were able to read the text stimuli without difficulty. Data from one participant (S03) was excluded from the analysis due to excessive head motion artifact (see Data analysis section below). Each experimental session had a scanning time of approximately one-hour. During the experiment, participants viewed a series of sentences and were instructed to read each one carefully in order to decide whether the last word completed the sentence appropriately (no behavioural response was required). To prevent motion artifacts, participants' heads were restrained physically within the head coil using adjustable horizontal braces and thick foam padding (prevented in-plane motion) as well as a strap secured over the top of the forehead (prevented out-of-plane motion). All participants were also instructed to remain as still as possible in order to minimize head movement while in the scanner. The study had ethical committee approval and all participants were debriefed fully following completion of the experiment.

II. Experimental paradigm

The experiment involved reading sentences adapted from a previous ERP N400 study (Connolly et al., 1995b). The sentence stimuli were presented through MR video goggles (Resonance Technology Inc.). A set of 15 sentences was adapted for event-related presentation format. An additional session (15 sentences), given to each

participant, was analyzed for control comparisons in order to ensure that the results were representative. The last trial for each data set was excluded from the analysis in order to equate the experimental conditions. The number of trials[14] was set to the upper limit of the scanner acquisition capabilities in order to maximize the sensitivity of the analysis. The effects of this factor are discussed later (see Discussion section).

Fourteen highly constrained sentences, obtained from a normative sentence base (Bloom and Fischler, 1980), were semantically congruent or incongruent (Appendix 3). For the congruent sentences (n = 7), the terminal words completed the sentences in a semantically acceptable manner (e.g., The pigs wallowed in the... mud). For the incongruent sentences (n = 7), the terminal words were semantically anomalous to the preceding sentence context (e.g., The pizza was too hot to... sing). The terminal words in both congruent and incongruent sentences also varied with respect to the expectancy of the initial orthographic features, the focus of a separate investigation (Connolly, D'Arcy, MacMaster, Marchand, and Service, 2002). The sentences were presented in a fixed pseudo-random order and average number of words per sentence was 7.1 (SD = 0.9).

Stimulus presentation used a basic event-related presentation format (Dale and Buckner, 1997). For a single trial, the body of the sentence (excluding the terminal word) was presented for 3 s and was followed, after a 1 s interval, by the terminal word of the sentence (duration = 1 s). The interval between the last word of a sentence and the onset of the next sentence was 8 s (Figure 16). All words were presented in yellow against a blue background.

---

[14] Functional MRI analyses typically use raw BOLD data (i.e., no signal averaging). While increasing the number of trial increases the statistical power, experimental effects can be imaged readily with a single trial (Dale and Buckner, 1997).

III. Data Acquisition

All experiments were performed on a Siemens 1.5 Tesla Vision MR Imager with echo planar imaging (EPI) capability. The functional MRI data were obtained using a gradient-recalled EPI sequence with TR/TE = 1760/61 ms. Whole brain imaging was performed with 11 axial slices, 8 mm thick, with a 0.8 mm gap between slices, a 220 mm FOV, and a 64x128 matrix (flip angle = 90 degrees). The axial slices were prescribed such that they were parallel to the AC-PC line on the mid-sagittal localizer slice. The sampling rate (i.e., TR) resulted in 128 (x 11 slices) data points per session (i.e., across the presentation of all sentences). Standard anatomical MRI scans were also obtained for each individual using an inversion recovery sequence (TR/TE = 9216/60 ms, TI = 400 ms, 11 axial slices, 0.8 mm gap between slices, 8 mm thick, FOV = 220 mm, and a 154 x 256 matrix).

IV. Data analysis

Data preprocessing and statistical analyses used Statistical Parametric Mapping Program 1996 (SPM '96) (Wellcome Department of Cognitive Neurology, Institute of Neurology, London, UK) (Friston, 1995) incorporated within the MEDx™ (Version 3.2) software package. Prior to preprocessing routines, the functional images were inspected visually in a cine loop and movement was quantified for all participants, one data set (S03) was excluded on the basis of excessive head motion artifact (Table 15). For the remaining individuals, the functional images were resliced and realigned in order to correct for head motion using a six-parameter (rigid body) transformation model.

Figure 16 - Caption

The experimental paradigm and event-related methodology. **A.** Participants read visual sentence stimuli. Highly contextually-constrained sentences were presented with the sentence body displayed for 3 s, a 1 s delay, and then the terminal word was displayed for 1 s. There was an 8 s delay before the next trial, in which the BOLD responses to the terminal words occurred. The terminal words completed the sentences in either a semantically acceptable (congruent) or unacceptable (incongruent) manner. **B.** Typical BOLD responses elicited by terminal words. A sensory response is presented from the primary visual area and a cognitive response from Broca's area. Note the BOLD response peaks in the range of 1.5 to 3.0% of signal change, is largest for sensory responses, and can be readily approximated by a half sine wave reference vector.

Figure 16

Experimental Paradigm: ERP N400 Paradigm in Event-related fMRI

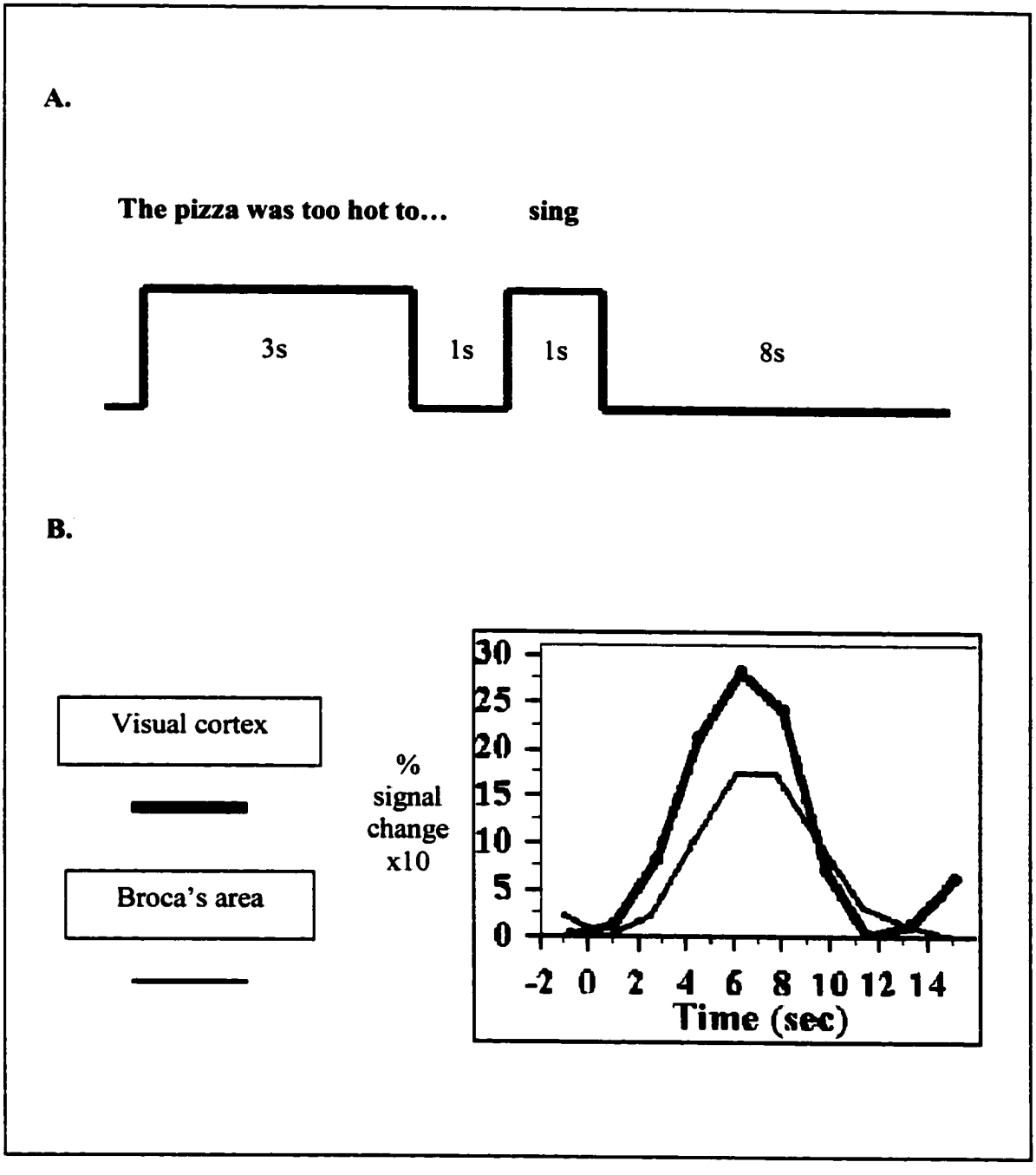

Table 15

Head Motion Summary Statistics

	ΔS	ΔL	ΔP	Roll	Pitch	Yaw
S01	-0.030	1.804	-0.064	-0.088	0.177	-0.019
S02	-0.164	1.117	-0.240	-0.051	-0.256	-0.282
S03	2.335	2.123	-1.014	-0.097	-1.047	-0.969
S04	-1.129	1.274	-0.053	-0.050	0.657	0.169
S05	-0.051	1.272	-0.091	0.114	-0.086	0.176
S06	-0.310	1.374	-0.310	0.166	0.076	0.013
S07	0.436	2.151	-0.279	0.101	0.002	-0.145
S08	-1.299	0.317	-0.977	0.089	0.293	-0.921

Absolute group means (and standard deviations) - excluding S03

S: 0.719	**ΔL:** 1.429	**ΔP:** 0.379	**Roll:** 0.095	**Pitch:** 0.324	**Yaw:** 0.337
(0.810)	(0.601)	(0.393)	(0.037)	(0.355)	(0.386)

ΔS: superior-inferior (positive = superior, mm)
ΔL: left-right (positive = left, mm)
ΔP: anterior-posterior (positive = posterior, mm)
Roll: rotation about inferior-superior axis (degrees counterclockwise)
Pitch: rotation about left-right axis (degrees counterclockwise)
Yaw: rotation about the anterior-posterior axis (degrees counterclockwise)

The realigned data were then spatially normalized to standard Talairach space (Talairach and Tournoux, 1988; Talairach, Tournoux, and Missir, 1993) using a template-bounding box defined by the SPM '95 brain. Following spatial transformation to Talairach co-ordinate space, all of the images were smoothed using an 8-mm isotropic Gaussian FWHM kernel. The spatial normalization and smoothing procedures allowed for inter-subject averaging in order to derive the group data.

Statistical activation maps (computed for individual voxels) used the general linear model in SPM '96. The hypotheses were evaluated within an appropriate linear contrast model (two contrasts, half sine wave, de-trended, and proportional scaling) with a Congruent-weighted contrast (Contrast 1: 1/-1) and an Incongruent-weighted contrast (Contrast 2: -1/1). The Incongruent-weighted contrast tested for activation elicited by the N400 congruency effect. The significance of global activation in the model was assessed using an F-statistic ($p < 0.001$, uncorrected), and provided threshold values for the computation of contrast activation maps. Contrast activation maps were tested using a t-statistic, transformed to unit normal distribution Z maps ($p < 0.01$, uncorrected). All Z values (> 3.0) and their respective p values were reported.

Activated anatomical regions were recorded as Brodmann's areas (BAs). BAs were identified using x (left-right), y (anterior-posterior), and z (superior-inferior) Talairach co-ordinates for all active regions (nearest gray matter areas). Activation is reported for both individual and group analyses, with the primary emphasis on Contrast 2 (i.e., N400 congruency effect). Individual activation maps were examined in order to determine whether the active regions correspond to N400 source regions. Group data

were also analyzed to evaluate whether any anatomical regions were active reliably across the individual data sets.

Chapter Four - Results

I. Individual Analyses

Overall, the individual activation maps showed similar global patterns ($F(2,92)$, $p < 0.001$, uncorrected) with regions of well-known reading involvement being identified (Figure 17). The results also highlighted known areas for N400 sources, but it was not clear which clusters were specific to correlates of the N400. Pronounced activity was present in the bilateral occipital, ventral occipital-temporal, middle/superior temporal, and inferior parietal regions. In addition, there was bilateral activation in frontal regions, predominating in the inferior lateral areas (i.e., Broca's area/right homologue and lateral prefrontal cortex). This pattern of results was remarkably consistent across individuals and demonstrated that general reading processes were activated (more detail is provided in the Group analysis section below).

The linear contrast analyses revealed prominent activation corresponding to the congruency effect in the Incongruent-weighted contrast. Six out of seven individuals showed activation in the Incongruent-weighted contrast. Figure 18 depicts the areas of activation for all of these individual data sets. A number of regions were identified as overlapping with N400 source locations (see Table 16). In particular, activation was present in the superior temporal gyrus (BA 22), middle temporal gyrus (BAs 21 and 39), inferior parietal lobule (BA 31 and 40), and frontal lobe (BAs 9, 10, 11, and 47). In addition, there was activation in the lingual gyrus and cuneus (BA 18), and the middle occipital gyrus (BA 19), likely related to visual word form processing. While the active areas were generally distributed in a bilateral manner, the temporal lobe activation was left asymmetrical, with a number of the regions corresponding to perisylvian N400

Figure 17 - Caption

Functional MRI activation for sentence reading. Participants (N = 7) read highly contextually constrained sentences the ended with either congruent or incongruent words. Statistical parametric *F* maps ($p < 0.001$, uncorrected) are presented for all individuals. The active areas were consistent with the task requirements and reliable across individuals (see text for detail). The maps display the maximum intensity projection (MIP) on a glass brain in sagittal, axial, and coronal orientations. The letter 'R' denotes the right hemisphere and darker regions reflect higher intensity activation (as measured by *Z* scores).

Figure 17

Global Activation Maps (N = 7)

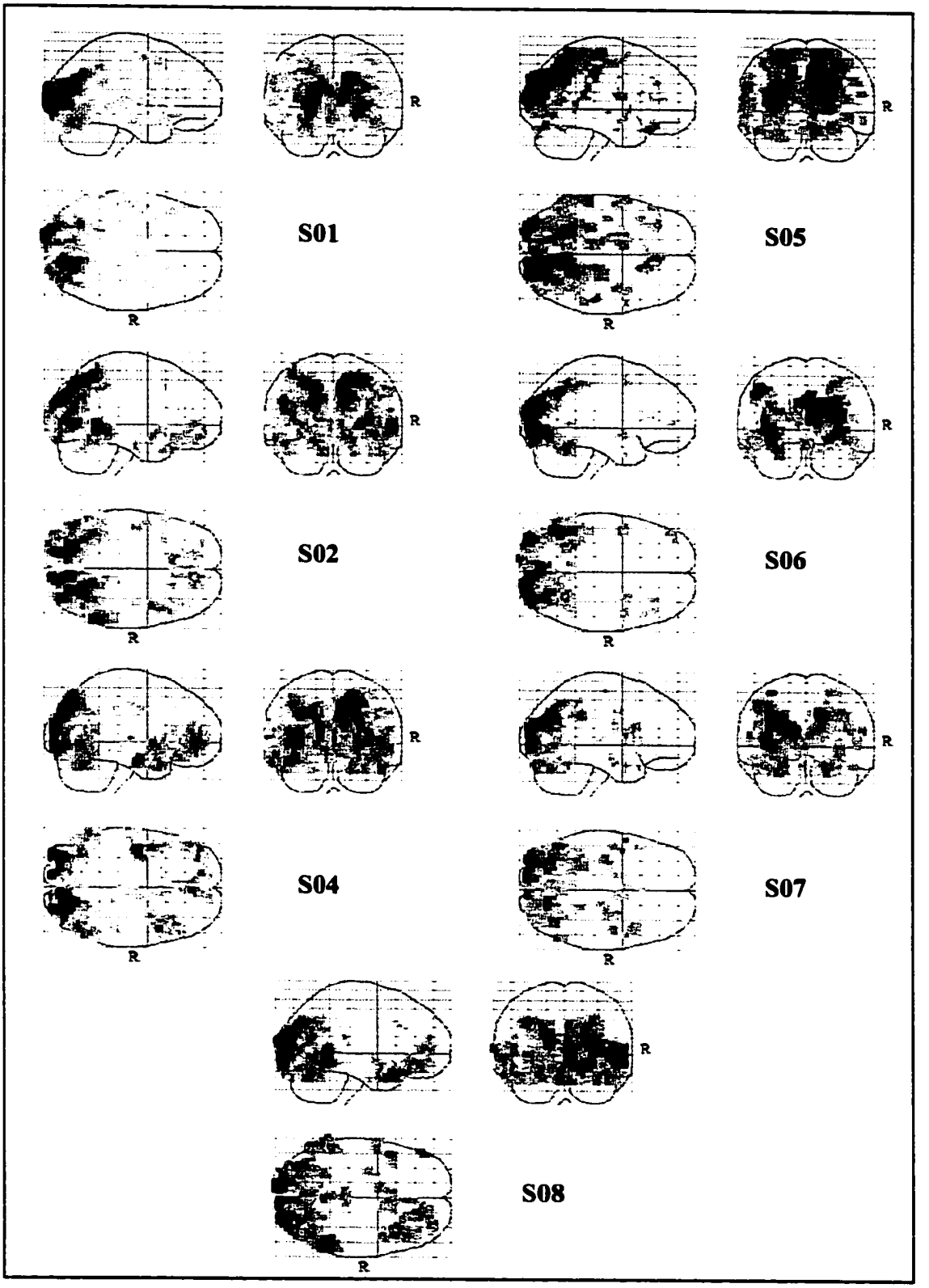

Figure 18 - Caption

Statistical parametric maps for the Incongruent-weighted contrast (Contrast 2). Active regions varied between individuals, but a number of regions were associated with processing semantically incongruent words including visual, temporal, inferior parietal, and frontal regions. The temporal lobe activation was predominately left asymmetrical, with a number of regions corresponding to those identified previously as N400 generators. All other details as for Fig. 17.

Figure 18

Incongruent-weighted Contrast Activation Maps (N = 6)

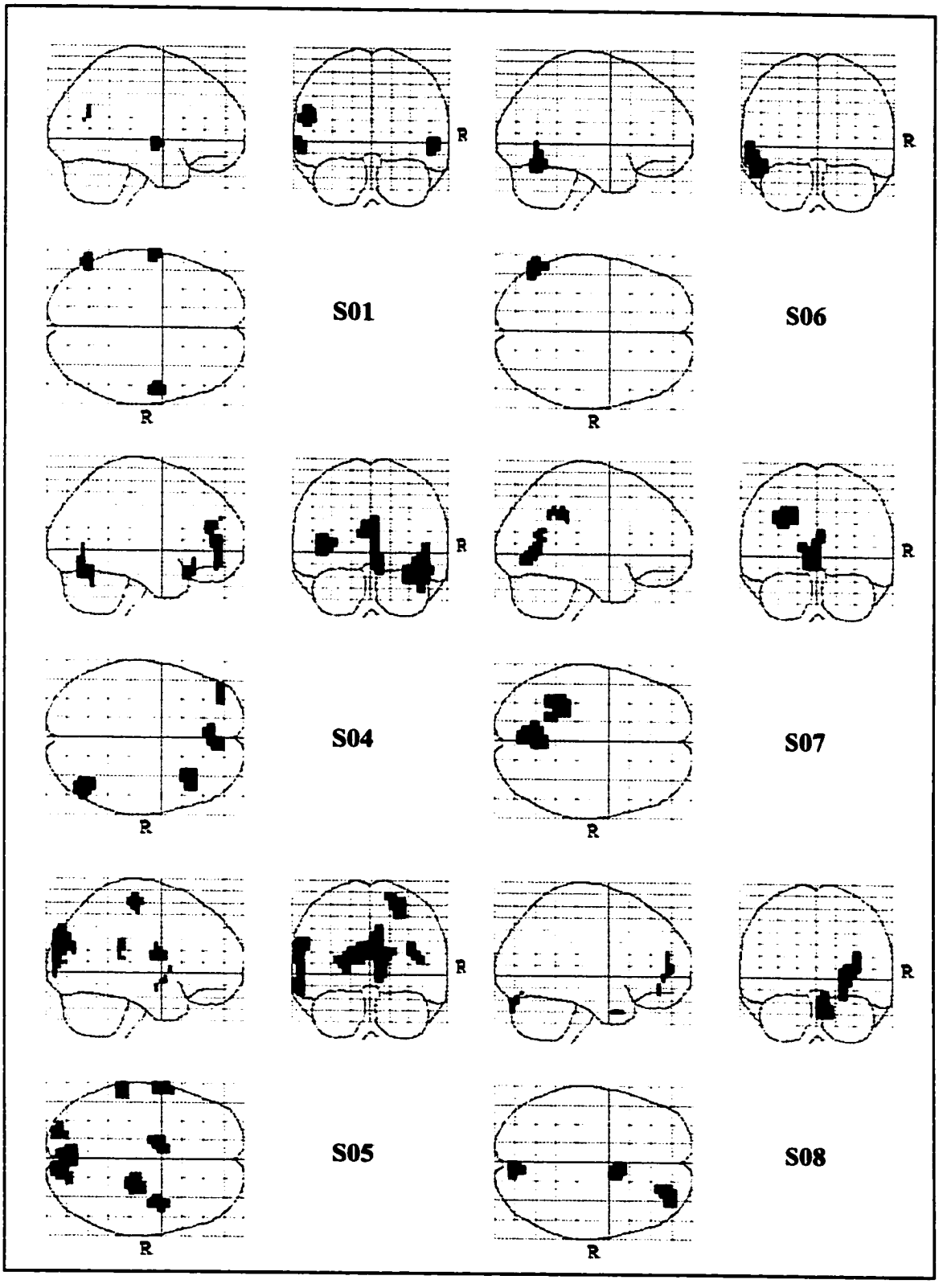

Table 16

Foci of Activation for the Incongruent-weighted Contrast

Subject Cluster	Hem.	BA	x	y	z	*Z*	Region	*p*
S01								
1	R	22	60	-4	4	4.36	sup. temp. gyr.	.00001
2	L	22	-60	-8	4	3.66	sup. temp. gyr.	.00012
3	L	39	-52	-64	24	3.57	mid. temp. gyr.	.00018
S04								
1	R	19	52	-68	-12	3.88	temp. fusiform	.00005
2	R	47	40	24	-16	3.59	inf. front. gyr.	.00017
3	R	11	12	48	-12	3.51	sup. front. gyr.	.00023
	L	9	0	40	24	3.18	mid. front. gyr.	.00072
S05								
1*†	R	18	12	-88	20	5.77	occ. cuneus	.00000
2*	L	n/a	-8	0	16	4.63	caudate-body	.00000
3	R	13	44	-8	20	4.47	insula	.00000
4	R	4	32	-24	60	4.34	precent. gyr.	.00001
5	L	21	-60	-4	-8	4.09	mid. temp. gyr.	.00002
6	L	40	-52	-32	28	3.90	inf. pariet. lobu.	.00005
7	L	18	-20	-92	16	3.24	mid. occ. gyr.	.00060
S06								
1	L	19	-52	-60	-4	4.07	mid. occ. gyr.	.00002
S07								
1	R	18	4	-68	4	4.32	lingual gyr.	.00001
	L	18	-4	-72	0	4.04	lingual gyr.	.00003
2	L	31	-16	-52	36	3.95	pariet. precuneus	.00004
S08								
1	R	~17	12	-84	-20	3.58	inf. occ. pole	.00017

Symbols *Z*: highest *Z* score within a region, *p*: uncorrected *Z* probability, *: height threshold $p < 0.05$, and †: spatial extent threshold $p < 0.05$

sources. However, examination of the activation across the group revealed that the specific regions identified varied between the individual data sets.

In contrast to the Incongruent-weighted condition, activation from the Congruent-weighted contrast (Contrast 1) was far less pronounced and did not fit well with N400 source patterns. Only four out of seven individuals showed activation in the Congruent-weighted contrast. Figure 19 depicts the areas of activation for all four individuals. With the exception of one individual (S05), the activation was predominately restricted to visual regions in the occipital lobe (BAs 18 and 19) (Table 17). S05, however, showed more pronounced activation in general (Tables 16 and 17). These results demonstrated that the Incongruent-weighted contrast was considerably more sensitive to N400 correlates than was the Congruent-weighted contrast.

II. Group Analysis

The results of the group analysis yielded global activation patterns that were highly consistent with the individual maps. Figure 20 presents the global activation anatomically rendered onto a standard brain (SPM '95). This reading-related activation pattern validated the N400 sentence paradigm. In the Incongruent-weighted contrast, there was one active cluster located in the left middle occipital gyrus (BA 37), bordering BA 19 (Figure 21). This result was consistent with the presence of pronounced activation in similar visual regions across all individuals. It also corresponded with the location of modality-specific N400 sources involved in visual perceptual processing along the ventral visual stream (Chapter Three). As expected, no reliable activation was found in the Congruent-weighted contrast.

Figure 19 - Caption

Statistical parametric maps for the Congruent-weighted contrast (Contrast 1). Active regions were consistently found in the visual areas (e.g., BAs 18 and 19). Only the results from one individual (S05) did not correspond to the group, showing pronounced activation in a number of areas (for both Contrast 1 and 2). Overall, the Congruent-weighted contrast was not sensitive to N400 correlates. All other details as for Fig. 17.

Figure 19

Congruent-weighted Contrast Activation Maps (N = 4)

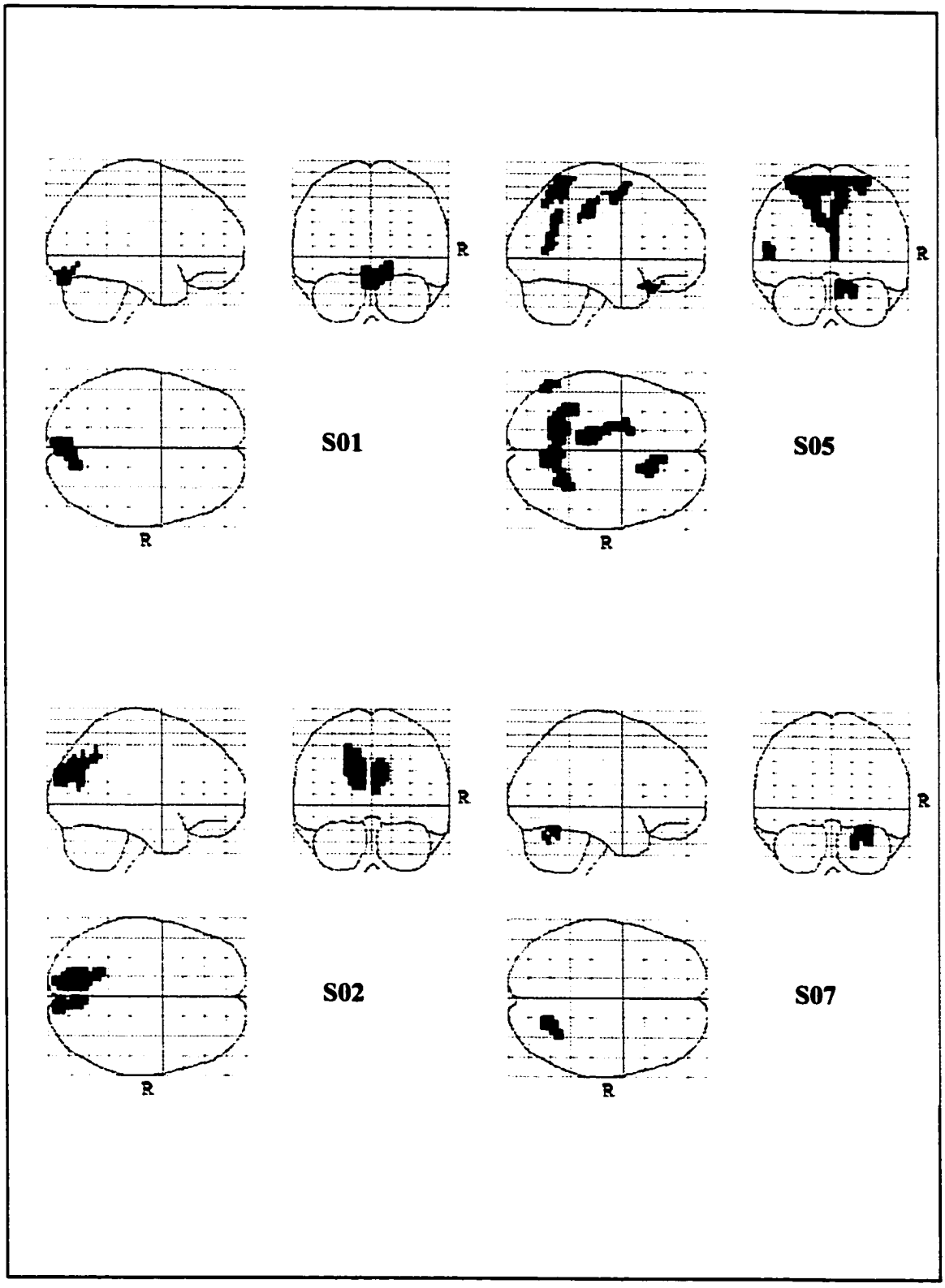

Table 17

Foci of Activation for the Congruent-weighted Contrast

Subject Cluster #	Hem.	BA	x	y	z	*Z*	Region	*p*
S01								
1	R	18	16	-76	-8	3.89	occ. ling. gyr.	.00005
S02								
1	L	19	-8	-80	28	4.01	occ. cuneus	.00003
2	R	19	12	-88	28	3.13	occ. cuneus	.00088
3	R	18	8	-76	28	3.11	occ. cuneus	.00092
S05								
1*†	L	6	-8	-24	48	5.79	front. paracent. lobu.	.00000
	L	31	-4	-28	40	4.92	limbic cing. gyr.	.00000
2*†	L	7	-16	-60	64	5.45	sup. pariet. lobu.	.00000
3*	R	11	20	24	-20	4.92	inf. front. gyr.	.00000
4*	L	6	-16	-4	56	4.71	front. lobe	.00000
5	R	31	8	-60	20	4.41	pariet. precuneus	.00001
S07								
1	R	37	36	-56	-16	3.39	temp. fusiform gyr.	.00035

Symbols *Z*: highest *Z* score within a region, *p*: uncorrected *Z* probability, *: height threshold $p < 0.05$, and †: spatial extent threshold $p < 0.05$

Figure 20 - Caption

Anatomically rendered maps for the global activation - group analysis. The location of the four axial slices (A, B, C, and D), depicted on a template brain. **A to D.** Four axial slices (superior to inferior, respectively) showing functional activation overlaid onto an anatomical background. The group data show reading-related activation in the visual (*), ventral occipital-temporal (†), superior temporal/inferior parietal (‡), and inferior/lateral frontal areas (#). The images are presented in radiological format (i.e., the left hemisphere is on the right).

Figure 20

Rendered Global Activation Maps - Group (N = 7)

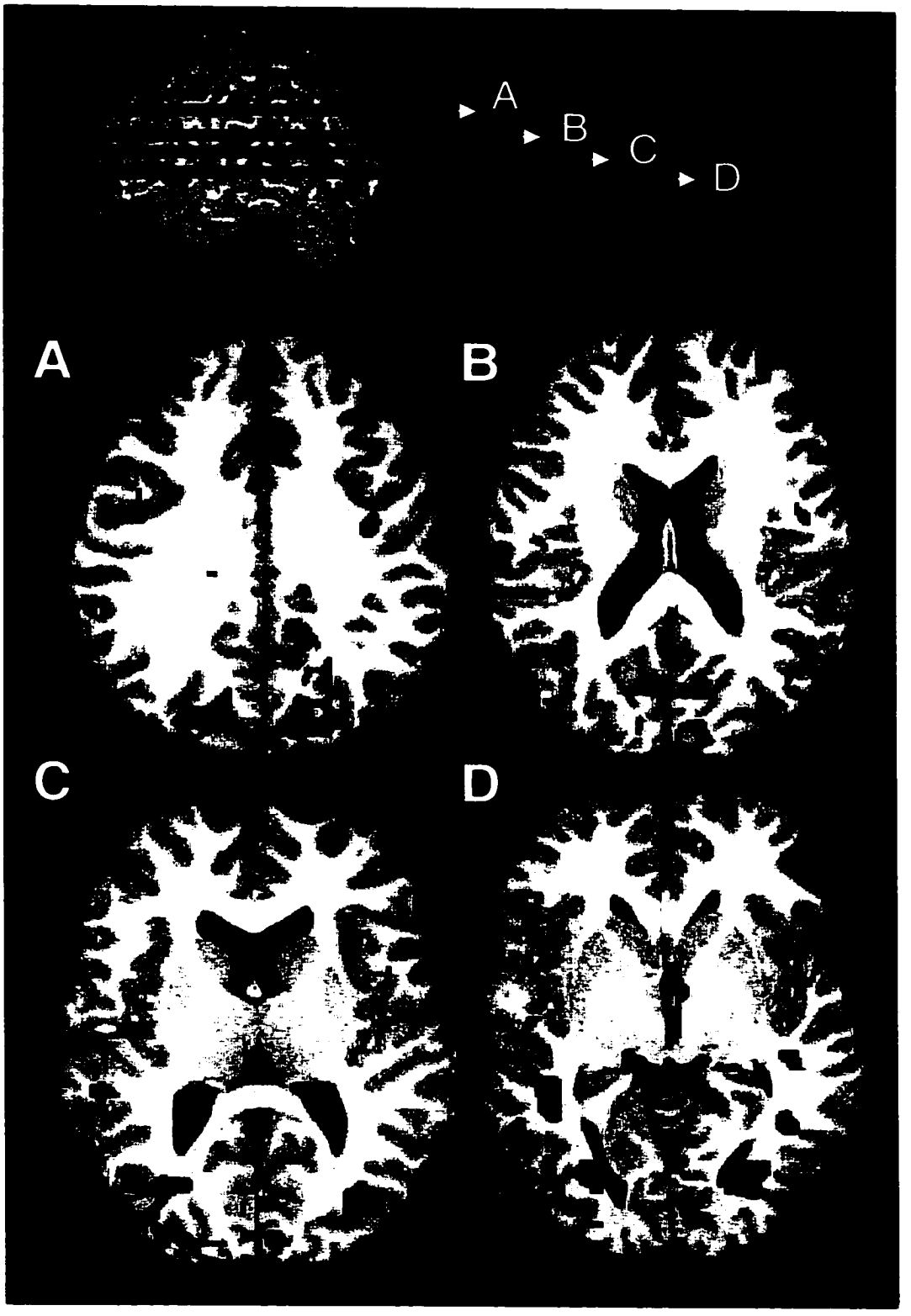

Figure 21 - Caption

Statistical parametric maps for the Incongruent-weighted contrast (Contrast 2) - group analysis. **A.** There was robust group activation in the left middle occipital gyrus, reflecting modality-specific visual word form processing. All other details as for Fig. 17. **B.** The SPM table showing the hemisphere, Brodmann's area, Talairach coordinates, *Z* score, region, and uncorrected *Z* score probability for the cluster.

Figure 21

Incongruent-weighted Contrast Activation Maps - Group (N = 7)

A.

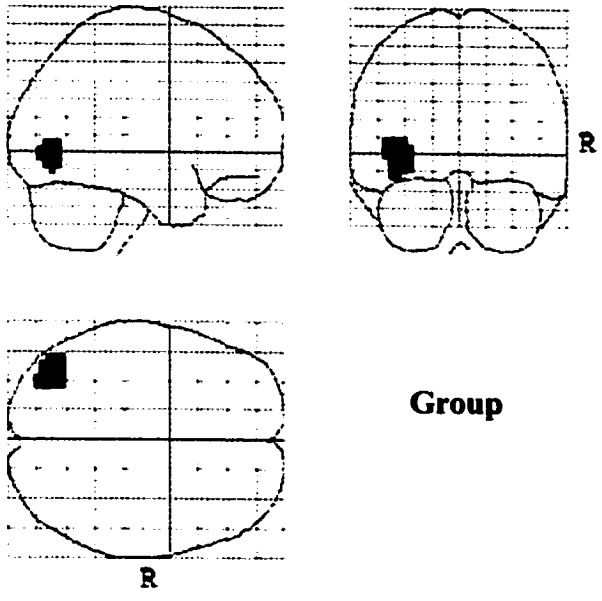

Group

B.

Group	Hem.	BA	x	y	z	*Z*	Region	*p*
Cluster 1	L	37(19)	-36	-68	0	3.51	mid. occ. gyr.	.00022

Chapter Four - Discussion

Overall, sentence reading activated a number of different brain regions (Figs. 17 and 20). The active regions corresponded with structures known to contribute to reading, consistent with previous findings (Fiez and Petersen, 1998). Also, it is noteworthy that this activation highlighted several of the areas implicated as N400 source locations, but it was not possible to determine which particular clusters were specific to N400 generation. Linear contrasts were used to detect activation that may be related to the congruency effect. The Incongruent-weighted contrast yielded notably more pronounced activation, in more individuals, than the Congruent-weighted contrast (Figs. 18 and 19). This finding supported the first hypothesis, providing preliminary evidence for hemodynamic correlates of the N400 in fMRI.

In the Incongruent-weighted contrast, several foci correspond to the locations of N400 sources for individual data sets. The Incongruent-weighted contrast yielded activation in the lingual gyrus and cuneus (BA 18), the middle occipital gyrus (BA 19), the superior temporal gyrus (BA 22), the middle temporal gyrus (BAs 21 and 39), the inferior parietal lobule (BA 31 and 40), and the frontal lobe (BAs 9, 10, 11, and 47). Much of the activation was distributed in a bilateral manner, but the temporal lobe foci were left asymmetrical, with some of the active regions matching perisylvian N400 sources. Interestingly, several of the foci identified in previous fMRI studies (see Introduction section) were replicated in the current study, providing further evidence for the role of temporal and temporal-parietal regions in semantic processing (Newman et al., 2001). In contrast, the activation in the Congruent-weighted contrast was far less pronounced and predominately restricted to visual areas, failing to match the location of

any N400 sources. The overlap between fMRI activation to semantically incongruent sentences and the location of N400 sources supported the second hypothesis. Taken together (i.e., Hypotheses 1 and 2), it would appear that hemodynamic N400 spatial correlates might exist.

While the preliminary findings in the individual data were promising, the results of the group analysis suggested that the N400 signal might be at or near BOLD threshold levels in the current study. The activation patterns elicited in the Incongruent-weighted contrast varied between individuals (Fig. 18). While inter-individual variance is common factor in fMRI studies (Aguirre, Zarahn, and D'Esposito, 1998), only three of the six individuals showed perisylvian foci (S01, S05, and S07; Fig. 18). Moreover, the group analysis for the Incongruent-weighted contrast did not reveal reliable activation in the left perisylvian region (Fig. 21). There was only reliable activation in the left middle occipital gyrus (BA 37), bordering BA 19. This result fit well with modality-specific N400 sources modeled in the same region (Chapter Three) and was likely associated with visual word form processing task requirements. However, the lack of group activation in general (and left perisylvian activation in particular) suggested that more work is needed to determine whether hemodynamic and electromagnetic signals can be reliably co-localized.

Several factors may be relevant to the absence of perisylvian activation in the group analysis, despite its presence within a subset of individuals. First, the BOLD signal tends to be larger for sensory-perceptual processing (e.g., visual processing) than for cognitive processes like semantics (Fig. 16). Second, the numbers of trials per contrast and sample size (see Methods section) are likely key factors that will increase the sensitivity of BOLD contrast imaging to this activation. In future work on hemodynamic

correlates of ERP/MEG signals, the signal-to-noise and statistical power should be maximized by: 1) the incorporation of an even larger numbers of trials; 2) the use of high-field strengths (3-4T); and 3) the selection of larger sample sizes to assist in partitioning the individual variance. Third, it must be noted that changes in the task due to the adaptation to event-related methodology may have led to corresponding changes in the underlying cognitive processes. In particular, the slower stimulus presentation rate may have altered the N400 congruency effect. It will be useful to demonstrate the N400 in ERPs and/or MEG using stimulus parameters similar to those used in event-related fMRI. Fourth, while group analysis provides valuable information about overall activation, by collapsing across individual data it becomes difficult (if not impossible) to account for multiple sources of spatial variance. In the case of the N400, there is known spatial variance in the distribution of sources (Haan et al., 2000). Therefore, it is critical to consider *both* the individual and group activation patterns (and potentially give more weight to the former in fMRI studies).

As expected, a one-to-one correspondence between fMRI activation and N400 dipoles was not apparent in the current investigation. But, it is nonetheless encouraging that there was a good degree of spatial co-localization between fMRI activation and N400 sources, suggesting that it is possible to co-localize key generators. Thus, the current data provided positive evidence that the 'task-related' activation observed in both ERPs/MEG and fMRI/PET studies may be physiologically comparable. Also, the findings stress the importance of examining spatiotemporal relationship between various imaging modalities (e.g., Dale et al., 2000; McCarthy, 1999; Puce, Allison, Spencer, Spencer, and McCarthy, 1997; Thierry, Doyon, and Démonet, 1998). Once these physiological phenomena can be

confirmed spatially, experimental manipulations that influence the temporal characteristics will be critical in demonstrating their unitary (or non-unitary) nature.

Chapter Four - Conclusion

Neuroimaging methods are providing critical insight into the functional neuroanatomy of language. By linking multimodal measures, our understanding of the neurobiological basis of these cognitive functions will also be enhanced greatly. In the present study, semantic congruency was varied using an event-related fMRI sentence reading task and the hemodynamic correlates of the semantic N400 response were investigated. Incongruent-weighted contrasts elicited pronounced activation, which overlapped with the location of N400 sources in the left ventral occipital-temporal and left perisylvian regions. However, individual variance in the activation patterns existed. While there was reliable group activation in the left ventral occipital-temporal region (visual word form analysis), no such activation was detected in the left perisylvian region (i.e., the principle region for N400 sources). Overall, the findings suggested that it is possible to detect hemodynamic correlates of the N400 using BOLD contrast imaging, but this activity may be at or near threshold levels.

Chapter Five

General Discussion – Towards the Functional Neural Architecture of Language

Chapter Five – Summary

In the present investigation, neural correlates of phonological and semantic processing were studied and the contribution of working memory (WM) was characterized. The phonological mismatch negativity (PMN) was localized primarily to Broca's area with WM sources in the left inferior parietal lobe. The PMN likely represents a specific electromagnetic marker of phonological analysis for speech sound categorization, which is elicited during matching of input against a cognitive template maintained in WM. Critically important was the fact that increased WM load also affected the N400 latency, demonstrating the source of timing delays in behavioural measures of semantic processing as a function WM load (i.e., the fan effect) and implicating left inferior parietal lobe involvement. Convergent evidence was obtained for the localization of primary dipoles for the N400 in the left superior (and middle) temporal region. The exact role of additional N400 sources remains to be determined fully. Given that hemodynamic correlates of the N400 were present in fMRI, it will be useful to use different imaging modalities to address this issue. Indeed, functional mapping of the human brain has improved with respect to identifying the underlying cognitive processes represented by activation. The next step will be to expand the scope of these techniques to better address the neurobiological basis of the particular cognitive function in question.

Chapter Five - Towards the Functional Neural Architecture of Language

Phonological processes, semantic processes, and working memory

Phonological analysis has traditionally been regarded as central to speech comprehension (Liberman, 1992) and, although the exact nature of its role has been debated (Frost, 1998), it is also critical for reading comprehension (Van Orden, 1988). Several ERP studies have now demonstrated that the phonological mismatch negativity (PMN) represents an electromagnetic phonological processing response (Chapter Two; Connolly, Byrne, and Dywan, 1995a; Connolly and Phillips, 1994; Connolly, Phillips, and Forbes, 1995b; Connolly, Service, D'Arcy, Kujala, and Alho, 2001; Dehaene-Lambertz, Dupoux, and Gout, 2000; Hagoort and Brown, 2000; Praamstra and Stegeman, 1993; van den Brink, Brown, and Hagoort, 2000). Connolly et al. (2001) observed that the PMN was associated with a left anterior distribution, and speculated about a source in Broca's area along with possible WM activation. The current investigation localized a PMN source to Broca's area along with another source in the inferior parietal lobe, the latter likely reflected phonological WM.

The findings indicate that the PMN activity represents a specific marker for phonological processing. In this respect, it is similar to the N400, which is a specific marker for semantic processing. As stated earlier, the phenomenon is hypothesized to represent utilization of incoming phonological information, during lexical search processes, in order to formulate candidate lists. Maximal activation can be observed in instances for which the speech input fails to match phonological expectation. However, even phonological matches can elicit PMN activation, particularly in cases where a larger

number of lexical units receive spreading activation. Thus, the term 'Phonological Mismatch Negativity' must be regarded as a description of those conditions in which this manifestation is most readily observed (Connolly et al., 2001).

Other event-related brain potential (ERP) and magnetoencephalographic (MEG) components have been associated with phonological processing in speech and reading. The mismatch negativity (MMN; Näätänen, 1995), a short-duration auditory component that reflects auditory 'echoic' memory, has been shown to be sensitive to phoneme representations (Alho et al., 1998; Näätänen et al., 1997; Szymanski, Yund, and Woods, 1999). However, the MMN is primarily regarded as a perceptual change detection mechanism that responds to various forms of auditory stimuli (i.e., it is not specific to phonological processing). There is also evidence that the N2b, which has been linked to voluntary attentional detection of stimulus deviance (Pritchard, Shappell, and Brandt, 1991), is sensitive to speech mismatches with an existing cognitive template that is stored in phonological WM (Celsis et al., 1999; D'Arcy, Connolly, and Crocker, 2000). But like the MMN, the N2b is not specific to speech input and appears to be related to voluntary attentional processing following deviance detection. Interestingly, a N270 may share similar properties to the PMN during written word processing (i.e., the visual modality counterpart). The N270 has been linked to orthographic deviations from expectancy in visual word processing (Connolly, Phillips, and Forbes, 1995b; Forbes and Connolly, 2002a,b). Recently, Newman and Connolly (2001) varied the orthographic, phonological, and semantic features of terminal words and suggested that it may in fact represent a distinct electrophysiological marker for the translation of orthographic units into

phonological representations. However, other work has suggested that the N270 reflects endogenous mental conflict processing that may occur with different forms of visual stimuli (e.g., digits and shapes; cf. Wang, Kong, Tang, Zhuang, and Li, 2000). It remains to be determined whether the different reports of the N270 are all investigating one phenomenon, which needs to be characterized better, or simply separate observations that happen to share similar response characteristics. Nonetheless, it is clear that both the PMN and N400 are relatively specific language components.

While the PMN is linked to phonological analysis in speech perception, it is also clear that WM activation contributes to the scalp recorded potential. This observation provides further insight into how semantic comprehension may be established. The component has been proposed to lie at the interface between sensory (bottom-up) and contextual (top-down) information, and this interface is not static in time but shifts with the incoming speech input (Connolly and Phillips, 1994). Accounts of speech perception emphasize the processes involved in speech sounds categorization (e.g., segmental, hierarchical, or course; Dehaene-Lambertz et al., 2000). In addition, sentential context and semantic memory structure exert top-down influences during comprehension processes (Chapter Two; Federmeier and Kutas, 1999). The degree to which top-down input is available to speech sound categorization will vary depending on the type of task and the number of possible candidates, which in turn affects the utilization of phonological information. Taking these circumstances into account, it is reasonable to suggest that PMN may represent a process in which continuous phonological analysis for speech sound categorization is matched against a cognitive template maintained in WM.

That is, a dynamic interaction between bottom-up and top-down phonological processing generates the PMN activity and facilitates access to the lexicon.

While WM may be a core process within the PMN, it also appears to interact with the semantic processes indexed by the N400. Increased WM load delayed significantly the latency of the N400, providing valuable insight into the source of WM timing delays measured behaviourally (i.e., the fan effect; Anderson, 1974, 1983). Further, it affected the processing of semantically acceptable items and resulted in the recruitment of additional cortical regions, particularly the left inferior parietal lobe. These results highlighted the ubiquitous influence of WM on cognitive processing. In the future, ERP work examining the effects of increased WM load on the PMN and N400 in the auditory modality as well as fMRI studies on related changes in hemodynamic activation is certainly warranted.

Convergent evidence for the intracranial PMN and N400 generators

The inverse problem has provided the primary challenge to localizing ERP/MEG components because the problem is highly underdetermined (i.e., an infinite number of solutions exist) and requires additional constraints (e.g. mathematical or physiological) to obtain a solution (Grave de Peralta-Menendez and Gonzalez-Andino, 1998). Nonetheless, it has been demonstrated that intracranial generators can in fact be localized for ERP/MEG components, two prominent examples being the auditory N100 in the primary auditory cortices (Verkindt, Bertrand, Perrin, Echallier, and Pernier, 1998) and the MMN in the auditory cortices and the frontal lobe (cf. Rinne, Alho, Ilmoniemi, Virtanen, and Näätänen, 2000). There are two critical factors that helped to substantiate these results: 1)

the source locations were established in a series of related studies for which convergent evidence was obtained; and 2) physiological confirmation of these solutions existed (e.g., the N100 is sensitive to tonotopic manipulations; Verkindt et al., 1998).

The PMN is a relatively small component and typically 'rides' on the N400 (i.e., it can be difficult to isolate). While the N400 has a large SNR (signal-to-noise ratio), it is a later higher order component and can have variable response characteristics (e.g., differences between the auditory and visual modality). Accordingly, both the PMN and the N400 require more advanced models in order to elucidate their respective intracranial generators. As discussed in previous chapters, a shared location for some of the generators irrespective of experimental differences (e.g., sensory modality) has been taken as a strong indication of critical involvement. For the PMN, the ability to show that the same source was modeled in Broca's area for averages with and without the N400 present provided strong evidence for activity in that area. For the N400, the left superior (and middle) temporal lobe (BA 22) responded in a robust manner to manipulations of semantic congruency in both auditory and visual modalities. Of particular relevance is the relative stability of the N400 dipole solutions even after increased WM load significantly changed its peak latency. Further evidence for activation in this region was observed using event-related functional magnetic resonance imaging (fMRI). While the strongest hemodynamic correlates were observed in visual perceptual processing regions, a number of individuals also showed strong activation in the left superior/middle temporal lobe region (Chapter Four). A summary of the spatial localization results, which demonstrates the convergent data, is presented in Figure 22.

Figure 22 - Caption

A schematic summary of the functional activation during speech perception and reading in the left hemisphere. The distribution of intracranial sources for the PMN (auditory) and N400 (auditory and visual) are depicted. Note that the primary PMN dipoles are localized to Broca's area and left inferior parietal regions (associated with WM), whereas the N400 dipoles are distributed throughout the perisylvian region (including WM regions), with differences related to sensory modality being readily apparent. The main regions of hemodynamic N400 correlates (identified by event-related fMRI) are depicted and highlight the convergence between electromagnetic and hemodynamic measures.

Figure 22

Summary of Functional Activation during Speech Perception and Reading

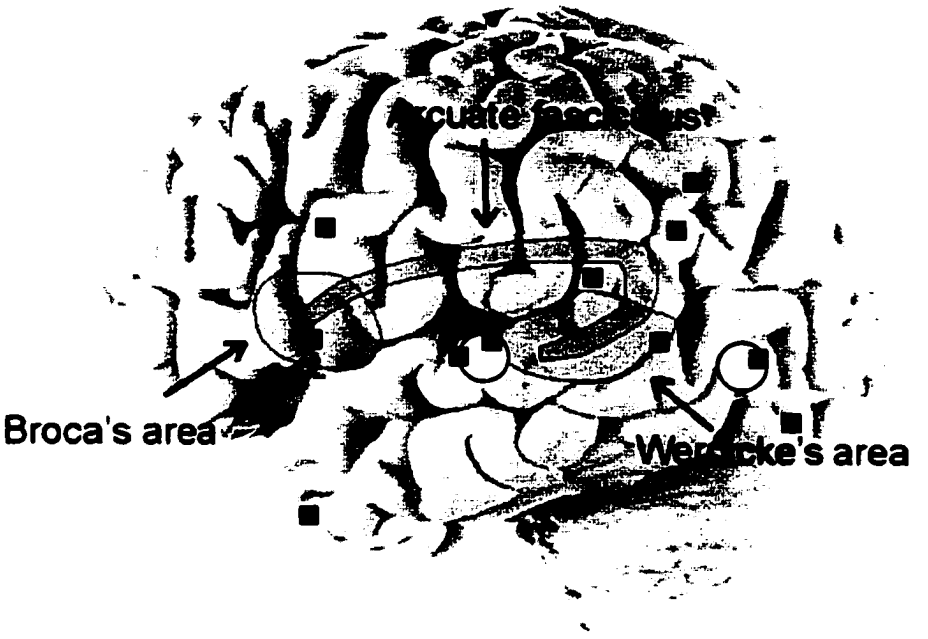

PMN ERP – auditory modality ■

N400 ERP – auditory modality ■

N400 ERP – visual modality ■

N400 fMRI – visual modality ○

The PMN and N400 activation fits well with neurological models of language organization (Chapter One). However, more evidence for physiological validation (second factor, above) is needed. Newman, Connolly, MacDonald, and Arnold (2001) have shown that the PMN is highly sensitive to phonological awareness deficits in dyslexics, with reduced latency and increased amplitude following phonological awareness training. It may be possible to investigate whether these changes exist in Broca's area and the left inferior parietal lobe in order to confirm the PMN source configuration. For the N400, the different functional roles of the various sources that were identified require further investigation For example, although less active, right hemisphere sources for the N400 were found in both auditory and visual modalities. This result fits well with speculation about right hemisphere contributions to accessing semantic memory (Federmeier and Kutas, 1999; St George, Kutas, Martinez, and Sereno; 1999). Presumably, manipulations directed at varying access to semantic memory structure (e.g., categorical relatedness; see Federmeier and Kutas, 1999) may be useful for elucidating the putative contributions of right hemisphere sources.

Insight from multimodal imaging: Multiple signals from neuronal activation

There is considerable potential for non-invasive imaging techniques to contribute to understanding information processing in the human brain. But, continued research is necessary in order to maximize the promise of these techniques. A number of methodological issues have been, or currently are, in the process of being solved. For example, the approach to dealing with differences in individual activation patterns is relatively straightforward (i.e., it is possible to obtain 'group' activation patterns or to

characterize individual differences). Similarly, event-related paradigms, instead of subtraction tasks, have allowed for the use of more sophisticated experimental designs in order to better isolate cognitive functions. Some criticisms have been leveled against the general notion of mapping cognitive systems in the brain. Typically, these arguments concentrate on the 'unknowns' about the cognitive roles of active regions (cf. Bub, 2000). This view may well be justified with respect to some of the earlier research that explored the possibility of imaging higher order functions (e.g., Petersen, Fox, Snyder, and Raichle, 1990), but it is simply incorrect with respect to contemporary work. Indeed, the findings of the current investigation have demonstrated unequivocally that it is possible to fractionate and characterize functional activation and begin exploring the underlying cognitive processes.

Another more serious criticism of brain imaging technologies focuses on physiological and anatomical limitations. Crick and Jones (1993) observed that our understanding of human neuroanatomy (particularly the cerebral cortex) lags behind that of the macaque monkey or rat. Not surprisingly, the difficulty in studying human neuroanatomy has stemmed largely from the fact that many of the experimental methods used with macaques cannot be used with humans. Currently, techniques like ERPs and fMRI provide non-invasive spatiotemporal information about active neural systems. However, this insight into brain function is obtained at the expense of other critical information. In this respect, the term 'neural' aptly describes the coordinated activity of large groups of cells. It is difficult to obtain non-invasive data at the 'neuronal' level. Ultimately, it will be important to non-invasively image cellular and intra-cellar activity

during higher order processes (like semantic processing). Multimodal investigations, which take advantage of the various signals generated either directly or indirectly from neuronal activity, will likely be critical for advancements of this type.

The primary challenge to functional localization at a cellular or intra-cellular level stems in part from current limitations on the absolute spatiotemporal resolution and also from the fact that functional anatomy of higher order processing is dynamic and highly variable in nature. Nonetheless, recent work has provided the initial model upon which to expand. Shulman and Rothman (1998) have emphasized an integrative neuroimaging approach that focuses on neurophysiological parameters of the imaging data (e.g., cerebral metabolic rate of oxygenation), the putative links to neuronal activity (e.g., nitric oxide; Jueptner and Weiller, 1995), and the contribution of neural activity (e.g., N400) to a particular cognitive process (e.g., semantic analysis). These researchers have developed this model largely on the basis of magnetic resonance spectroscopy (MRS) studies of humans and rats. Specifically, they have investigated the coupling of glutamate and γ-aminobutyric acid (GABA) neurotransmitter release to functional neuroenergetics and global electromagnetic activity (Magistretti, Pellerin, Rothman, and Shulman, 1999; Mason et al., 1995; Rothman, Petroff, Behar, and Mattson, 1993; Sibson et al., 1998; Sibson et al., 1997). This type of approach will enable key links to be established between cognition, functional brain activation, and neurobiology. For example, the N400 neural marker can be spatiotemporally isolated (ERPs/MEG; Chapters Two and Three) and linked to neuroenergetic requirements (fMRI; Chapter Four). Future MRS investigations can in turn link neurotransmitter activity to the neuroenergetic changes (fMRI) associated

with the N400 and semantic analysis. While this type of integrated multimodal approach will still be limited by absolute spatial resolution (which is constantly being improved), it has the potential to provide indirect information about cellular (neuronal and glial) and intra-cellular (neurotransmitter) involvement. Thus, this style of functional brain mapping (and its related goals) differs considerable from straightforward comparisons to cartographers; it involves linking functional processes to their neurobiological foundations.

Appendices

Appendix 1

Chapter Two – Experimental Stimuli

High Congruent (1) High Incongruent (2) Low Congruent (3) Low Incongruent (4)

1. The girl is crying in the crib.

   The girl is in the: bedroom – 3

2. The girl is waiting at the luggage carousel.

   The girl is in the: airport – 1

3. The man is swimming in the wave.

   The man is in the: museum (ocean) – 2

4. The woman is singing in the soprano section.

   The woman is in the: choir – 1

5. The woman is cooking in the galley.

   The woman is in the: ship – 3

6. The man is practicing the script lines.

   The man is in the: play – 1

7. The woman is living in the cellblock.

   The woman is in the: traffic (prison) – 2

8. The woman is fixing the furnace.

   The woman is in the: disco (basement) – 2

9. The woman is viewing the light at the end.

   The woman is in the: tunnel – 1

10. The man is experimenting at the Bunsen burner.

The man is in the: biathlon (laboratory) – 2

11. The girl is sitting in the cockpit.

The girl is in the: church (airplane) – 2

12. The boy is storing the safety deposit box.

The boy is in the: bank – 1

13. The boy is riding on the Ferris wheel.

The boy is in the: fair – 3

14. The woman is fighting on the battlefield.

The woman is in the: orchestra (war) – 2

15. The woman is dancing in an evening gown.

The woman is in the: ballroom – 1

16. The girl is ordering at the sandwich counter.

The girl is in the: deli – 3

17. The boy is exploring inside the rocks.

The boy is in the: parlor (cave) – 2

18. The girl is singing in the recording booth.

The girl is in the: wagon (studio) – 2

19. The woman is voting at the ballot box.

The woman is in the: polls – 3

20. The boy is carrying the coffin.

The boy is in the: derby (funeral) – 4

21. The boy is struggling in the rushing winds.

The boy is in the: storm – 3

22. The woman is lounging in the mud bath.

    The woman is in the: car (spa) – 2

23. The woman is swimming in the sunken ship.

    The woman is in the: ocean – 3

24. The man is collecting the toll.

    The man is in the: pool (tollbooth) – 2

25. The man is washing under the water nozzle.

    The man is in the: precession (shower) – 4

26. The girl is playing the video game.

    The girl is in the: arcade – 1

27. The girl is looking across the flat land.

    The girl is in the: prairies – 1

28. The woman is dancing by the DJ booth.

    The woman is in the: stable (bar) – 4

29. The woman is viewing the Pharaoh's tomb.

    The woman is in the: office (pyramid) – 2

30. The woman is shooting at the target.

    The woman is in the: range – 3

31. The woman is reporting the top-story.

    The woman is in the: fighter (newsroom) – 2

32. The boy is climbing in the tree.

    The boy is in the: truck (forest) – 4

33. The girl is buying some shrubs.

The girl is in the: greenhouse – 3

34. The boy is paying the taxi driver.

The boy is in the: sea (taxi-cab) – 2

35. The girl is storing the mop and bucket.

The girl is in the: closet – 3

36. The man is running the 20th mile.

The man is in the: marathon – 1

37. The girl is hiding in the closet.

The girl is in the: pageant (house) – 4

38. The man is leading in the polls.

The man is in the: election – 1

39. The girl is participating in the scientific test.

The girl is in the: laboratory – 3

40. The man is standing at the lotto booth.

The man is in the: tree (mall) – 4

41. The woman is heading towards the subway.

The woman is in the: desert (city) – 4

42. The boy is skating on the ice.

The boy is in the: kitchen (rink) – 4

43. The girl is riding in the coaster car.

The girl is in the: roller coaster – 3

44. The boy is sitting in the barber chair.

The boy is in the: woods (barber) – 4

45. The boy is waving from the decorative float.

    The boy is in the: parade – 1

46. The man is diving in the coral.

    The man is in the: canteen (ocean) – 4

47. The girl is writing on the chalkboard.

    The girl is in the: classroom – 1

48. The girl is swimming away from the crocodiles.

    The girl is in the: swamp – 3

49. The man is sitting with the senators.

    The man is in the: pond (senate) – 4

50. The man is watching the movie.

    The man is in the: theatre - 1

51. The boy is climbing in the rafters.

    The boy is in the: barn – 3

52. The woman is working in the office.

    The woman is in the: river (building) – 4

53. The boy is standing at the fax machine.

    The boy is in the: office – 1

54. The man is entering through the swinging doors.

    The man is in the: marsh (saloon) – 4

55. The girl is sitting on the Queen's throne.

    The girl is in the: sawmill (palace) – 4

56. The boy is working at the cappuccino machine.

The boy is in the: café – 3

57. The boy is relaxing in the swirling hot water.

The boy is in the: hot-tub – 3

58. The girl is buying some fresh meat.

The girl is in the: mailroom (butchers) – 4

59. The girl is sitting in the driver's seat.

The girl is in the: car – 1

60. The boy is playing with trucks in the sand.

The boy is in the: war (sandbox) – 2

61. The woman is appearing on the front page.

The woman is in the: garage (newspaper) – 2

62. The man is working at the power-saw.

The man is in the: workshop – 3

63. The man is crossing the crosswalk.

The man is in the: street – 1

64. The man is cooking at the stove.

The man is in the: tornado (kitchen) – 2

65. The boy is driving the team of horses.

The boy is in the: air force (race) – 4

66. The girl is riding in the caboose.

The girl is in the: train – 1

67. The boy is bidding for the artwork.

The boy is in the: sky (auction) – 2

68. The girl is climbing over the sand dune.

    The girl is in the: desert – 3

69. The woman is watching the outdoor movie.

    The woman is in the: survey (drive-in) – 2

70. The man is standing on the medal podium.

    The man is in the: Olympics – 3

71. The woman is riding on the bucking horse.

    The woman is in the: rodeo – 1

72. The man is organizing the mail.

    The man is in the: yacht (post-office) – 4

73. The girl is running towards the net.

    The girl is in the: game - 3

74. The man is escaping from the torture chamber.

    The man is in the: bus (dungeon) – 4

75. The woman is swinging in the hammock.

    The woman is in the: restaurant (backyard) – 2

76. The girl is selling the old clothing.

    The girl is in the: Jacuzzi (flee-market) – 4

77. The boy is swimming in shallow end.

    The boy is in the: pool – 1

78. The girl is waiting by the trains.

    The girl is in the: boutique (station) – 2

79. The man is circling in the glider.

The man is in the: air – 3

80. The boy is appearing on the big screen.

The boy is in the: movie – 1

81. The man is running on the inside lane.

The man is in the: race – 3

82. The woman is getting into the fire engine.

The woman is in the: supermarket (fire-station) – 2

83. The woman is acting in the play.

The woman is in the: lagoon (theatre) – 2

84. The woman is sleeping in the tent.

The woman is in the: department (campground) – 4

85. The woman is trading the gold shares.

The woman is in the: stock market – 1

86. The man is working at the assembly line.

The man is in the: vault (factory) – 2

87. The girl is playing on the basketball court.

The girl is in the: gym – 3

88. The man is standing at the punch bowl.

The man is in the: jail (party) – 4

89. The boy is standing in the pastry section.

The boy is in the: campaign (bakery) – 4

90. The boy is playing the drums.

The boy is in the: band – 1

91. The boy is looking at the tiger cage.

    The boy is in the: zoo – 1

92. The boy is helping the superintendent.

    The boy is in the: rodeo (apartment) – 4

93. The man is waiting on the batting bench.

    The man is in the: dugout – 3

94. The woman is looking at the ring display.

    The woman is in the: orchard (jewelers) – 2

95. The man is dousing water on the hot rocks.

    The man is in the: sauna – 1

96. The boy is running past the ten-yard line.

    The boy is in the: casino (game) – 4

Appendix 2

Chapter Three – Experimental Stimuli

High Congruent (1) High Incongruent (2) Low Congruent (3) Low Incongruent (4)

Level 1

1. The man is collecting the toll.

   The man is in the: tollbooth - 1

2. The man is experimenting at the Bunsen burner.

   The man is in the: laboratory - 1

3. The boy is storing the lawn mower.

   The boy is in the: shed - 3

4. The boy is exploring inside the rocks.

   The boy is in the: parlor (cave) - 2

5. The boy is standing in the pastry section.

   The boy is in the: bakery - 3

6. The woman is sunning on the beach chair.

   The woman is in the: beach - 3

7. The girl is paying at the teller.

   The girl is in the: bank - 1

8. The man is circling in the glider.

   The man is in the: nunnery (air) - 4

9. The woman is sleeping in the tent.

   The woman is in the: campground - 3

10. The woman is lying in the sleeping bag.

The woman is in the: tent - 1

11. The girl is waiting by the trains.

The girl is in the: dance (station) - 2

12. The man is working under the vehicle hoist.

The man is in the: garage - 1

13. The boy is standing in the dockyard.

The boy is in the: navy - 3

14. The girl is climbing over the sand dune.

The girl is in the: snowfall (desert) - 4

15. The boy is paying the taxi driver.

The boy is in the: sea (taxi-cab) - 2

16. The man is watching the movie.

The man is in the: freeway (theatre) - 2

17. The boy is pulling the 'next-stop' cord.

The boy is in the: bus - 1

18. The man is washing the parked car.

The man is in the: driveway - 3

19. The boy is singing on the stage.

The boy is in the: car (concert) - 4

20. The woman is swinging in the hammock.

The woman is in the: tour (backyard) - 2

21. The girl is climbing out of the manhole.

The girl is in the: sewer - 1

22. The man is leading in the polls.

    The man is in the: airfield (election) - 2

23. The girl is selling the old clothing.

    The girl is in the: chimney (flee-market) - 4

24. The boy is standing at the punch bowl.

    The man is in the: jail (party) - 4

25. The boy is skating on the ice.

    The boy is in the: rink - 3

26. The girl is staying in the bunkhouse.

    The girl is in the: jet (camp) - 4

27. The man is soaking in the hot water.

    The man is in the: bathtub - 1

28. The girl is sitting in the driver's seat.

    The girl is in the: volcano (car) - 2

29. The man is escaping from the collapsed building.

    The man is in the: earthquake - 3

30. The woman is living in the cellblock.

    The woman is in the: prison - 1

31. The man is working at the assembly line.

    The man is in the: vault (factory) - 2

32. The girl is fixing the barbwire fence.

    The girl is in the: yacht (field) - 4

33. The woman is getting into the fire engine.

The woman is in the: fire station - 1

34. The boy is pushing through the many people.

The boy is in the: hammock (crowd) - 2

35. The woman is struggling under the snow.

The woman is in the: puddle (avalanche) - 4

36. The woman is singing in the soprano section.

The woman is in the: choir - 1

37. The woman is appearing on the front page.

The woman is in the: district (newspaper) - 2

38. The man is sitting with the senators.

The man is in the: pond (senate) - 4

39. The boy is visiting the injured pet.

The boy is in the: lagoon (veterinarian) - 2

40. The boy is building the tree fort.

The boy is in the: backyard - 3

41. The woman is trapped in the crashed car.

The woman is in the: accident - 1

42. The man is diving in the coral.

The man is in the: street (ocean) - 4

43. The girl is buying some fresh meat.

The girl is in the: butchers - 3

44. The girl is sitting on the highest branch.

The girl is in the: bunker (tree) - 2

45. The girl is hiding in the closet.

    The girl is in the: river (house) - 4

46. The woman is trying on a dress.

    The woman is in the: rally (store) - 4

47. The man is washing under the water nozzle.

    The man is in the: shower - 3

48. The boy is eating by the lunch tray rack.

    The boy is in the: runway (cafeteria) - 2

49. The girl is viewing the art exhibit.

    The girl is in the: gallery - 1

50. The woman is blowing the foghorn.

    The woman is in the: lighthouse - 1

51. The boy is riding on the Ferris wheel.

    The boy is in the: lobby (fair) - 4

52. The man is entering through the swinging doors.

    The man is in the: saloon - 3

53. The girl is sitting in the pew.

    The girl is in the: vehicle (church) - 2

54. The man is reporting the agenda.

    The man is in the: jungle (meeting) - 4

55. The woman is carrying the picket sign.

    The man is in the: strike - 3

56. The boy is helping the superintendent.

The boy is in the: apartment - 3

57. The girl is sharing the room with other students.

The girl is in the: pasture (dormitory) - 2

58. The woman is paying at the cash register.

The woman is in the: store - 1

59. The woman is voting at the ballot box.

The woman is in the: everglades (polls) - 4

60. The girl is crossing the clearing.

The girl is in the: field - 3

Level 2

1. The woman is riding on the underground train.

   The woman is lounging in the mud bath.

   The woman is in the: spa – 1

2. The girl is waiting by the receptionist desk.

   The girl is running past the ten-yard line.

   The girl is in the: office – 3

3. The woman is sitting in the space capsule.

   The woman is at performing on the piano.

   The woman is in the: dingy (spaceship) – 4

4. The boy is sitting on the witness stand.

   The boy is standing at the grave.

   The boy is in the: courtroom - 1

5. The boy is bidding for the artwork.

   The boy is storing the safety deposit box.

   The boy is in the: sky (auction) - 2

6. The woman is viewing the Pharaoh's tomb.

   The woman is fixing the furnace.

   The woman is in the: basement - 1

7. The boy is working in the office.

   The boy is opening the drawbridge.

   The boy is in the: castle - 3

8. The boy is riding in the caboose.

The boy is competing in the 100-metre sprint.

The boy is in the: art-class (race) - 2

9. The man is waiting on the batting bench.

The man is standing at the dairy case.

The man is in the: dugout – 3

10. The boy is shooting at the target.

The boy is relaxing in the swirling hot water.

The boy is in the: hot-tub – 3

11. The girl is standing by the washing machines.

The girl is sitting in the cockpit.

The girl is in the: snow fort (Laundromat) – 2

12. The boy is cooking in the galley.

The boy is waiting at the pharmacy counter.

The boy is in the: graveyard (drugstore) – 4

13. The girl is lying in the operating room.

The girl is digging in the coal pit.

The girl is in the: hospital – 1

14. The man is standing at the lotto booth.

The man is fixing the parked airplane.

The man is in the: mall – 3

15. The boy is waving from the decorative float.

The boy is looking at the tiger cage.

The boy is in the: zoo – 1

16. The girl is cooking at the stove.

    The girl is sitting at a table-for-two.

    The girl is in the: marsh (restaurant) – 2

17. The girl is appearing on the big screen.

    The girl is eating in the dining car.

    The girl is in the: movie – 1

18. The man is sitting at the slot machine.

    The man is crossing the crosswalk.

    The man is in the: glacier (casino) – 2

19. The girl is riding in the coaster car.

    The girl is running towards the net.

    The girl is in the: bunk bed (roller coaster) – 4

20. The woman is looking through the periscope.

    The woman is reporting the top-story.

    The woman is in the: fighter (newsroom) – 2

21. The man is swimming away from the crocodiles.

    The man is examining the new cars.

    The man is in the: dealership – 3

22. The boy is crying in the crib.

    The boy is climbing in the tree.

    The boy is in the: union (forest) – 4

23. The man is swinging in the sand trap.

    The man is drinking from the beer tap.

The man is in the: playpen (bar) – 4

24. The boy is looking across the flat land.

    The boy is tending to the apple trees.

    The boy is in the: orchard – 1

25. The girl is sitting on the Queen's throne.

    The girl is participating in the scientific test.

    The girl is in the: food court (palace) – 4

26. The woman is paddling in the stern seat.

    The woman is organizing the mail.

    The woman is in the: canoe – 3

27. The boy is working at the cappuccino machine.

    The boy is buying some shrubs.

    The boy is in the: bathroom (café) – 4

28. The man is boxing the challenger.

    The man is sleeping in the barracks.

    The man is in the: ring – 1

29. The woman is dousing water on the hot rocks.

    The woman is looking at the ring display.

    The woman is in the: blizzard (jewelers) – 2

30. The girl is dancing with the ballerinas.

    The girl is fighting on the battlefield.

    The girl is in the: whirlpool (ballet) – 2

31. The woman is carrying the coffin.

The woman is mushing the pack of huskies.

The woman is in the: arctic – 3

32. The girl is stopping the penalty shot.

The girl is ordering at the sandwich counter.

The girl is in the: sauna (deli) – 4

33. The woman is flying in the fighter plane.

The woman is sitting in the barber chair.

The woman is in the: stadium (airforce) – 4

34. The woman is trading the gold shares.

The woman is standing at the fax machine.

The boy is in the: lake (office) – 2

35. The girl is writing on the chalkboard.

The girl is balancing on the high wire.

The girl is in the: classroom – 1

36. The man is living with the monks.

The man is looking through the telescope.

The man is in the: hurricane (monastery) – 2

37. The girl is climbing in the rafters.

The girl is playing on the basketball court.

The girl is in the: monarchy (gym) – 4

38. The man is escaping from the torture chamber.

The man is on the bottom bunk.

The man is in the: dungeon – 3

39. The girl is waiting in the lobby.

    The girl is watching the wild gorillas.

    The girl is in the: tunnel (hotel) – 4

40. The man is studying in the carrel.

    The man is watching the outdoor movie.

    The man is in the: blimp (drive-in) – 2

41. The man is standing on the medal podium.

    The man is cursing at the stalled car.

    The man is in the: Olympics – 3

42. The boy is struggling in the rushing winds.

    The boy is standing at the dog cages.

    The boy is in the: tavern (kennel) – 4

43. The boy is swimming in shallow end.

    The boy is sitting in the detention room.

    The boy is in the: school – 1

44. The girl is browsing in the fiction section.

    The girl is storing the mop and bucket.

    The girl is in the: closet – 3

45. The man is paddling down the rapids.

    The man is sitting on the slide.

    The man is in the: car-lot (river) – 4

46. The boy is playing with trucks in the sand.

    The boy is singing in the recording booth.

The boy is in the: congress (sandbox) –2

47. The girl is raising the main sail.

The girl is playing the drums.

The girl is in the: band – 1

48. The woman is viewing the light at the end.

The woman is dancing in an evening gown.

The woman is in the: safari (ballroom) – 2

49. The man is swimming in the sunken ship.

The man is moving to the music.

The man is in the: disco – 3

50. The man is building the igloo.

The man is running on the sidewalk.

The man in the: amazon (city) – 4

51. The woman is acting in the play.

The woman is running the 20th mile.

The woman is in the: theater – 1

52. The man is swimming in the wave.

The man is playing the video game.

The man is in the: treasury (ocean) – 2

53. The boy is practicing the script lines.

The boy is running towards the finish line.

The boy is in the: race – 1

54. The woman is singing in the shower.

The woman is kissing the groom.

The woman is in the: electorate (wedding) – 2

55. The woman is dancing by the DJ booth.

The woman is working at the power-saw.

The woman is in the: bar – 3

56. The woman is storing the sports gear in the locker.

The woman is living with the nuns.

The woman is in the: convent – 3

57. The man is standing on the doormat.

The man is appearing on the billboard picture.

The man is in the: corral (porch) – 4

58. The woman is heading towards the subway.

The woman is standing at the craft tent.

The woman is in the: city – 3

59. The girl is riding on the bucking horse.

The girl is tending to the rose bushes.

The girl is in the: rodeo – 1

60. The boy is waiting at the luggage carousel.

The boy is getting some suit alterations.

The man is in the: tailor – 1

Appendix 3

Chapter Four – Experimental Stimuli

Stimulus codes:

Congruent initial orthographic match (1)

Incongruent initial orthographic match (2)

Congruent initial orthographic mismatch (3)

Incongruent initial orthographic mismatch (4)

Experimental Session

1) Sharon dried the bowels with a... towel. - 1

2) Shuffle the cards before you... tree. - 4

3) He mailed the letter without a... stampede. - 2

4) Ray fell down and skinned his... knee. - 1

5) The academic year began in the... grow. - 4

6) Water and sunshine help plants... grow. - 1

7) At last the time for action had... arrived. - 3

8) At night the old woman locked the... door. - 1

9) She called her husband at his... convenience. - 3

10) The children went outside to... placement. - 2

11) George could not believe his son stole a... truck. - 3

12) Her job was easy most of the... time. - 2

13) The teacher wrote the problem on the... heat. - 4

14) He hung her coat in the... marathon. - 4

15) Pete won the cross-country... event. - 3

Control Session

1) He lay down and went to... sleeves. - 2

2) The exit was marked by a large... sign. - 1

3) When the shooting started, they ran for... safety. - 3

4) The pigs wallowed in the... pen. - 3

5) The man was caught selling an illegal... weapon. - 3

6) The pizza was too hot to... sing. - 4

7) He liked lemon and sugar in his... coffee. - 3

8) It's hard to admit when one is... rock. - 2

9) Jean hurriedly shoveled her way through the... crouch. - 2

10) The gambler had a streak of bad... luggage. - 2

11) The baby cried and upset her... sitter. - 3

12) The lawyer feared his client was... velvet. - 4

13) The picnic was ruined by the... ants. - 3

14) Most shark attacks occur very close to... trees. - 4

15) Don't touch the wet... painful. - 2

References

Aguirre, G. K., Zarahn, E., & D'Esposito, M. (1998). The variability of human BOLD hemodynamic responses. *NeuroImage, 8*, 360-369.

Alexander, M. P. (1997). Aphasia: Clinical and anatomic aspects. In: T.E. Feinberg & M.J. Farah (Eds.), *Behavioral neurology and neuropsychology* (pp. 133-149). New York, McGraw-Hill.

Alho, K., Connolly, J. F., Cheour, M., Lehtokoski, A., Huotilainen, M., Virtanen, J., Aulanko, R., & Ilmoniemi, R. J. (1998). Hemispheric lateralization in preattentive processing of speech sounds. *Neuroscience Letters, 258*, 9-12.

American Electroencephalographic Society: Guidelines for standard electrode position nomenclature. (1991). *Journal of Clinical Neurophysiology, 8*, 200-202.

Anderson, J. R. (1974). Retrieval of propositional information from long-term memory. *Cognitive Psychology, 6*, 451-474.

Anderson, J.R. (1983). A spreading activation theory of memory. *Journal of Verbal Learning and Verbal Behavior, 22*, 261-295.

Baddeley, A. D. (1992). Working memory. *Science, 255*, 556-559.

Baddeley, A. D. (1996). The fractionation of working memory. *Proceedings of the National Academy of Sciences USA, 93*, 13468-13472.

Baddeley, A. D., & Hitch, G. J. (1974). Working memory. In: G. H. Bower (Ed.). *The Psychology of Learning and Motivation: Advances in Research and Theory* (pp. 47-89). New York: Academic Press.

Becker, J. T., MacAndrew, D. K., & Fiez, J. A. (1999). A comment on the functional localization of the phonological storage subsystem of working memory. *Brain and Cognition, 41*, 27-38.

Bentin, S., McCarthy, G., & Wood, C. (1985). Event-related potentials, lexical decision and semantic priming. *Electroencephalography and Clinical Neurophysiology, 60*, 343-355.

Berg, P., Kakigi, R., Scherg, M., Dobel, C., & Zobel, E. (1999). Source modeling of the EEG and MEG oddball response in a subject with a large P300. *Electroencephalography and Clinical Neurophysiology, Supplemental, 49*, 189-193.

Binder, J. R., & Mohr, J. P. (1992). The topography of callosal reading pathways: A case-control analysis. *Brain, 115*, 1807-1826.

Bloom, P. A., & Fischler, I. (1980). Completion norms for 329 sentence contexts. *Memory and Cognition, 8*, 631-641.

Braver, T. S., Cohen, J. D., Nystrom, L. E., Jonides, J., Smith, E. E., & Noll, D. C. (1997). A parametric study of prefrontal cortex involvement in human working memory. *NeuroImage, 5*, 49-62.

Broca, P. (1861). Remarques sur le siège de la faculté du langage articulé; suivies d'une observation d'aphemie. *Bulletin de la Société Anatomique de Paris, 6*, 330-357.

Brown, C., & Hagoort, P. (1993). The processing nature of the N400: Evidence from masked priming. *Journal of Cognitive Neuroscience, 5*, 34-44.

Bub, D. (2000). Methodological issues confronting PET and fMRI studies of cognitive function. *Cognitive Neuropsychology, 17*, 467-484.

Cabeza, R., & Nyberg, L. (2000). Imaging cognition II: An empirical review of 275 PET and fMRI studies. *Journal of Cognitive Neuroscience, 12*, 1-47.

Cantor, J., & Engle, R. W. (1993). Working memory capacity as long-term memory activation: An individual difference approach. *Journal of Experimental Psychology: Learning, Memory, and Cognition, 19*, 1101-1114.

Caplan, D., Carr, T., Gould, J., & Martin, R. (1999). Language and communication. In: M. J. Zigmond, F. E. Bloom, S. C. Landis, J. L. Roberts, & L. R. Squire (Eds.). *Fundamental neuroscience* (pp. 1487-1520). San Diego: Academic Press.

Caplan, D., & Hildebrandt, N. (1988). *Disorders of syntactic comprehension.* Cambridge, MA: MIT Press.

Celsis, P., Doyon, B., Boulanouar, K., Pastor, J., Démonet, J.F., & Nespoulous, J.L. (1999). ERP correlates of phoneme perception in speech and sound contexts. *NeuroReport, 10*, 1523-1527

Chiappa, K. H. (1997). *Evoked potentials in clinical medicine.* New York: Raven Press.

Connolly, J. F., Byrne, J. M., & Dywan, C. A. (1995a). Assessing adult receptive vocabulary with event-related potentials: An investigation of cross modal and cross form priming. *Journal of Clinical and Experimental Neuropsychology, 17*, 548-565.

Connolly, J. F., D'Arcy, R. C. N., MacMaster, F. P., Marchand, Y., & Service, E. (2002). Orthographic and semantic fMRI activation in sentence reading. In preparation.

Connolly, J. F., & Phillips, N. A. (1994). Event-related potential components reflect phonological and semantic processing of the terminal word of spoken sentences. *Journal of Cognitive Neuroscience, 6*, 256-266.

Connolly, J. F., Phillips, N. A., Forbes, K. A. K. (1995b). The effects of phonological and semantic features of sentence-ending words on visual event-related brain potentials. *Electroencephalography and Clinical Neurophysiology, 94*, 276-287.

Connolly, J. F., Phillips, N. A., Stewart, S. H., & Brake, W. (1992). Event-related potential to acoustic and semantic properties of terminal words in sentences. *Brain and Language, 43*, 1-18.

Connolly, J. F., Service, E., D'Arcy, R. C. N., Kujala, A., & Alho, K. (2001) Phonological aspects of word recognition as revealed by high-resolution spatio-temporal brain mapping. *NeuroReport, 12*, 237-243.

Connolly, J. F., Stewart, S. H., & Phillips, N. A. (1990). The effects of processing requirements on neurophysiological responses to spoken sentences. *Brain and Language, 39*, 302-318.

Coslett, H. B. (1997). Acquired dyslexia. In: T.E. Feinberg & M.J. Farah (Eds.), *Behavioral neurology and neuropsychology* (pp. 197-208). New York, McGraw-Hill.

Cowan, N. (1995). *Attention and memory: An integrated framework.* Oxford Psychology Series, No. 26. New York: Oxford University Press.

Cowan, N., Winkler, I., Teder, W., & Näätänen, R. (1993). Memory prerequisites of the mismatch negativity in the auditory event-related potential (ERP). *Journal of Experimental Psychology: Learning, Memory, and Cognition, 19*, 909-921.

Crick, F., & Jones, E. (1993). Backwardness of human neuroanatomy. *Nature, 361*, 109-110.

Dale, A. M., & Buckner, R. L. (1997). Selective averaging of rapidly presented individual trials using fMRI. *Human Brain Mapping 5*, 329-340.

Dale, A. M., Liu, A. K., Fischl, B. R., Buckner, R. L., Belliveau, J. W., Lewine, J. D., & Halgren, E. (2000). Dynamic statistical parametric mapping: Combining fMRI and MEG for high-resolution imaging of cortical activity. *Neuron, 26*, 55-67.

Damasio, A. R., & Damasio, H. (1983). The anatomical basis of pure alexia. *Neurology, 33*, 1573-1583.

Daneman, M., & Carpenter, P. A. (1980). Individual differences in working memory and reading. *Journal of Verbal Learning and Verbal Behavior, 19*, 450-466.

D'Arcy, R. C. N. (1996). *Neuropsychological assessment of receptive language comprehension with event-related brain potentials*. M.Sc. Thesis. Halifax: Dalhousie University.

D'Arcy, R. C. N., Connolly, J. F., & Crocker, S. F. (2000). Latency shifts in the N2b component track phonological deviations in spoken words. *Clinical Neurophysiology, 111*, 40-44.

D'Arcy, R. C. N., Marchand, Y., Eskes, G. A., Harrison, E. R., Phillips, S. J., Major, A., & Connolly, J. F. (2002). Evoked potential assessment of language function following stroke. Submitted.

Deacon, D., Hewitt, S., Yang, C. M., & Nagata, M. (2000). Event-related potential indices of semantic priming using masked and unmasked words: Evidence that the N400 does not reflect a post-lexical process. *Cognitive Brain Research, 9*, 136-146.

DeArmond, S. J., Fusco, M. M., & Dewey, M. M. (1989). Structure of the human brain: A photographic atlas 3rd Ed. New York: Oxford University Press.

Dehaene-Lambertz, G., Dupoux, E., & Gout, A. (2000). Electrophysiological correlates of phonological processing: A cross-linguistic study. *Journal of Cognitive Neuroscience, 12,* 635-647.

Déjerine, J. (1891). Sur un cas de cecite verbale avec agraphie, suivi d'autopsie. *Mémoires de la Société de Biologique, 3,* 197-201.

Déjerine, J. (1892). Contribution a l'étude anatomoclinique et clinique des differentes varieties de cecite verbal. *Compte Rendu Hebdomadaire des Séances et Mémoires de la Société de Biologie, 4,* 61-90.

Démonet, J. F., Chollet, F., Ramsay, S., Cardebat, D., Nespoulous, J. L., Wise, R., Rascol, S., & Frackowiak, R. S. J. (1992). The anatomy of phonology and semantic processing in normal subjects. *Brain, 115,* 1753-1768.

Démonet, J. F., Price, C., Wise, R., Frackowiak, R. S. J. (1994). Differential activation of right and left posterior sylvian regions by semantic and phonological tasks: A positron-emission tomography study in normal human subjects. *Neuroscience Letters, 182,* 25-28.

Démonet, J. F., & Thierry, G. (2001). Language and the brain: What is up? What is coming up? *Journal of Clinical and Experimental Neuropsychology, 23,* 49-73.

D'Esposito, M. (2000). Functional neuroimaging of cognition. *Seminars in Neurology, 20,* 487-498.

Engle, R. W. (1996). Working memory and retrieval: An inhibition-resource approach. In: J. T. E. Richardson, R. W. Engle, L. Hasher, R. H. Logie, E. R. Stoltzfus, & R. T. Zacks (Eds). *Working Memory and Human Cognition.* (89-119). New York: Oxford University Press.

Engle, R. W., Cantor, J., & Carullo, J. J. (1992). Individual differences in working memory and comprehension: A test of four hypotheses. *Journal of Experimental Psychology: Learning, Memory, and Cognition, 18*, 972-992.

Ericsson, K. A., & Kintsch, W. (1995). Long-term working memory. *Psychological Reviews, 102*, 211-245.

Federmeier, K. D., & Kutas, M. (1999). A rose by any other name: Long-term memory structure and sentence processing. *Journal of Memory and Language, 41*, 469-495.

Federmeier, K. D., & Kutas, M. (2001). Meaning and modality: Influences of context, semantic memory organization, and perceptual predictability on picture processing. *Journal of Experimental Psychology, 27*, 202-224.

Feiz, J. A., & Petersen, S. E. (1998). Neuroimaging studies of word reading. *Proceedings of the National Academy of Sciences USA, 95*, 914-921.

Forbes, K. A. K., & Connolly, J. F. (2002a). Event-related brain potentials (ERPs) measure the influence of orthographic, phonological, and semantic representations during silent reading. In preparation.

Forbes, K. A. K., & Connolly, J. F. (2002b). Evidence for phonological influence during silent reading involving homophones and pronounceable non-words. In preparation.

Friston, K. J. (1994). Functional and effective connectivity: A synthesis. *Human Brain Mapping, 2*, 56-78.

Friston, K. J. (1995). Commentary and opinion: II. Statistical parametric mapping: Ontology and current issues. *Journal of Cerebral Blood Flow and Metabolism, 15*, 361-370.

Friston, K. J., Price, C. J., Fletcher, P., Moore, C., Frackowiak, R. S., & Dolan, R. J. (1996). The trouble with cognitive subtraction. *NeuroImage, 4*, 97-104.

Frost, R. (1998). Toward a strong phonological theory of visual word recognition: True issues and false trails. *Psychological Bulletin, 123*, 71-99.

Ganis, G., Kutas, M., & Sereno, M. I. (1996). The search for "common sense": An electrophysiological study of the comprehension of words and pictures in reading. *Journal of Cognitive Neuroscience, 8*, 89-106.

Goldman-Rakic, P. S. (1990). Cellular and circuit basis of working memory in prefrontal cortex of nonhuman primates. *Progress in Brain Research, 85*, 325-335.

Goodglass, H. (1993). Understanding aphasia. In: L. S. Cermak LS, (Ed.). *Foundations of neuropsychology*. San Diego: Academic Press.

Grave de Peralta-Menendez, R., & Gonzalez-Andino, S. L. (1998). A critical analysis of the linear inverse solution to the neuroelectromagnetic inverse problem. *IEEE Transactions on Biomedical Engineering, 45*, 440-448.

Greenhouse, S. W., & Geisser, S. (1959). On methods in the analysis of profile data. *Psychometrika, 24*, 95-112.

Gunter, T. C., Jackson, J. L., & Mulder, G. (1995). Language, memory, and aging: An electrophysiological exploration of the N400 during reading of memory-demanding sentences. *Psychophysiology, 32*, 215-229.

Haan, H., Streb, J., Bien, S., & Rösler, F. (2000). Individual cortical current density reconstructions of the semantic N400 effect: Using a generalized minimum norm model with different constraints (L1 and L2 norm). *Human Brain Mapping, 11*, 178-192.

Hagoort, P., & Brown, C. (2000). ERP effects of listening to speech: Semantic ERP effect. *Neuropsychologia, 38*, 1518-1530.

Hämäläinen, M., Hari, R., Ilmoniemi, R. J., Knuutila, J., & Lounasmaa, O. V. (1993). Magnetoencephalography-theory, instrumentation, and applications to noninvasive studies of the working human brain. *Reviews of Modern Physics, 65*, 413-497.

Helenius, P., Samelin, R., Service, E., & Connolly, J. F. (1998). Distinct time courses for word and context comprehension in the left temporal cortex. *Brain, 121*, 1133-1142.

Helenius, P., Samelin, R., Service, E., Connolly, J. F., Leinonen, S., & Lyytinen, H. (2002). Cortical activation during spoken-word segmentation in non-reading-impaired and dyslexic adults. *Journal of Neuroscience,* manuscript accepted.

Hickok, G., & Poeppel, D. (2000). Towards a functional neuroanatomy of speech perception. *Trends in Cognitive Science, 4*, 131-138.

Hoge, R. D., & Pike, B. (2001). Oxidative metabolism and the detection of neuronal activation via imaging. *Journal of Chemical Neuroanatomy, 22*, 43-52.

Holcomb, P. J. (1993). Semantic priming and stimulus degradation: Implications for the role of the N400 in language processing. *Psychophysiology, 30*, 47-61.

Holcomb, P. J., & Neville, H. J. (1990). Auditory and visual semantic priming in lexical decision: A comparison using evoked potentials. *Language and Cognitive Processes, 5*, 281-312.

Honey, G. D., Bullmore, E. T., & Sharma, T. (2000). Prolonged reaction time to a verbal working memory task predicts increased power of posterior parietal cortical activation. *NeuroImage, 12*, 495-503.

Jasper, H. H. (1958). The ten-twenty electrode system of the international federation. *Electroencephalography and Clinical Neurophysiology, 10*, 371-375.

Jueptner, M., & Weiller, C. (1995). Review: Does measurement of regional cerebral blood flow reflect synaptic activity? Implications for PET and fMRI. *Neuroimage, 2*, 148-156.

Kim, D. S., Duong, T. O., & Kim, S. G. (2000). High-resolution mapping of iso-orientation columns by fMRI. *Nature Neuroscience, 3*, 164-169.

King, J., & Just, M. A. (1991). Individual differences in syntactic processing: The role of working memory. *Journal of Memory and Language, 30*, 580-602.

Kintch, W. (1977). *Memory and cognition.* New York: John Wiley & Sons.

Knight, R. T. (1997). Electrophysiological methods in behavioral neurology and neuropsychology. In: T. E. Feinberg & M. J. Farah (Eds.), *Behavioral neurology and neuropsychology* (pp. 101-120). New York, McGraw-Hill.

Kolb B., & Whishaw, I. Q. (1996). *Fundamentals of human neuropsychology.* New York: H. Freeman and Company.

Kuriki, S., Takeuchi, F., & Hirata, Y. (1998). Neural processing of words in the human extrastriate visual cortex. *Cognitive Brain Research, 6*, 193-203.

Kutas, M. (1997). Views on how the electrical activity that the brain generates reflects the functions of different language structures. *Psychophysiology, 34*, 383-398.

Kutas, M., & Hillyard, S. A. (1980). Reading senseless sentences: Brain potentials reflect semantic incongruity. *Science, 207*, 203-205.

Kutas, M., & Van Petten, C. (1994). Psycholinguistics electrified: Event-related brain potential investigations. In: M.A. Gernsbacher (Ed.). *Handbook of Psycholinguistics*. (83-143). San Diego: Academic Press.

Lichtheim, L. (1885). On aphasia. *Brain, 7*, 433-484.

Liberman, A. M. (1992). On the relation for speech to reading and writing. Pp. 167-178. In: R. Frost, & L. Latz (Eds.). *Orthography, phonology, morphology, and meaning.* Amsterdam: North Holland.

Loftus, E. F., Freedman, J. L., & Loftus, G. R. (1970). Retrieval of words from subordinate and superordinate categories in semantic hierarchies. *Psychonomic Science, 21*, 235-236.

Magistretti, P. J., & Pellerin, L. (1996). Cellular bases of brain energy metabolism and their relevance to functional brain imaging: evidence for a prominent role of astrocytes. *Cerebral Cortex, 6*, 50-61.

Magistretti, P. J., Pellerin, L., Rothman, D. L., & Shulman, R. G. (1999). Energy on demand. *Science, 283*, 496-497.

Marslen-Wilson, W. D. (1984). Function and process in spoken word recognition: A tutorial review. In: H. Bourma & D. G. Bouwhuis (Eds.). *Attention and performance X: Control of language processes* (pp. 125-150). Hillsdale, NJ: Lawrence Erlbaum Associates.

Mason, G. F., Gruetter, R., Rothman, D. L., Behar, K. L., Shulman, R. G., & Novotny, E. J. (1995). Simultaneous determination of the rates of the TCA cycle, glucose utilization, α-ketoglutarate/glutamate exchange, and glutamine synthesis in human brain by NMR. *Journal of Cerebral Blood Flow and Metabolism, 15*, 12-25.

McCarthy, G. (1999). Event-related potentials and functional MRI: A comparison of localization in sensory, perceptual, and cognitive tasks. *Electroencephalography and Clinical Neurophysiology Supplemental, 49*, 3-12.

McCarthy, G., Nobre, A. C., Bentin, S., & Spencer, D. D. (1995). Language-related field potentials in the anterior-medial temporal lobe: I. Intracranial distribution and neural generators. *The Journal of Neuroscience, 15*, 1080-1089.

McCarthy, G., & Wood, C. C. (1985). Scalp distribution of event-related potentials: An ambiguity associated with the analysis of variance models. *Electroencephalography and Clinical Neurophysiology, 62*, 203-208.

Mecklinger, A., Kramer, A. F., & Strayer, D. L. (1992). Event-related potentials and EEG components in a semantic memory search task. *Psychophysiology, 29*, 104-119.

Menon, R. S., & Goodyear, B. G. (1999). Submillimeter functional localization in human striate cortex using BOLD contrast at 4 Tesla: Implications for the vascular point-spread function. *Magnetic Resonance in Medicine, 41*, 230-235.

Menon, R. S., & Kim, S. G. (1999). Spatial and temporal limits in cognitive neuroimaging with fMRI. *Trends in Cognitive Science, 3*, 207-216.

Meyer, D. E., & Schvaneveldt, R. W. (1971). Facilitation in recognizing pairs of words: Evidence of a dependence between retrieval operations. *Journal of Experimental Psychology, 90*, 227-234.

Miyake, A., & Shah, P. (1999). *Models of Working Memory.* Cambridge, UK: Cambridge University Press.

Näätänen, R. (1995). The mismatch negativity: a powerful tool for cognitive neuroscience. *Ear and Hearing, 16*, 6-18.

Näätänen, R., Lehtokoski, A., Lennes, M., Cheour, M., Huotilainen, M., Iivonen, A., Vainio, M., Alku, P., Ilmoniemi, R. J., Luuk, A., Allik, J., Sinkkonen, J., & Alho, K. (1997). Language-specific phoneme representations revealed by electric and magnetic brain responses. *Nature, 385*, 432-434.

Neely, J. H. (1991). Semantic priming effects in visual word recognition: A selective review of current findings and theories. In: D. Besner, & Y. W. Humphreys (Eds.). *Basic processes in reading.* Hillsdale, NJ: Lawrence Erlbaum Associates.

Newman, A. J., Pancheva, R., Ozawa, K., Neville, H. J., & Ullman, M. T. (2001). An event-related fMRI study of syntactic and semantic violations. *Journal of Psycholinguistic Research, 30*, 339-364.

Newman, R. L., & Connolly, J. F. (2002). Determining the role of phonology in silent reading using event-related brain potentials. Submitted.

Newman, R. L., Connolly, J. F., MacDonald, W., & Arnold S. (2001). Identifying phonological awareness deficits with event-related brain potentials (ERPs). *Psychophysiology, 38*, s71.

Nigam, A., Hoffman, J. E., & Simons, R. F. (1992). N400 to semantically anomalous pictures and words. *Journal of Cognitive Neuroscience, 4*, 15-22.

Nobre, A. C., & McCarthy, G. (1995). Language-related field potentials in the anterior-medial temporal lobe: II. Effects of word type and semantic priming. *The Journal of Neuroscience, 15*, 1090-1098.

Nunez, P. L. (1981). Electric fields of the brain: The neurophysics of EEG. New York, Oxford University Press.

Nystrom, L. E., Braver, T. S., Sabb, F. W., Delgado, M. R., Noll, D. C., & Cohen, J. D. (2000). Working memory for letters, shapes, and locations: fMRI evidence against stimulus-based regional organization in the human prefrontal cortex. *NeuroImage, II*, 424-446.

Ogawa, S., & Lee, T. (1990). Magnetic resonance imaging of blood vessels at high fields: in vivo and in vitro measurements and image simulation. *Magnetic Resonance in Medicine, 16*, 9-18.

Oldfield, R. C. (1971). The assessment and analysis of handedness: the Edinburgh inventory. *Neuropsychologia, 9*, 97-113.

Orrison, W. W., Lewine, J. D., Sanders, J. A., & Hartshorne, M. F. (1995). *Functional brain imaging.* St. Louis: Mosby-Year book, Inc.

Owen, A. M. (2000). The role of the lateral prefrontal cortex in mnemonic processing: The contribution of functional imaging. *Experimental Brain Research, 133*, 33-43.

Paulesu, E., Frith, C. D., Frackowiak, R. S. J. (1993). The neural correlates of the verbal component of working memory. *Nature, 362*, 342-344.

Petersen, S. E., Fox, P. T., Snyder, A. Z., & Raichle, M. E. (1990). Activation of the extrastriate and frontal areas by visual word and word-like stimuli. *Science, 249*, 1041-1044.

Picton, T. W., Lins, O., & Scherg, M. (1995). The recording and analysis of event-related potentials. In: F. Boller, J. Graftman (Eds.) R. Johnson Jr. (Section Ed.) *Handbook of neuropsychology. Event-related brain potentials and cognition, 10*, (3-73). Amsterdam: Elsevier.

Praamstra, P., & Stegeman, D.F. (1993). Phonological effects on the auditory N400 event-related brain potential. *Brain Research: Cognitive Brain Research, 1*, 73-86.

Price, C. (2000). The anatomy of language: Contributions from functional neuroimaging. *Journal of Anatomy, 197*, 335-359.

Pritchard, W. S., Shappell, S. A., & Brandt, M. E. (1991). Psychophysiology of the N200/N400: A review and classification scheme. In: P. K. Ackles, J. R. Jennings, & M. G. H. Coles (Eds.). *Advances in Psychophysiology* (pp. 43-106). Greenwich, CT: JAI Press.

Polich, J., & Kok, A. (1995). Cognitive and biological determinants of the P300: An integrative review. *Biological Psychology, 41*, 103-146.

Puce, A., Allison, T., Spencer, S. S., Spencer, D. D., & McCarthy, G. (1997). Comparison of cortical activation evoked by faces measured by intracranial field potentials and functional MRI: Two case studies. *Human Brain Mapping, 5*, 298-305.

Revonsuo, A., Portin, R., Juottonen, K., & Rinne, J. O. (1998). Semantic processing of spoken words in Alzheimer's Disease: An electrophysiological study. *Journal of Cognitive Neuroscience, 10*, 408-420.

Rinne, T., Alho, K., Ilmoniemi, R. J., Virtanen, J., & Näätänen, R. (2000). Separate time behaviors of the temporal and frontal mismatch negativity sources. *NeuroImage, 12*, 14-19.

Rösler, F., Heil, M., & Glowalla, U. (1993). Monitoring retrieval from long-term memory by slow event-related brain potentials. *Psychophysiology, 30*, 170-182.

Rothman, D. L., Petroff, O. A. C., Behar, K. L., & Mattson, R. H. (1993). Localized ^{1}H NMR measurements of γ-aminobutyric acid in human brain *in vivo*. *Neurobiology, 90*, 5663-5666.

Rugg, M. (1995). Event-related potential studies of human memory. In: M.S. Gazzaniga (Ed.). *The Cognitive Neurosciences* (pp. 789-801). Cambridge, MA: MIT Press.

Scherg, M., & Berg, P. (1996). Brain electromagnetic source analysis - BESA. Munich: MEGIS version 3.

Scherg, M., & Picton, T. W. (1991). Separation and identification of event-related potential components by brain electric source analysis. *Electroencephalography and Clinical Neurophysiology, Supplemental, 42*, 24-37.

Scherg, M., Vajsar, J., Picton, T. W. (1989). A source analysis of the late human auditory evoked potentials. *Journal of Cognitive Neuroscience, 4*, 336-355.

Schumacher, E. H., Lauber, E., Awh, E., Jonides, J., Smith, E. E., & Koeppe, R. A. (1996). PET evidence for an amodal verbal working memory system. *NeuroImage, 3*, 29-88.

Schwartz, T. J., Kutas, M., Butters, N., Paulsen, J. S., & Salmon, D. P. (1996). Electrophysiological insights into the nature of the semantic deficits in Alzheimer's disease. *Neuropsychologia, 34*, 827-841.

Segalowitz, S. L., & Chevalier, H. (1998). Event-related potential (ERP) research in neurolinguistics. In: B. Stemmer & H. A. Whitaker (Eds.). Handbook of neurolinguistics (pp. 96-122). San Diego: Academic Press.

Shulman, R. G., & Rothman, D. L. (1998). Interpreting functional imaging studies in terms of neurotransmitter cycling. *Neurobiology, 95*, 11993-11998.

Sibson, N. R., Dhankhar, A., Mason, G. F., Rothman, D. L., Behar, K. L., & Shulman, R. G. (1997). *In vivo* ^{13}C NMR measurements of cerebral glutamine synthesis as evidence of glutamate-glutamine cycling. *Neurobiology, 94*, 2699-2704.

Sibson, N. R., Dhankhar, A., Mason, G. F., Rothman, D. L., Behar, K. L., & Shulman, R. G. (1998). Stoichiometric coupling of brain glucose metabolism and glutamatergic neuronal activity. *Neurobiology, 95*, 316-321.

Simos, P. G., Basile, L. F. H., & Pananicolaou, A. C. (1997). Source localization of the N400 response in a sentence-reading paradigm using evoked magnetic fields and magnetic resonance imaging. *Brain Research, 762*, 29-39.

Smith, E. E., & Jonides, J. (1998). Neuroimaging analyses of human working memory. *Proceedings of the National Academy of Sciences USA, 95*, 12061-12068.

Smith, E. E., Jonides, J., & Koeppe, R. A. (1996). Dissociating verbal and spatial working memory using PET. *Cerebral Cortex, 6*, 11-20.

Smith, E. E., Jonides, J., Marshuetz, C., & Koeppe, R. A. (1998). Components of verbal working memory: Evidence from neuroimaging. *Proceedings of the National Academy of Sciences USA, 95*, 876-882.

Sternberg, S. (1969). Memory-scanning: Mental processes revealed by reaction-time experiments. *American Science, 57*, 421-457.

St. George, M., Kutas, M., Martinez, A., & Sereno, M. I. (1999). Semantic integration in reading: Engagement of the right hemisphere during discourse processing. *Brain, 122*, 1317-1325.

Szymanski, M. D., Yund, E. W., & Woods, D. L. (1999). Phonemes, intensity and attention: differential effects on the mismatch negativity (MMN). *Journal of the Acoustic Society of America, 106*, 3492-3505

Talairach, J., & Tournoux, P. (1988). *Co-planar stereotaxic atlas of the human brain: A 3-dimensional proportional system, an approach to cerebral imaging.* G. Thieme, (Ed.). Stuttgart/New York: Thieme Medical.

Talairach, J., Tournoux, P., & Missir, O. (1993). *Referentially oriented cerebral MRI anatomy: An atlas of stereotaxic anatomical correlations for gray and white matter.* G. Thieme, (Ed.). Stuttgart/New York: Thieme Medical.

Thierry, G., Boulanouar, K., Kherif, F., Ranjeva, J. P., & Démonet, J. F. (1999). Temporal sorting of neural components underlying phonological processing. *NeuroReport, 10*, 2599-2603.

Thierry, G., Doyon, B., & Démonet, J. F. (1998). ERP mapping in phonological and lexical semantic monitoring tasks: A study complementing previous PET results. *NeuroImage, 8*, 391-408.

Ungerleider, L. G., & Mishkin, M. (1982). Two cortical visual systems. In: D. J. Ingle. M. A. Goodale, & R. J. W. Mansfield (Eds). *Analysis of visual behavior.* Cambridge, MA: MIT press.

van Den Brink, D., Brown, C., & Hagoort, P. (2001) Electrophysiological evidence for early contextual influences during spoken-word recognition: N200 versus N400 effects. *Journal of Cognitive Neuroscience, 13*, 967-985.

Van Orden, G. C., Johnston, J. C., & Halle, B. L. (1988). Word Identification in reading proceeds from spelling to sound to meaning. *Journal of Experimental Psychology: Learning, Memory, and Cognition, 14*, 371-386.

Van Orden, G. C., Pennington, B. F., & Stone, G. O. (1990). Word identification in reading and the promise of subsymbolic psycholinguistics. *Psychological Review, 97*, 488-522.

Vanzetta, I., & Grinvald, A. (1999). Increased cortical oxidative metabolism due to sensory stimulation: Implications for functional brain imaging. *Science, 286*, 1555-1558.

Verkindt, C., Bertrand, O., Perrin, F., Echallier, J. F., & Pernier, J. (1995). Tonotopic organization of the human auditory cortex: N100 topography and multiple dipole model analysis. *Electroencephalography and Clinical Neurophysiology, 96*, 143-156.

Wang, Y., Kong, J., Tang, X., Zhuang, D., & Li, S. (2000). Event-related potential N270 is elicited by mental conflict processing in human brain. *Neuroscience Letters, 293*, 17-20.

Waters, H. S. (1978). Superordinate-subordinate structure in semantic memory: The roles of comprehension and retrieval processes. *Journal of Verbal Learning and Behavior, 17*, 587-597.

Wechsler, D. (1987). *Wechsler Memory Scale-Revised*. New York: Psychological Corporation.

Wernicke, C. (1874). *Der aphasiche symptomenkomplex*. Breslau, Poland: Cohen and Weigert.

Zwitserlood, P. (1989). The locus of the effects of sentential-semantic context in spoken word processing. *Cognition, 32*, 25-64.